Co-adaptive myoelectric control for upper limb prostheses

December 2020

Author: Carles Igual Bañó

Supervisor: Jorge Igual García

The work of Carles Igual Bañó to carry out this research and elaborate this dissertation has been supported by the Ministerio de Educación, Cultura y Deporte under the FPU Grant FPU15/02870. One visiting research fellowships (EST18/00544) was also funded by the Ministerio de Educación, Cultura y Deporte of Spain.

Acknowledgments

Durante los cuatro años de elaboración de la tesis, muchas son las personas a las que tengo que agradecer su presencia y ayuda permitiéndome, finalmente, alcanzar los objetivos propuestos para la finalización del proyecto.

En primer lugar, agradecer a Jorge su dedicación desde el primer día ya que sin su ayuda nunca podríamos haber conseguido la beca que permitió empezar los estudios de doctorado. El tiempo dedicado, su disponibilidad en cualquier momento, incluso estancias en su casa para trabajar codo con codo y su confianza en el trabajo que estábamos realizando han sido fundamentales para lograr los objetivos. No olvidar tampoco de agradecer las tempranas comidas en la universidad de donde tan buenas ideas han surgido.

En segundo lugar, reconocer la enorme labor y mostrar mi gratitud a aquellas otras personas que han formado parte de mi entorno laboral a lo largo de la tesis. A Enrique J. Bernabeu por su enorme ayuda dentro de la escuela y su labor como tutor, siempre dispuesto para todo lo que necesitase. A Janne M. Hahne y Lucas C. Parra por su continua supervisión y ayuda, tanto para el desarrollo de la tesis como para la posibilidad de llevar a cabo las diversas estancias. A Arndt Schilling, Marko Markovic, Luis A. Pardo y Miguel A. Bravo Cabrera por el apoyo y colaboración durante la estancia en Alemania. A Hernán Makse por su disposición y ayuda en mi estancia en Nueva York, y por abrirme la posibilidad de tantos fascinantes proyectos. Agradecer también a Alberto Castillo, compañero de carrera con el que inicié simultaneamente el doctorado y con el que he podido compartir penurias y eternos procesos administrativos culminando la tesis con una publicación conjunta.

Por otro lado, agradecer a mi familia, a mis padres, todo el esfuerzo y dedicación en mi vida universitaria. Su conocimiento de la universidad y del campo académico ha servido para que fuesen un pilar fundamental para cada una de las decisiones a tomar, mi ejemplo a seguir. A su vez, su confianza en la importancia de la tesis me ha ayudado a seguir en momentos críticos donde no han dudado en ofrecerme toda su ayuda y apoyo. También reconocerles todo el cariño durante todos estos años que tanto ha ayudado en los momentos más duros.

Y por último, agradecerle a Laura toda su comprensión y ánimo durante estos años tan turbulentos. Estancias, proyectos, estrés, decisiones, momentos muy malos, momentos muy buenos, pero para todos ellos siempre ha estado dispuesta a apoyarme y entenderme las veces que hiciese falta, y no han sido pocas, siendo también siempre la primera en alegrarse por los éxitos. Sin su ayuda este proyecto no habría podido terminarse.

Abstract

Many people in the world suffer from the loss of a limb (predictions estimate more than 3 million people by 2050 only in the USA). In spite of the continuous improvement in the amputation rehabilitation and prosthetic restoration, living without a limb keeps limiting the daily life activities leading to a lower quality of life. In this work, we focus in the upper limb amputation case, i.e., the removal of any part of the arm or forearm.

This thesis is about upper limb prosthesis control using electromyographic signals (the superficial electric potentials generated during muscle contractions). Studies in this field have grown exponentially in the past decades trying to reduce the gap between a fast growing prosthetic research field, with the introduction of machine learning, and a slower prosthetic industry and limited manufacturing innovation. This thesis contributes to the field from different perspectives. The main goal is to provide and implementable new controller based on adaptive filtering that overcomes the most common state of the art concerns.

From the theoretical point of view, there are two main contributions. First, we propose a new system to model the relationship between electromyographic signals and the desired prosthesis movements; this new model takes into account previous states for the estimation of the current position generating a new human-machine synergy. Second, we introduce a new and more efficient autonomously personalized training paradigm, which can benefit not only to our new proposed controller but also other state of the art regressors. As a consequence of this new protocol, the human-machine structure differs with

respect to current state of the art in two features: the controller learning process and the input signal generation strategy.

As a direct aftereffect of all of this, the experimental phase design results more complex than with traditional controllers. The current state dependency on past states forces the experimentation to be in real time, a very high demanding task in human and time resources. Therefore, a major part of this thesis is the associated fieldwork needed to validate the new model and training strategy. Since the final goal is to provide an implementable new controller, the last part of the thesis is devoted to test the proposed methods in real cases, not only analyzing the robustness and reliability of the controller in real life situations but in real prosthetic devices.

As a conclusion, this work provides a new paradigm for the myoelectric prosthetic control that can be implemented in a real device. Once the thesis has proven the system's viability, future work should continue with the development of a physical device where all these ideas are deployed and used by final patients in a daily basis.

Resumen

Mucha gente en el mundo se ve afectada por la pérdida de una extremidad (las predicciones estiman que en 2050 habrá más de 3 millones de personas afectadas únicamente en los Estados Unidos de América). A pesar de la continua mejora en las técnicas de amputación y la prostética, vivir sin una extremidad sigue limitando las actividades de los afectados en su vida diaria, provocando una disminución en su calidad de vida. En este trabajo nos centramos en los casos de amputaciones de extremidades superiores, entendiendo por ello la pérdida de cualquier parte del brazo o antebrazo.

Esta tesis trata sobre el control mioeléctrico (potenciales eléctricos superficiales generados por la contracción de los músculos) de prótesis de extremidades superiores. Los estudios en este campo han crecido exponencialmente en las últimas décadas intentando reducir el hueco entre la parte investigadora más dinámica y propensa a los cambios e innovación (por ejemplo, usando técnicas como la inteligencia artificial) y la industria prostética, con una gran inercia y poco propensa a introducir cambios en sus controladores y dispositivos. El principal objetivo de esta tesis es desarrollar un nuevo controlador implementable basado en filtros adaptativos que supere los principales problemas del estado del arte.

Desde el punto de vista teórico, podríamos considerar dos contribuciones principales. Primero, proponemos un nuevo sistema para modelar la relación entre los patrones de la señales mioélectricas y los movimientos deseados; este nuevo modelo tiene en cuenta a la hora de estimar la posición actual el valor de los estados pasados generando una nueva sinergia entre máquina y ser humano.

En segundo lugar, introducimos un nuevo paradigma de entrenamiento más eficiente y personalizado autónomamente, el cual puede aplicarse no sólo a nuestro nuevo controlador, sino a otros regresores disponibles en la literatura. Como consecuencia de este nuevo protocolo, la estructura humano-máquina difiere con respecto del actual estado del arte en dos características: el proceso de aprendizaje del controlador y la estrategia para la generación de las señales de entrada.

Como consecuencia directa de todo esto, el diseño de la fase experimental resulta mucho más complejo que con los controladores tradicionales. La dependencia de la posición actual de la prótesis con respecto a estados pasados fuerza a la realización de todos los experimentos de validación del nuevo controlador en tiempo real, algo costoso en recursos tanto humanos como de tiempo. Por lo tanto, una gran parte de esta tesis está dedicada al trabajo de campo necesario para validar el nuevo modelo y estrategia de entrenamiento. Como el objetivo final es proveer un nuevo controlador implementable, la última parte de la tesis está destinada a testear los métodos propuestos en casos reales, tanto en entornos simulados para validar su robustez ante rutinas diarias, como su uso en dispositivos prostéticos comerciales.

Como conclusión, este trabajo propone un nuevo paradigma de control mioélectrico para prótesis que puede ser implementado en una prótesis real. Una vez se ha demostrado la viabilidad del sistema, la tesis propone futuras líneas de investigación, mostrando algunos resultados iniciales.

Resum

Molta gent en el món es veu afectada per la pèrdua d'una extremitat (les prediccions estimen que en 2050 hi haurà més de 3 milions de persones afectades únicament als Estats Units d'Amèrica). Malgrat la contínua millora en les tècniques d'amputació i la prostètica, viure sense una extremitat continua limitant les activitats dels afectats en la seua vida diària, provocant una disminució en la seua qualitat de vida. En aquest treball ens centrem en els casos d'amputacions d'extremitats superiors, entenent per això la pèrdua de qualsevol part del braç o avantbraç.

Aquesta tesi tracta sobre el control mioelèctric (potencials elèctrics superficials generats per la contracció dels músculs) de pròtesis d'extremitats superiors. Els estudis en aquest camp han crescut exponencialment en les últimes dècades intentant reduir el buit entre la part investigadora més dinàmica i propensa als canvis i innovació (per exemple, usant tècniques com la intel·ligència artificial) i la indústria prostètica, amb una gran inèrcia i poc propensa a introduir canvis en els seus controladors i dispositius. Aquesta tesi contribueix a la investigació des de diversos punts de vista. El principal objectiu és desenvolupar un nou controlador basat en filtres adaptatius que supere els principals problemes de l'estat de l'art.

Des del punt de vista teòric, podríem considerar dues contribucions principals. Primer, proposem un nou sistema per a modelar la relació entre els patrons de la senyals mioelèctrics i els moviments desitjats; aquest nou model té en compte a l'hora d'estimar la posició actual el valor dels estats passats generant una nova sinergia entre màquina i ésser humà. En segon lloc, introduïm un nou

paradigma d'entrenament més eficient i personalitzat autònomament, el qual pot aplicar-se no sols al nostre nou controlador, sinó a uns altres regresors disponibles en la literatura. Com a conseqüència d'aquest nou protocol, l'estructura humà-màquina difereix respecte a l'actual estat de l'art en dues característiques: el procés d'aprenentatge del controlador i l'estratègia per a la generació dels senyals d'entrada.

Com a conseqüència directa de tot això, el disseny de la fase experimental resulta molt més complex que amb els controladors tradicionals. La dependència de la posició actual de la pròtesi respecte a estats passats força a la realització de tots els experiments de validació del nou controlador en temps real, una cosa costosa en recursos tant humans com de temps. Per tant, una gran part d'aquesta tesi està dedicada al treball de camp necessari per a validar el nou model i estratègia d'entrenament. Com l'objectiu final és proveir un nou controlador implementable, l'última part de la tesi està destinada a testar els mètodes proposats en casos reals, tant en entorns simulats per a validar la seua robustesa davant rutines diàries, com el seu ús en dispositius prostètics comercials.

Com a conclusió, aquest treball proposa un nou paradigma de control mioelèctric per a pròtesi que pot ser implementat en una pròtesi real. Una vegada s'ha demostrat la viabilitat del sistema, la tesi proposa futures línies d'investigació, mostrant alguns resultats inicials.

Contents

List of Figures

List of Tables

Chapter 1

Introduction

This chapter presents the motivations behind this thesis, its objectives and main contributions. In addition, it also introduces the thesis framework and its outline.

Contents

1.1 Motivation

Living without a limb can have tremendous consequences in people lives. The development of cutting-edge prostheses technology is vital for minimizing the inconveniences. Artificial limbs have made great progress in the last years moving from static prostheses to intelligent ones with machine learning algorithms. However, the rejection and low functionality has always been a problem, specially with upper-limb amputation cases (Biddiss and Chau, 2007a; Datta et al., 2004). The satisfaction with prostheses is reported limited (Davidson, 2002; Østlie et al., 2012) generating a gap between the academia progress and an industry that faces a decreasing demand as prostheses do not fulfill the users expectations.

The fast evolution of the Machine Learning field and the integration in upper limb prostheses impulsed the last decades research. The goal is to develop an optimal and robust prosthesis control helping the thousands of people that suffer a major upper-limb loss to overcome their daily limitations. The general idea of an intelligent controllable prosthesis is to infer the user's intentions from an available biological signal and move the prosthesis accordingly. In the last 15 years, the literature presented a diversified bundle of approaches combining different signal sources and control methods. The high performance achieved with completely different proposals proves the nonexistence of a unique solution for the prosthesis control problem.

Despite the major progress into more efficient, powerful and complex systems, not many of them have reached the market. The gap between the industry and the academia is still large due to the lack of functionality of the novel proposals in real environments. As a consequence, the research shifted into generating more natural, robust and intuitive controls (Dohnálek et al., 2013; Marasco et al., 2018; Scheme and Englehart, 2011; Scheme et al., 2010). Despite of this effort, prostheses are far from replacing a natural human limb. Nevertheless, a positive trend was observed in the last years decreasing the rejection rate to a 20% (Biddiss and Chau, 2007a; Biddiss and Chau, 2007b) in upper limb prostheses and 30% for body-powered devices in general (Vujaklija et al., 2016) suggesting that the research is going in the right direction.

The motivation of this PhD thesis is to contribute into continue closing the gap between the academia and the industry providing a functional proportional and simultaneous prosthesis control. The thesis proposes a regression based algorithm combined with an autonomous personalized training, developing a prosthesis controller that presents excellent performance metrics while ensures a smooth, robust and natural control.

1.2 Objectives

The main goal of this work is the development of an intelligent control for upper limb prostheses that achieves robust performance in controlled and not controlled scenarios with a novel training based on co-adaptation. The thesis is a closed project (from beginning to end) that starts with the proposal of a new algorithm and ends with its implementation in real life scenarios on a final product. The novel system presents a different approach to the EMG prostheses control and appeases several specific objectives related to the state of the art research:

- Selection of the best input source and definition of the state of the art for prostheses control. Implementation of an electromyographic (EMG) signal acquisition process.
- Development of an intelligent adaptive auto-regressive controller for a proportional and simultaneous control. Implementation of a novel infinite impulse response (IIR) model and integration with state of the art finite impulse response (FIR) regressors into a unique algorithm.
- Development of a co-adaptive training system where both agents, machine and human, learn simultaneously and interact with each other. Analysis and improvement of the training protocol and the user interface to exploit the benefits of the regression based controller.
- Test the system in a representative sample. Large experimentation with a significant sample of participants including subjects with limb deficiencies, all tested in controlled and non-controlled environments.
- Development of a robust system capable of overcoming disturbances such as: donning and doffing the prosthesis, arm movements during its use, muscle fatigue and long term use; all this avoiding tedious and inefficient re-training protocols.

1.3 Main contributions

Understanding the prosthesis control state of the art research is essential to generate a useful and optimized model that could help to solve the problems this field is facing nowadays. Therefore, a deep study about the literature is carried out contributing with a paper that gathers the history, highest performance systems (input signals and models), caveats and future work of the

field. This research revealed that the main caveats are non optimal regression based algorithms and a low acceptance due to a lack of robustness in non-controlled environments (Igual et al., 2019b).

This thesis is shaped in order to contribute at some of these caveats. Note that not only the machine learning algorithms play a critical role in the prosthesis control task and its issues. As recent studies pointed out, the analysis of the training protocols is essential for an optimal controller. One relevant contribution of this work is the introduction of the co-adaptation concept into the learning phase. This technique gives two agents of the system, human and machine, a similar relevance for the learning process. In this situation both are active learners that interact with each other in real time. The key is to develop the right training such that the interaction between them enhances the qualities of both learners (Igual et al., 2021a).

The major contributions of this thesis is a novel regression based algorithm for simultaneous and proportional myoelectric upper limb prosthesis control. The novelty relies on the development of an intelligent autoregressive–moving-average (ARMA) model capable of learning a velocity or position control choosing the best protocol to maximize the performance with 2 controllable degrees of freedom (DoFs) (Igual et al., 2019a) that can be extended to include a third DoF.

Trying to generate the most efficient training, this document presents a new autonomously personalized training protocol, which exploits all the strengths of regression based algorithms. The contribution resides in generating a training that explores the complete continuous space and adapts efficiently the training time distribution for each particular case depending on the user performance (Igual et al., 2020b).

One of the main drawbacks the academia has faced in the last decades is the robustness problem. This manuscript presents as a solution the introduction of directly trained IIR models in real time with an optimal training that includes the previously described features. This approach obtains controllers that remain robust through time and other daily disturbances such as removing and relocating the sensor generating small electrode shifting or altering the EMG signals due to arm movements or fatigue. The system overcomes this obstacles without needing any type of re-training or re-calibration, commonly used as an acceptable but not completely efficient solution (Igual et al., 2020a).

The promising results of this PhD thesis lead to start assembling a final product (prototype) as part of a possible future post-doctoral research. Preliminary

tests proved the successful deployment of the algorithm into a real commercial prosthesis. The training experience is also improved using a more immersive environment based on Virtual Reality (VR) technologies. Finally, a prototype based on 3D printing technology is being developed.

1.4 Framework

This thesis stands within the framework of the research FPU grant FPU15/02870 funded by the Spanish *Ministerio de Educación, Cultura y Deporte* supporting all the work carried out by Carles Igual Bañó on this research and the elaboration of this manuscript.

The project has its origin in the visiting research fellowship Jorge Igual did in 2015 at the *Parra Lab*[1] belonging to the *City College of New York*. The main purpose of this visit was to develop a high performance lineal regressor for myoelectric prosthesis control. The *Parra Lab* had previously collaborated with Janne M. Hahne, a german researcher nowadays working for the *ART-Lab*[2] a world leader group in prosthesis control, developing a novel lineal regressor for prosthesis control (Hahne et al., 2014). The thesis project started with the goal of continuing the development of the algorithm initiated by Jorge Igual and creating viable prosthesis controlling system.

In addition, the *Ministerio de Educación, Cultura y Deporte* funded Carles Igual one visiting research fellowship. In 2019 Carles Igual visited the german group *ART-Lab* in Göttingen to collaborate with Janne M. Hahne, the research leader in the work used as basis for this thesis, and work in a world reference laboratory of this field. The goal of this scholarship was to perform test in real prosthesis and use all the german group infrastructure to implement the research in real world applications. A second non-funded visit occurred in 2020 to the *Parra Lab*[3] of the *City College of New York*. As this group has other research projects that involve other biological signals as input for prosthesis control, the aim of this visit was to gain knowledge about those other input sources and optimize the training strategy used with the current myoelectric control. The two visits had a great impact in this thesis. The work developed in those two periods is included along the present manuscript.

[1] `www.parralab.org`
[2] `http://cuop-umg.de/forschung/forschungsthemen/artlab`
[3] `www.parralab.org`

1.5 Outline

The manuscript is divided in 8 chapters. This chapter has done a brew introduction to the history and motivation about the topic of this research, myoelectric control for upper limb prosthesis. It also describes the main contributions to the field and the framework that supported the project.

In Chapter 2 an exhaustive analysis about the prosthesis control problem and the state of the art controllers is carried out. This chapter introduces the problem of the loss of an upper limb and the possible limbs anatomies describing the different biological signals used as input for prosthesis control. Classification and regression methods are presented along with the training paradigms and learning systems used in the literature. At the same time, a deeper analysis about the electromyographic signals and its data acquisition process is conducted.

Chapter 3 gives an especial attention to the new co-adaptive concept and its value in the controller training. So far only one learner, machine or human, was active during the learning phase. With this new technique both learners are active at the same time influencing the other learning and optimizing the controller training.

Chapter 4 introduces to the reader the novel co-adaptive auto-regressive filter algorithm for myoelectric control tested for 2 controllable DoFs. A velocity control strategy with a regression based model is used to train a controller in a virtual environment. To measure the new model performance an experiment is conducted comparing the proposed model with other state of the art regressors and evaluating our model strengths and weaknesses.

Chapter 5 details the training procedure and the basics of an optimal learning. In particular, a novel training protocol to optimize and personalize the learning process is explained in depth. The performance of the user shapes the duration and target distribution during the training period, fitting it to the user's needs.

Chapter 6 emphasizes the problems the academia is facing to reach the market. Several disturbances from the daily use of a real prosthesis are analyzed. On one hand, experiments with the new model are used to test the robustness and capabilities to overcome these disturbances such as time, arm movements and donning/doffing the sensor.

In Chapter 7 an introduction of the future work is carried out. This chapter presents the preliminary tests developed to prove the benefits of all the previously proposed methodologies for the control of 3 DoFs. In order to

keep improving the model's capabilities, a new virtual reality (VR) user interface (UI) designed to improve the user experience when carrying out the experiments. It also shows some preliminary results from the deployment of the algorithm in a real prosthesis.

A final Chapter 8 presents the conclusions obtained from the thesis ending with the citation of the scientific publications derived from the work.

The organization of the thesis follows the temporal workflow from the review of the state of art to the deployment and testing of the new ideas in real environments. In Figure 1.1 we show the different modules and the paper associated to each of them. They correspond to each chapter in this manuscript. Some of these chapters are extended/adapted versions of the corresponding papers. That explains why some content (introductions) might overlap.

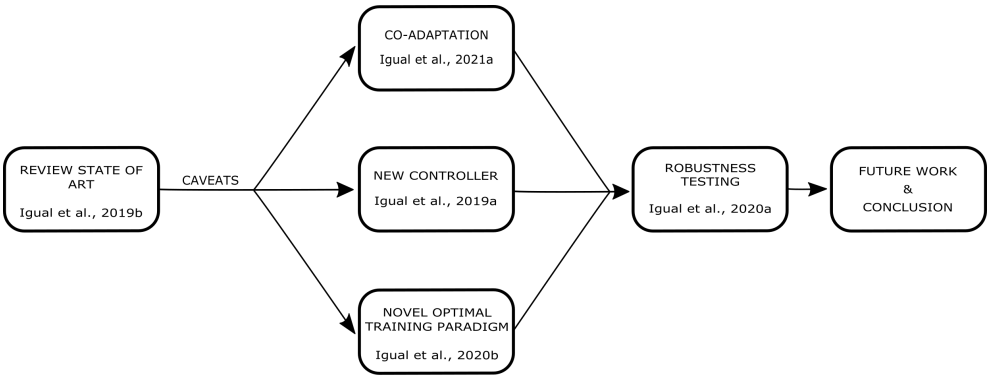

Figure 1.1: Thesis workflow diagram.

Chapter 2

Myoelectric control for upper limb prostheses

This chapter reviews the state-of-the-art and provides a taxonomy emphasizing the challenges in the field. High-end prostheses are electro-mechanically devices able to provide a great variety of movements in order to functionally replace a human limb. This chapter reviews the most recent literature in upper limb prosthetic control. It covers commonly used variants of possible biological inputs, state of the art prosthesis models, its signal processing and translation to actual control, mostly focusing on electromyograms as well as the problems it will have to overcome in the near future.

Chapter based on **Igual, C.**, Pardo, L.A., Hahne, J.M. and Igual, J. (2019). Myoelectric Control for Upper Limb Prostheses. In *Electronics*, vol. 8, nº 11: 1244. JCR Impact factor: 2.41 (Q2).

Contents

2.1 Introduction

In the USA alone, each year around 158,000 persons undergo amputations (Dillingham et al., 2002). In 2005, 1.6 million persons were living in the USA with the loss of a limb, with a 3.6 million prediction by the year 2050 (Ziegler-Graham et al., 2008). For amputees, the use of artificial limbs (prostheses) is vital for their quality of life. Unfortunately, rejection and non-functional use has been traditionally high, specially in upper-limb amputation cases (Biddiss and Chau, 2007a; Datta et al., 2004) and satisfaction with prostheses was reported limited (Davidson, 2002; Østlie et al., 2012).

Upper limb prosthesis control has been a growing research topic in the last decades. Different studies focused on developing robust prosthesis control to help the thousands of people that suffer a major upper-limb loss. Trying to predict the user's intent from available biological signals has been a challenging problem. Electromyography (EMG) is the most important input source for upper limb prosthesis control. Numerous methods have been tested in the last 15 years presenting different approaches to this problem and leading to a diversified literature. The performance of the different methods strongly depends on the environment and experimental setup, proving the nonexistence of a unique solution for prosthesis control.

Despite the great number of different attempts, not many of the recent, complex and powerful proposals have emerged as a daily functional option. Some companies have developed prostheses using sophisticated classification controllers, but the difference between academia and industry is still one of the most intriguing situations. As a consequence, clinical usability has become a key issue in the research community. The need for more intuitive, natural and robust controls is the main topic in many recent papers (Dohnálek et al., 2013; Marasco et al., 2018; Scheme and Englehart, 2011; Scheme et al., 2010). Prostheses have to improve a lot to naturally replace a human limb. The prosthesis rejection decreased to a 20% in the last years (Biddiss and Chau, 2007a; Biddiss and Chau, 2007b). This rejection percentage goes up to a 35% for body-powered devices in general (Vujaklija et al., 2016).

Diverse signal sources were considered for a better estimation of the user's intent. Non-invasive and invasive methods have been compared in order to establish a preference depending on the user's condition. Contingent to the physiology of the patient, there are differences in the availability of muscles and signals. For the data acquisition process (see Figure 2.1), surface EMG signals are the most common ones. They are used to obtain the features in the time or frequency domain that are the basis for the prosthesis control algorithm.

Depending on how data is collected and processed, offline and online methods can be used, i.e., learning can be done with prerecorded signals or in real time. The opportunity for the user to adapt during an online experimentation and in real life makes these versions more realistic and accurate.

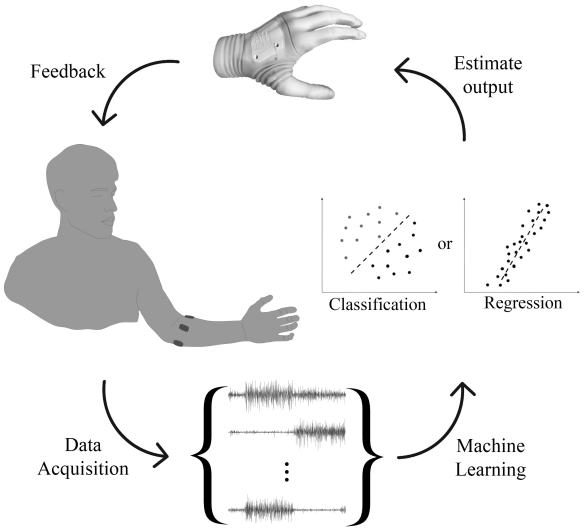

Figure 2.1: Closed loop for prosthetic myoelectric control. First step, acquisition of multiple EMG channels from upper limb muscles. Second, mapping into control signals with machine learning techniques (classification or regression) using the EMG features as inputs. Third, model estimation of the prosthesis output for control, and last, feedback to the user from the prosthesis (or other output interface).

Another fundamental challenge is the learning model, the second step of the control loop in Figure 2.1. Commercial systems generally work with a hard-coded control using two channels. One option is that with a co-contraction, the user switches between functions. Furthermore, contractions in different channels generate outputs in the selected function. The other one is where the slope in each channel signal determines the function used. The prosthesis does not have any learning process. Here, the user adjusts the parameters to the best fitting, but the machine is already programmed to work in a specific way. As opposed, machine learning models have to be trained to learn. They know what the goal is, typically, an error cost function to be minimized, and try to learn from the input data. During training, the machine finds the most suitable transformation for the input data to estimate the best output according to the

goal set and the model parameters. This is known as machine adaptation; the machine adapts itself to improve its performance using the input information. After training, it is tested in unknown conditions to evaluate its performance. Classification models, which assign the current data to specific movements (a finite length alphabet of allowed movements) were the most common models in past research. Seeking for a more natural and smooth control, researchers are recently implementing regression models with high performance. This allows a more continuous control of the model's output.

To complete the closed loop structure of Figure 2.1, the last element is the feedback channel. The most common feedback is the visual channel, when the user is observing the prosthesis reactions or graphical representations of the model output in virtual tasks. The importance of feedback has been proven as critical in the learning process (Jiang et al., 2012), optimizing the performance if the user is able to predict the prosthesis' behaviour and to interact with the system. At the beginning, studies were focused only in the machine adaptation process. But recently, researchers found out that the human adaptation is as important and should be studied with the same effort. Human adaptation is the process in which a human learns from the machine's actions and changes his behavior to achieve the best results (Ison et al., 2016). The great impact of the concept of human adaptation in prosthesis control motivated the researchers to further investigate it. Due to this, co-adaptation emerged (Hahne et al., 2015). The application of this concept, understood as the simultaneous adaptation of machine and user, has shown promising results. Both learners are able to adapt to the other's response. This helps the control to be more dynamic and accurate in real time, avoiding non-optimal solutions. Another interesting concept developed is transfer learning, which allows previous knowledge from a different task to be used to perform a new task with high accuracy and within a shorter training period (Ameri et al., 2019).

Algorithms achieved peak performance in controlled environments, but adapting these to realistic environments and daily life situations exhibited issues in robustness (Jiang and Farina, 2014; Scheme et al., 2011). Many factors, such as changes in arm position (Fougner et al., 2011), small electrode shifts (Young et al., 2011), skin conditions (Jiang et al., 2012), mechanical load due to the weight of the prosthesis (Cipriani et al., 2011) or time between algorithm training and application (Amsüss et al., 2013) can impact the reliability and contribute to the limited usage of more sophisticated prosthesis control methods in final users. Trying to deal with this, a new research area focused on clinical usability has been initiated. Studying i.e., sensor shifting effects or long-term use, helps to improve the prosthesis' performance in the

real world. Furthermore, testing in real prostheses has become more regular, being aware of the need to analyze the theoretical progress in real environments (Hargrove et al., 2017; Vujaklija et al., 2017).

This chapter presents an overview of literature related to upper limb prosthesis control. We seek to clarify the different methods that have been used by research laboratories around the world. This review made it possible to identify the large number of alternatives used for prosthesis control in the literature. These were analyzed in depth, in order to present their advantages and disadvantages. In the next Sections, we review in detail, each of the blocks in Figure 2.1 and in the last Section, we discuss the future challenges in myoelectric upper limb prosthetic control.

2.2 Data acquisition

2.2.1 Muscle contraction physiology

The body movements are generated by muscle forces applied to the skeleton when contracting. The signals responsible of muscle contractions are generated in the brain's motor system which is mostly located in the frontal lobes. The motor cortex is divided in several areas each controlling different parts of the body. The motor cortex will plan, control and execute the voluntary movements. In the premotor areas the complex movements will be planed and coordinated to finally send from the primary motor cortex through the spinal cord the output signal. The process will generate voltage fluctuations in the brain resulting from ionic current within the neurons. Afterwards, this signal will reach its target and generate a contraction and movement of the muscles.

Muscles are composed of fibers controlled by the central nervous system (CMS). The CMS controls through motor neurons different fibers. A single motor neuron can control more than one fiber creating groups of fibers that will contract simultaneously named as motor units (MU) (Buchthal and Schmalbruch, 1980). Therefore, a muscle is composed by several MU (Al-Faiz and Al-Mashhadany, 2009). The axons from the spinal cord carry action potentials (generated by depolarizations of the motor neurons membranes) towards the muscles. Once the action potential reaches the muscles, they will trigger the release of neurotransmitters that will depolarize the muscle fibers of the MU to achieve the desired contraction. The level of the force depends on the number of activated MUs and the firing rates of each MU (Despopoulos, 2003). The local depolarizations will travel through the conductive tissue reaching the

skin surface. There we will be capable of measuring a surface electromyogram (sEMG) of the superposition of all MUs depolarizations.

2.2.2 Input signals

Decoding information transmitted from the brain to the muscles is a complicate task. The access to it can be performed invasive or noninvasive and can be seen as a straight forward procedure, but its decoding, interpretation and usage as control input for a prosthesis are more challenging. In principle, an expectation of a human's movement intention can usually be extracted from different stages of the transmission.

It is possible to access signals directly from the brain, using i.e., electroencephalography (EEG) (Frisoli et al., 2012; Hochberg et al., 2006; McMullen et al., 2014; Velliste et al., 2008). Ganguly and Carmena (2009) were able to generate a stable cortical map for prosthetic function. The problem is to create a stable neural interface that remains unchanged over time. Due to the plasticity of cortical circuits, neural representations for natural movements have been proven unstable, but with long-time use of prosthetic control, a stable map can be created. This representation can persist over time even with the addition of other cortical maps. Finding a stable EEG feature is key to a prosthesis brain control. Galán et al. (2008) controlled a wheelchair after users were able to perform stable EEG features that maximize separability between tasks. Nevertheless, the data acquisition process, as well as its necessary hardware are still not suitable for daily use.

Another option is to access it directly from activated muscles using EMGs. Nowadays, these are the most commonly used signals for upper limb prosthesis control and they have been utilized since the 1940s (Childress, 1985; Marquardt, 1965; Sherman, 1964). EMG measures electrical potentials generated in a muscle during its contraction representing neuromuscular activities. Therefore, they contain information about the neural signal sent to attempt a specific movement. The amplitude of the EMGs reflects the number of activated MUs and the firing rates (up to a few millivolts for strong contractions). Because of its easy access and the available information, EMGs are the first option for prosthesis control. They can be recorded placing non invasive superficial electrodes on the skin of the stump or other active muscles. Working with EMGs as inputs for user-intent estimation models has trained systems with excellent performance (Englehart and Hudgins, 2003; Fougner et al., 2012; Parker et al., 2006; Resnik et al., 2018; Scheme and Englehart, 2011; Scheme et al., 2010; Scheme et al., 2011). A deeper study on EMGs

was developed by Sartori et al. (2018), in which they generated a biomimetic model-based decoder that synthesizes the dynamics of the musculo-skeletal system controlled by the residual EMG measured. Additionally, it is possible to extract the central nervous system (CNS) "force functions" of muscular synergies from EMG recordings, which represent the Degrees of Freedom (DoFs) control signals that models have to estimate.

In addition, if the availability of active muscles is limited, Targeted Muscle Reinnervation (TMR) (A. et al., 2004; Huang et al., 2008; Kuiken et al., 2009; Miller et al., 2008; Souza et al., 2014), is an effective procedure to generate meaningful inputs and to treat phantom limb pain (Dumanian et al., 2019). With TMR, residual nerves are surgically transferred to alternative muscles where surface EMGs can be recorded. After successful reinnervations, the new muscles contract on motor commands sent to the lost limb. Thus new hot spots for intuitive EMG driven prostheses are created (Mioton and Dumanian, 2018). The experiments on patients who underwent TMR surgery prove that the nerve activity is amplified to an acceptable amplitude level. Using this it is possible to develop a control with the generated EMGs as good as the systems with biologically natural EMGs. This situation is more frequent in patients with a high level of amputation like transhumeral or shoulder-disarticulation amputations were some nerves are no longer bio-mechanically useful (Mioton and Dumanian, 2018). Moreover, for these individuals, the need to create additional signal sources is particularly large, as a high number of functions need to be replaced while only few natural sources are available. The TMR surgery helps to overcome this paradox and offers these patients a functional use of prostheses.

As the EMG signals are the most suitable and the most common in the literature, we will focus on them from now on.

2.2.3 Data amount: number of channels and sampling frequency

Larger amounts of acquired data contain more information to be used as an input for a prosthesis. Nevertheless, this additional information might not always be valuable. At a certain point, increasing the number of channels in a limited space will provide a lot of redundant, and therefore, useless information. This occurs to be a problem if it increases the computational cost needed to process the data in a reasonable amount of time, consequently decreasing the overall efficiency and performance of the system. Therefore, before performing acquisition, it is necessary to establish the number of channels to record from and, therewith, the amount of data to collect. Some studies use a high-density

data acquisition system reaching up to 192 channels of EMG signals (Hahne et al., 2014, 2012b; Ison et al., 2016; Young et al., 2013), but this amount of data is not necessary for high performance. Young et al. (2013) tested the effect of the number of channels during EMG data acquisition suggesting that having more than six channels did not reduce the estimation error, therewith, performance did not improve. Hahne et al. (2014) performed a similar study and showed that fewer channels were more optimal, due to the lower amounts of training data required. The increase of performance was not significant regarding the computational cost implied and most of the extra information obtained was redundant. The state-of-the-art methods are typically based on four to twelve channels using EMGs (Chen et al., 2013; Oskoei and Hu, 2007; Parker et al., 2006; Peerdeman et al., 2011; Pilarski et al., 2011; Sensinger et al., 2009). Within this range, models reach their peak performance with a high efficiency during the data acquisition process.

Since the bandwidth of EMG signals is around 400–500 Hz (Clancy et al., 2002), a typical sampling frequency is 1000 Hz (Nyquist–Shannon sampling theorem) (Ajiboye and Weir, 2005; Chu et al., 2006; Farina et al., 2004). Other studies use a lower sampling frequency with similar results. For a comparison of sampling frequencies and performance see Li et al. (2011). In some commercial devices, the sampling frequency is reduced to 200 Hz in order to capture enough signal information at a lower cost (Phinyomark et al., 2018).

2.2.4 Data segmentation: sample size for feature extraction

Once the input source has been digitized and the number of channels have been properly set, the EMG signal must be processed in order to use it afterwards to feed the system. Therefore, the next phase consists of segmentation, where input signal is windowed for feature extraction purposes: from all the data, only a specific amount (simple size defined by the window size) will be used to extract the information at each time step as it is sketched in Figure 2.2. The window is continuously moving accepting new samples. Farrell and Weir (2007) proposed a maximum delay of 300 ms to avoid unacceptable delays in real-time operations. The optimal window length was between 100 and 125 ms. Finding the trade-off between accuracy and time response is clue to window sizing. Nielsen et al. (2011) establish that the system decreases performance with windows smaller than 100 ms.

The second point in data segmentation is the windowing technique. The shape of the window is the rectangular one. With respect to the displacement, there are two options: adjacent windowing (disjoint segments) and overlapped

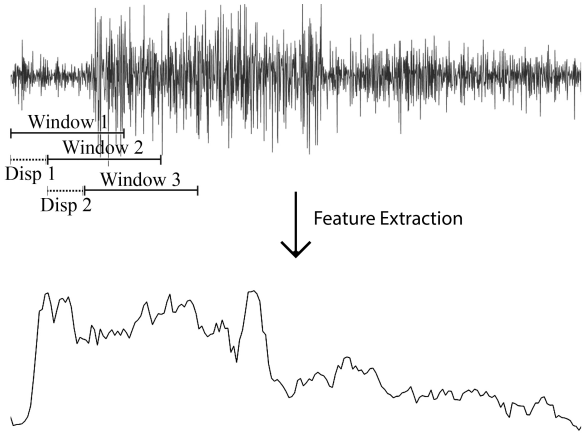

Figure 2.2: Feature extraction process. The upper plot represents EMG raw data from which only a portion is processed at each time step. The currently processed portion, named window, is displaced in time each iteration with a defined step-size (Disp 1 for the first iteration, Disp 2 for the second). This example uses an overlapping scheme where consecutive windows overlap in order to compensate the data acquisition delay and smooth the feature vector. The data in the window is updated to the most recent data recorded. Features (the root mean square RMS) are constantly extracted from the current window at each time step. The lower plot corresponds to the extracted features of the data. (Neither window nor displacement sizes exemplify actual dimension, but had to be enlarged for visual simplicity).

windowing (windows slide over each other, smoothing the feature vector). While variance can also be reduced in non overlapping windowing by using greater windows, they are slower and introduce delays. These delays exacerbate the user experience in real-time operations. Overlapping will reduce these delays, not having to wait for a time set by the window size to generate a new output. At the same time, overlapping uses enough data to not generate high-variance outputs. Phinyomark et al. (2013) tested different overlapping options, suggesting that overlapping does not improve the accuracy of the methods but helps reducing the delay using larger window sizes.

2.2.5 Feature extraction

As previously stated, feeding the system directly with myoelectric signals is unpractical due to the randomness and non-stationarity of the inputs. Some recent studies have been working with full EMG signals using a Convolutional Neural Network (CNN) to extract the main information (Ameri et al., 2019), but the common workflow consists of mapping the signals into smaller dimensions, increasing the information density. This method is called feature extraction and resides on the condensation of the relevant information, drafted in Figure 2.2. This process is critical for the success of any model.

There are three different categories of features for feature extraction: time domain (TD), frequency domain (FD) and time-scale domain (TSD). Oskoei and Hu (2007) did a deep theoretical study on the different categories and features that can be extracted from EMGs. Time domain features often investigate amplitude and related features of the EMGs, while frequency domain features are more focused on the power spectrum parameters. The use of wavelets falls into time-scale domain features. Time domain features are the most common in myoelectric controls due to their simplicity and since they are computed rapidly. The root mean square (RMS) is an example of TD features that works better with high level contractions following a Gaussian Model. Others, like mean absolute value (MAV), work better with low level contractions (or fatigue effects) using a Laplacian model. Phinyomark et al. (2018) studied 26 different, individual features and eight sets of multiple features. With lower sampling frequencies, that can reduce power-consumption and computational costs in a clinical application, the selection of the feature has a critical effect. The effect of dropping the sampling frequency was unavoidable, but signal amplitude or power features incurred less reductions. Features like EMG amplitude estimators, e.g., integrated absolute value (IAV), mean absolute value (MAV), root mean square (RMS), and waveform length (WL)) and power features, e.g., difference absolute mean value (DAMV), difference absolute standard deviation value (DASDV) and mean value of the square root (MSR)) obtained good results.

2.3 Learning

Extracted features are the input to the learning system. Features will be used to train the model for estimating the user's intent. It will map the features to an output of various degrees of freedom.

The majority of commercial devices are non-learning systems that control one DoF at a time. An activation pattern allows the user to switch between the functions available. While using other patterns, the user can control the output of the prosthesis in the activated function. Which DoF is controlled will depend on the function. Looking for a more realistic and natural control of the output, researchers developed more complex algorithms.

There are two agents that participate in this learning process: the machine and the human. Focusing on the machine learning system first, the models are mostly based on two fundamental approaches: classification and regression. Depending on the final application we want it for, we will use one or the other.

2.3.1 Classification

A classifier is designed to identify patterns in data and to categorize them. Classifiers recognize patterns in the data generated during the training phase and assign a particular input to the corresponding target motion class during the application phase. The concept can thus be applied to recognizing and separating EMG signals and to relate them to the intention of the user. Several linear and non-linear approaches were investigated in the last decades. Early attempts used a linear approach based on time series parameters that was able to correctly separate classes (Graupe and Cline, 1975). Artificial Neural Networks, which are mathematically modeled networks inspired by biological neurons, added the ability to learn the distinction between different conditions in patterns and therewith, the linear and nonlinear relationships directly from the data being classified. Kelly et al. (1990) showed that a discrete Hopfield model is capable of generating the same time series parameters as those produced by the conventional sequential least-squares-algorithm with higher computational efficiency. Furthermore, the model could distinguish between four separate arm functions using a two-layer perceptron, although at still high computational costs.

Heretofore, many classifiers have been explored, such as Linear Discriminant Analysis (LDA) (Englehart and Hudgins, 2003; Spanias et al., 2015), Gaussian mixture models (Castellini and Van der Smagt, 2009; Huang et al., 2005),

Support Vector Machines (SVM) (Alkan and Günay, 2012; Oskoei and Hu, 2007; Al-Timemy et al., 2013), Hidden Markov Models (HMM) (Chan and Englehart, 2004), K-Nearest Neighbors (KNN) (Zardoshti-Kermani et al., 1995), Multi-Layer Perceptrons (MLP) (Karlik et al., 2003; Kelly et al., 1990), Quadratic Discriminant Analysis (QDA) (Scheme et al., 2011) and Hyper-Dimensional Computing (HDC) (Rahimi et al., 2016).

Currently, it is widely accepted that a simple time-domain feature-set, as proposed by Hudgins et al. (1993) in combination with an LDA classifier is sufficient and presents a good balance between classification accuracy and computational usage, as well as robustness towards some non-stationarities (Young et al., 2011).

Due to the usage of multiple channels for signal acquisition, the extracted feature vector dimension can become large. In order to overcome problems with dimensionality, feature-reduction (FR) or feature selection (FS) are commonly performed. Using Principal Component Analysis as a method for FR decreases computational costs by projecting the high dimensional feature set into a relatively low dimensional space, still preserving the linearity (Hargrove et al., 2008b). FS is achieved with methods such as Sequential Forward Selection (Hargrove et al., 2008b; Li et al., 2017), Genetic Algorithms (Oskoei and Hu, 2006; Peleg et al., 2002), Kohonen's Self-organizing Map (Huang et al., 2003) and Particle Swarm Optimization (Khushaba and Al-Jumaily, 2007). Moreover, Common Spatial Patterns (CSP), a method generally employed to overcome binary classification problems of EEG signals, has been shown to also improve performance and robustness against noise in EMG pattern recognition Hahne et al. (2012a).

In fact, not many classification methods reached clinical usage, in part due to missing reliability outside of laboratory conditions (Almström et al., 1981; Farina et al., 2014; Jiang et al., 2012; Lorrain et al., 2011). All classifiers need thorough training to identify the intention of the user and the high performance levels obtained with the applied techniques often drop when natural variations in the EMG patterns and noise-sources, typical for real-world conditions, are introduced (Amsüss et al., 2013; He et al., 2015; Vidovic et al., 2015). These non-stationarities (Samek et al., 2012; Von Bünau et al., 2009) may be caused by changed electrode impedances due to sweat or dry skin (Jiang et al., 2012), altered armpositions (Fougner et al., 2011; Radmand et al., 2014), mechanical loads due to the weight of the prosthesis (Cipriani et al., 2011; Roy et al., 2007), small shifts of electrode positioning (Hargrove et al., 2008a; Young et al., 2011) or variations in the user's contractions. Furthermore, a classifier provides only an estimation about the executed movement but not the level of

contraction that is needed to control the velocity or grip force of a prosthesis. To obtain a proportional control, which is clinically important, the discrete signals of the classifier output are combined with a force-estimate (Castellini and Van der Smagt, 2009), achieved by averaging of the amplitude of all EMG channels (Jiang et al., 2012).

2.3.2 Regression

Regression models do not classify input signals in a discrete set of classes, but approximate continuous multivariate outputs. Classifiers have the disadvantage that only a finite number of pre-trained patterns can be learned. Regressors do not have that handicap and give the user more freedom. A continuous mapping of the output allows a complete control and lots of combinations of values. The user can perform any movement generated by the controlled DoFs activation even if it has not been trained.

Classification has other limitations. The need of re-training for the non-stationary EMGs is one of them. As mentioned before, small changes in the EMG signals, e.g., fatigue, electrode shifting or sweat, are not well handled by classifiers. The user is more able to adapt to these effects in regression (Hahne et al., 2017). Small changes in the input signal can generate small variations in the prediction, which could lead to a missclassification. A small variation in the prediction on a regressor is better handled due to its continuity. There are no abrupt changes as class-boundaries, so the user can directly react and better compensate for potential errors in the estimation.

In summary, regression models include the control for all DoFs simultaneously, independent and proportional, generating a smoother and more natural behavior of the prosthesis (Fougner et al., 2012). Therefore, a large amount of different motions could be used for prosthesis control. But for now, only two to three DoFs can be reliably controlled (Ameri et al., 2014a,b,c; Hahne et al., 2014, 2015, 2012b; Huang et al., 2017; Hwang et al., 2017; Jiang et al., 2008). Regression allows the user to skip the separate and sequential control of different DoFs that classification proposes.

Hahne et al. (2014) compared different linear and non linear regression techniques for two DoFs control. These techniques include linear regression (LR), mixture of linear experts (ME), multilayer-perceptron, and kernel ridge regression (KRR). Results have shown that KRR outperformed the other regressors. But with a basic linearization in the feature space, simpler regressors as ME or LR were able to perform as well as KRR, showing

that simple linear models with the correct features are perfectly suitable for prosthesis control, increasing the efficiency of the model. It was also shown in the study how regressors were able to generalize for DoF combinations, where no training data was provided, proving their robustness against unknown situations for the model.

This more natural control was taken to a realistic manipulation scenario by Strazzulla et al. (2017). They were able to control two robotic arms that had ten independent DoFs between both, using a linear regressor for each DoF. With them they controlled the torque and force for each of the motors. The learning models were based on incremental ridge regression with random Fourier features. They achieved a completion rate of 95% of single-handed tasks and 84% of bimanual tasks.

Another very common regression approach is the support vector machine regression-based (rSVM). Ameri et al. (2019) compared this regressor to a new regression convolutional network (rCNN). Regressors showed advantage over previous CNN classification studies facing independent simultaneous control of motions. Furthermore, the ability of the rCNN to extract underlying motor information in the EMG with no need for feature selection was presented as an advantage over rSVM and an option to solve robustness issues.

In regression control, there have been two strategies. One can either control the position (Hahne et al., 2015, 2017) or the velocity (Ameri et al., 2019; Hwang et al., 2017; Smith et al., 2016) of movement. Those two approaches were hard coded and fix i.e, they lack the ability to adapt continuously. In Chapter 4 we present a new controller that overcomes this limitation. In fact, we show there that these state of the art regression methods can be seen as particular cases od the proposed new one. This was the first adaptive strategy to directly learn proportional velocity control. The machine is who learns one protocol or the other, depending on the user's actions. The studies showed a clear trend to velocity control. This option seems to be more natural to the user and has a number of benefits in practice (Engeberg et al., 2008) such as less overall effort and no limitations on range of motion.

2.3.3 Feedback

Biological myoelectric control does not only consist of the brain activating a muscle in order to control a limb. A fundamental feature of our motor apparatus is a highly efficient sensory feedback system. In a human hand, this feedback carries information about its position, the pressure it is applying on something or even the stretch level of its tendons. Without sensory feedback, a prosthesis will keep being a simple tool with no possibilities of completely replace a missing limb.

Therefore, after generating the data and learning a prediction model, feedback is the last element of the state-of-the-art closed loop structure. Feedback increases the efficiency of the learning process. It is shown that, providing feedback to the user, the movement can be intuitively corrected by him. Problems appearing in the model learning process as estimation errors and poor robustness in changing conditions can be avoided with an appropriate feedback. This also will help to avoid local minimum solutions and give the user the ability to interact with the system when the output is not the desired.

There have been different approaches through time. One way of generating feedback and replacing the affected limb was bilateral mirror training (Muceli and Farina, 2012). The user is asked to perform the desired movement with both arms. Nielsen et al. (2011) used this to generate data to control the force and torque of the affected limb. Executing the task with the complete limb helps the user to reproduce the movement on the other side while EMG generation is not as easy. In the same study, they also proved that by generating both signals at the same time models in one limb are also suitable for the other limb. They recorded data of the force and torque in the healthy limb and generated a model to control those outputs with the EMGs. Then, they applied that model to the other limb so force and torque could be controlled with its own EMGs. Ameri et al. (2012, 2014c) used the same training procedure to also help the user and to mirror the recorded data of the intact limb to the phantom limb.

This feedback method is natural but it is not functional for bilateral amputees, where there is no intact limb to measure from. So, Ameri et al. (2014a) proposed a virtual visual feedback. With this approach, the system generates a visual representation of the users' performance. It is essential that the users understand the meaning of the visual feedback. The higher the relationship between the visual representation and the realistic movement, the easier the comprehension for the participants. Virtually showing the users' output has been the most common feedback used by researchers. Users can control cursors

as in Figure 2.3a (Ameri et al., 2014a,b,c; Fang et al., 2017; Hahne et al., 2015; Hochberg et al., 2006) or even virtual prostheses. Powell et al. (2014) developed a virtual prosthesis that executed the system's output for the user's intent. Then, the user was able to compare that to the desired output and try to correct it if necessary.

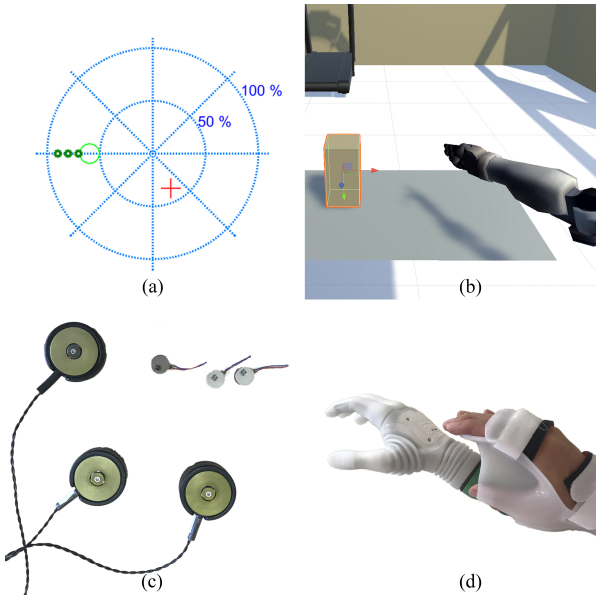

Figure 2.3: Common used feedbacks. (a) Visual interface representing the model estimation output as a red cross and the target as a green circle; (b) Virtual Reality environment to perform upper limb prosthesis control tasks; (c) Vibrotactors used to provide sensory-motor feedback to the user; (d) An actual prosthesis with two degrees of freedom and changeable grasp type used by an able-bodied participant.

The next level of visual feedback came with Virtual Reality (VR) (Figure 2.3b) (Ison et al., 2016). This allows the user to train in a realistic environment where the patient can use the prosthesis as it is going to be used in real life. The user sees how the prosthesis will react to the inputs and can adjust the behavior in a more realistic way, which helps to the user's acceptance and adaptation.

Another class of feedback is based on mechanical communication. This looks for generating some kind of non visual stimulation in the user. Peerdeman et al. (2011) developed a study among prosthesis users to find out which were their needs. The need for a proper environmental feedback was one of the main request that users had in common. They found that an implementation of a

proper environmental feedback system that helps them control the prosthesis and interact with its surroundings is extremely important.

On the one side, non-invasive methods, as vibrotactors (Figure 2.3c), are easily introduced into the prosthesis (Guémann et al., 2018; Thomas et al., 2019). On the other side, invasive electrodes directly innervating the nerves might simulate human sensory feedback to a much higher degree. Markovic et al. (2018b) showed that providing non-invasive feedback in form of vibrations on the remaining stump, subjects were able to scale the force of their prostheses better.

2.3.4 Human adaptation

The machine is not the only learner in the control system. Humans have to learn how to use the system in order to generate more stable and consistent signals. Practice makes the human a better user, therefore, everything that helps the human to adapt to the system will increase the system's performance (Radhakrishnan et al., 2008). Ison et al. (2016) proved that these learning skills positively influence the system. Human learning is consistent with the stages of typical motor skill learning for new tasks. First, it requires gathering a lot of information. Then, with repetition, the user starts to understand the task and gets used to it. Finally, the task becomes autonomous. The effects of this human adaptation were also described by Strazzulla et al. (2017). Experienced users (the ones familiar with the experimental setup) needed less time to complete the tasks while naive subjects were much slower. The completion rates were similar for both groups of patients which made the researchers conclude that it was not a machine effect, but a human effect. Expert users were more adapted to the system so had a more efficient behaviour.

The data can be collected offline and used to train the model. Afterwards, the user gets online control creating a closed loop with a fixed algorithm. This online control has shown improvement with respect to its offline counterpart (Hwang et al., 2017; Vidovic et al., 2015; Zhu et al., 2017). They found out that including the user into the learning loop and allowing him to interact in real-time helps to solve problems like arm position change or other non-stationary situations. The real-time feedback the user receives allows him to overcome the impact of interference and to interact with the system instantaneously. Hahne et al. (2017) added noise to the EMG signals to test how regression and classification methods behaved. Results exhibit that in online control experiments the user was more capable to compensate these

external disturbances and that this ability was better for regression than for classification, due to the continuous feedback regression offers.

The data can also be collected, and the model trained, online. Therewith, the user becomes part of the closed loop while the algorithm is adapting, giving him the ability to interact with the machine learning process (Betthauser et al., 2018; Nishikawa et al., 2001). This leads to the concept of co-adaptation studied in Chapter 3.

2.4 Usability

While the research and prototype models are continuously upgraded, the transfer into commercial prostheses is still limited. The great majority of prostheses are still fit with simple two-electrode systems without machine learning and only two simple classification-based controllers that do not allow for simultaneous motions are on the market (*Coapt Engineering Website* 2020; *Ottobock Website* 2020). Newer and better models have been developed, but these control schemes do not have a consistent performance in non controlled environments yet. With the first tests of the algorithms in clinical situations a lot of problems that were not being taken into account appeared. So far the models relied on the EMG used to train, but with time, those EMG signals showed a non stationary behaviour. This has been related to electrode shifting (Ison et al., 2016), fatigue (Huang et al., 2017), donning/doffing (Hwang et al., 2017), arm position (Betthauser et al., 2018; Fougner et al., 2011), etc. Researchers had to overcome this situation to get a decent level of functionality for real life activities with more robust and stable systems, especially when user motivation and emotions must be taken into account.

One of the proposed solutions is the use of re-training or re-calibration (Zhu et al., 2017). The idea is to add a small amount of data that represents the untrained conditions to the training set. Chen et al. (2013) also used this technique. Adding the data used for the test to the training set once the data was labeled correctly during the testing phase, improved the classification process. Increasing the amount of training data helps to deal with unknown inputs. Yeung et al. (2019) proposed a new re-training system, in which depending on the new data added to the training set specific old data was erased. This directional forgetting deleted old data that was in the same direction that the new one added. So, this updating process of the direction induced less distortion to each region, while discarding training data that was obsolete.

Re-training is used in order to correct system's performance degradation. However, with the development of newer and more robust models the re-training needs have been minimized (Hahne et al., 2018). Nevertheless, on the basis of this concept, the transfer learning protocol was developed (Ameri et al., 2019; Paaßen et al., 2018). Researchers saw that different tasks or movements had some relation between them (Braun et al., 2010). After having learned a task or a movement, they realized that there are associated movements that can take advantage of the previous task's model. Some tasks are similar to others, so the base of the information is related. This allows to, instead of re-training the entire system for a new move, learn new motion models using the previous data and adding a small amount of new data to overcome the differences. It can also be used when the data had suffered greater changes, so that the fundamental information is the same but the old model does not work. Paaßen et al. (2018) used the transfer learning concept instead of re-learning a new model, re-using an old version and adapting it to the new situation.

Long term use is also a problem for prosthesis control. Users have to wear the prosthesis during several hours during the day and the control has to be stable. Initially, this was associated with less efficient re-training protocols that were needed frequently (Sensinger et al., 2009). Re-training, however, has been developed into more efficient ones (Vidovic et al., 2015; Zhu et al., 2017). Additionally, models have been developed taking this undesired needs in consideration, trying to avoid them. That is why some studies have focused on the long term use of their models (Powell et al., 2014; Vidovic et al., 2015) achieving models that perform properly during 8 hours without re-training. These training protocols usually take several days, where in different days the model is trained to learn the non-stationarities that time and fatigue could generate in the EMGs. At the end, users want to re-train as fast (better re-training methods) and as less (long term stability) as possible.

Once the models improve their robustness against the possible non-stationarities of EMG data, it is interesting to see how they perform in real life tasks using prosthesis (Figure 2.3d). Daily life will challenge prosthesis control to perform tasks that have not been considered in a lab environment. Testing the control in tasks like the Clothespin Relocation Test (Hahne et al., 2018) and holding and grasping objects (Castellini and Van der Smagt, 2009; Strazzulla et al., 2017). These tasks represent a more realistic performance of what the end user will experience. Results showed that the academic algorithms that outperformed the commercial ones in lab environments are reducing the gap in usability terms with the industry. Some of them even started to outperform

the commercial algorithms in daily life applications. In Chapter 6 we test the robustness of the new controller in this kind of scenarios.

2.5 Open problems

Hitherto, the ultimate goal to fully replace a human limb is far from being reached and more deep knowledge about neural and behavioral changes that result from amputation is mandatory (Wheaton, 2017). However, the field of prosthesis control has been constantly growing for the last decades. Great advantages have been achieved recently and the rate of improvement seems to constantly grow. As we have seen, despite the major goal of reaching high functionality, some of the advancements in academia have not reached the industry due to a lack of robustness and usability. Thus, some newer proposals, the prosthetic technology could benefit from, are not appropriate for a daily use. Therewith, giving the user a more natural control that comes closer to the way an intact hand is actuated and a better evaluation of device adaptation, utility, and motor learning is to remain an essential objective.

Some recent classification systems are being used by some prosthetic devices, applying sequential control, which is far from being an accurate implementation of a biological limb behavior. Overall, the new developed learning models achieve great results in laboratory environments but they do not reach the commercial use. This is due a lack of robustness and overcoming non-stationarities that appear in a real-life use. Reducing this functionality problem has become the focus of the recent years with promising results. Users have to deal with systems that are very distant to offer a natural limb condition with antiquated one DoF control in a switching-between-functions system. New studies are starting to propose more natural controls (Amsuess et al., 2015b; Kuiken et al., 2016; Velliste et al., 2008). Consequently, regressors need to be improved to develop a robust control in more than two to three DoFs, to be able to be implemented into commercial prostheses. Alternatively, instead of using classification or regression by their own, a merger of both systems could be favorable. With this system, the benefits of one method could be used to overcome the limitations of the other. This idea is the focus of some ongoing studies. Being there yet no perfect learning model, a mixed model of classification and regression seems to be a good proposal (Amsuess et al., 2015b).

Feedback implementation is another of the main open and active fields. How to integrate the user into the system seems to be one of the keys to improve

prosthesis control and give a more suitable handling to the user. Able-bodies with intact limbs are provided with several feedback information: touch, vision, pressure, etc. Therefore, as a next step, it is necessary that these information gathered by the sensors of the prosthesis become accessible for the users, to get closer to the functionality of a biological limb. Nowadays, actual prostheses are mostly limited to intrinsic visual and acoustic feedback, available by observation of the prosthesis and sounds of the motors, therefore, the implementation of all other kinds of feedback has to be further investigated, as it is the case for vibrotactors or pressure (Markovic et al., 2018a). This will increase the acceptance of the prosthesis with the corresponding positive effects.

The computational power required by the new systems are higher than the ones actually used in commercial prostheses. In terms of hardware, the use of complex features, models, the control of multiple DoFs and the implementation of feedback requires high computational resources (Dargazany et al., 2019). For some of the proposed features, it is still to be shown whether they can be computed on a minimalist low-power hardware within the short time available in order to meet real-time constraints. Some examples of complex systems working in real time using computer front-ends are (Ameri et al., 2019, 2014b). Furthermore, some other of the novel models have been tested in embedded systems proving their capability to achieve the desired performance and overcoming the technological limitations (Hahne et al., 2018; Kuiken et al., 2016), but they are still under development.

Currently, the market of upper limb prostheses is relatively small. Therefore, development becomes slow and expensive. However, the prosthetic industry can take advantage of additional new emerging technologies and benefit from the fast developments such as the smartphone sector, intelligent robotics and other consumer and industry sectors. Prostheses could take advantage of the fast growing 3D printing field lowering manufacturing cost (Dargazany et al., 2019; Silva et al., 2015). The computational capabilities of low-power processors is constantly increasing, pushed in part by the large smart device market. This situation will help to generate new embedded systems, suitable for prosthesis control. Furthermore, Internet-of-Things (Farahani et al., 2018; Hiremath et al., 2014; LeMoyne, 2016; Li et al., 2019) or 5G (Wubben et al., 2014) could rise as a possible solution, using e.g., real-time cloud computing to withdraw the high computational requirements from the device. These new technologies allow the integration of new processing protocols such as data fusion. Cloud computing could be used to collect data from different users generating larger datasets. The use of this datasets to extract common

information between patients could improve the model's performance and adaptability. This can be understood as a transfer learning process between different users.

Prostheses have to be adapted to the significant variability in the population of users (Cordella et al., 2016). This variability demands to the prosthesis control to be usable in a wide range of physiological conditions. Moreover, prostheses have to be simple, in order to be configured by a non-signal processing expert such as orthopaedic technicians. The end user needs to have an easy usable prosthesis and he has to be able to understand how to use it without help. A simple user learning is necessary to reach a wider population. Complicated learning processes of the prosthesis control will not be suitable for beginners who could quit under the difficulty and consider it as not useful. The systems have to be accessible for everyone and not only for advanced users. So, working on the final training protocol and the setup of the prosthesis to make it as easy as possible, even using complex models, is a future task for the research community.

Lastly, one of the biggest problems is that most models have been tested extensively in controlled environments but the prove for robustness under the non-stationary conditions of daily life is often missing. This needs to be reflected in the evaluation procedures, that should include factors such as fatigue, arm positioning, sweat and long time use. The final proof of robustness has to be conducted in the daily life of the end users, revealing the need for large scale tests in clinical environments.

Chapter 3

User-prosthesis co-adaptation

Machine and human are capable of learning. But so far, each agent learns for its own interest. Making them co-operate and learn in the behalf of the whole system is what has been recently named as co-adaptation. The different agents have an online learning focusing on the same goal in order to maximize the model performance. In this case there will be two learners: human and machine. Co-adaptation also allows simpler algorithms to obtain high performance.

Chapter based on **Igual, C.**, Igual, J., Hahne, J. M. and Nazarpour, K. (2021). 'User-prosthesis co-adaptation' in Nazarpour, K. (ed.) Control of Prosthetic Hands: Challenges and Emerging Avenues (Healthcare Technologies). London: *Institution of Engineering & Technology*, pp. 159-174.

Contents

3.1 Introduction

In the early stages of myoelectric control for upper limb prostheses, researchers focused on obtaining the a more efficient model for the prosthesis control (Figure 3.1) (Englehart and Hudgins, 2003; Huang et al., 2005; Karlik et al., 2003; Kelly et al., 1990; Nazarpour et al., 2014; Parker et al., 2006). The focus was on the fast growing machine-learning field, where a wide range of potential methods were available. Having already developed machine-learning models in other areas leads to an accelerated evolution of the research in the prosthetic field. A broad variety of algorithms were applied to estimate the user's intent in upper limb movements among others. High-performance models were generated facing the task with completely different perspectives not finding a unique solution for the problem (Ameri et al., 2014a; Castellini and Van der Smagt, 2009; Hochberg et al., 2006). Despite these promising results and the newer developments of more complex and powerful algorithms, the older and simpler models remained as the main option for the prostheses control. A clear example of this is the most commonly used control protocol for commercial prosthesis: a basic one degree of freedom (DoF) control switching system. The machine-learning developments have so far not succeeded to replace the conventional 2-channel systems in a large scale. Even if these approaches presented an excellent behavior in controlled and specific environments, migrating to the real world has become a challenging task. In daily use, reliability of machine-learning modes remains an issue and regular re-calibration may be required for some users. These first approaches were considering the machine as the only agent that could learn. But the machine's learning is not the only factor that can be used to improve the overall system's performance, the user's learning can be integrated too.

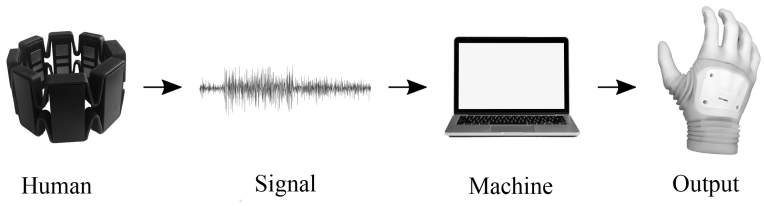

Figure 3.1: Generic prosthesis control scheme. The human patterns are used as input (in this case EMG signals extracted form an armband) by the machine to estimate an output (applied to a prosthesis or in a virtual environment) of the user's attempted action.

Originally, the models were mainly developed via off-line investigations (Hahne et al., 2012b; Jiang et al., 2008; Nazarpour et al., 2007; Nielsen et al., 2011).

The data was previously recorded and then the model was trained and tested in an off-line scenario. The machine and the participant did not interact in those phases. The two agents of the process were completely separated. Later on, the researchers realized that while testing the algorithms on-line (Ison et al., 2016), the users were able to correct behaviors where the machine was failing in the off-line evaluation. The reason on-line tests were outperforming off-line protocols was the human adaptation (Dyson et al., 2018, 2020; Ghazaei et al., 2017; Hahne et al., 2017; Krasoulis and Nazarpour, 2020; Krasoulis et al., 2019a,b; Pistohl et al., 2013, 2014; Radhakrishnan et al., 2008; Strazzulla et al., 2017). The human modified their behavior to compensate errors induced by the machine or by external perturbation. Because of the real-time feedback, the user could adapt to the machine's behavior. From here, human adaptation has been considered an essential element of the closed-loop structure learning and a powerful tool for improving the system's performance. Two learners were participating in the learning process: the machine and the human. The common, but not necessary, way to make the user interact with the machine was during the test phase once the model was learned. All along the learning process the user and the machine remained separated. The users were meant to perform the requested signals during a data acquisition period. Afterward, the machine was being trained with the recorded data. The user did not play any active role in the process of learning the model and that was only machine learning. Human learning was adapting the human behavior to the previously learned model with the goal of achieving the highest performance possible during the test. On-line studies allowed the users to adapt to the systems' output and correct the EMG signals they were generating in order to achieve the desired target. This improved the systems' performance but the gap between the academia and the industry remained significant.

Seeking to boost the benefits of human–machine interaction, some groups tried including the user as an adaptive agent into the model learning phase as well (Dyson et al., 2020; Hahne et al., 2015). These first trials triggered the concept of co-adaptation. The essence is that both agents adapt at the same time with a common goal of helping each other to learn the optimal model. Before getting deeper in the co-adaptation benefits, it is necessary to identify the role each learner plays in the learning process so we can understand the interaction between them.

3.2 Machine adaptation

We will focus our attention on the machine's learning process first. The objective for the machine here is to learn the underlying information of the data used as input. Since the beginning, it is necessary to define which kind of information we want the machine to understand and learn. The models are divided into two approaches: classification (Castellini and Van der Smagt, 2009; Krasoulis et al., 2019b; Rahimi et al., 2016; Spanias et al., 2015) and regression (Ameri et al., 2014c; Fang et al., 2017; Guémann et al., 2018; Hochberg et al., 2006; Krasoulis and Nazarpour, 2020; Krasoulis et al., 2019a; Markovic et al., 2018b; Thomas et al., 2019). The difference relies on the system's output: a label to tag the input data in a class (classification) or a continuous mapping of the output (regression). However, for our interests both approaches follow the same learning procedure.

As it is shown in Figure 3.2, the initial step is to feed the system with the input data that forms the base for the variables the machine should estimate. A proper choice of input variables is crucial for the system's performance. If the data is not appropriate, the machine will not be able to learn what is desired. We will go deeper in this later as it involves the human also. For now, the goal is to understand the learning that both learners go through individually.

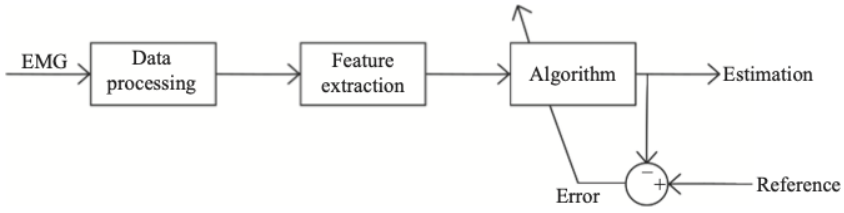

Figure 3.2: Example of a machine-learning process. EMG's signals are used as input for feature extraction. The features are used to train an adaptive model with an error-based cost function.

Once the data acquisition is complete, features are extracted in a block-wise manner (Oskoei and Hu, 2007). Features will then be the input for the learning algorithm. Feature extraction isolates meaningful information from the input data and simplifies the learning task for the machine, discarding irrelevant information. The executed patterns should correspond to features as independent as possible for different motions, so the model is capable of differentiating them.

During algorithmic training, the machine receives the data and forms a model to estimate the output. In the case of myoelectric control, this is to extract the user intend from the EMG features. Depending on the complexity of the machine learner, the provided repetitions for each of the contraction patterns need to be consistent within each class and separable across different classes. Similar constraints apply in the case of regression. The number of independent patterns the user is able to generate in a repetitive way determines the maximal number of functions or DoFs that can be controlled.

This could be a limitation for some users because of their limb deficiencies. The physiology of the stump could limit the capability of generating enough EMG patterns (Cordella et al., 2016). Algorithms that work with multiple DoFs in able-bodied have also to be tested in amputees for this reason. The system's final goal is to achieve a natural and proportional control of multiple DoFs. Usually commercial devices can control only one DoF at a time without any machine-learning program. The selection of the DoF is done with an activation function that allows the user to switch between DoFs. The output value depends on a metric extracted from the EMGs as it could be the amplitude of the signal. Obviously, this mapping is not natural and requires long training sessions for the user to learn how to control the prosthesis. Due to the non-learning protocols, all the adaptation lies on the human. With the newer machine-learning models, it has been tried to learn the underlying correlations between the EMG signals and the movement generated (Sartori et al., 2018). This gives the prosthesis control a more natural movement and intuitive relation with the signals. The similarities with a real hand are higher, due to the machine's ability to learn. The modeling of EMG-movement relationship helps the user to learn a more intuitive control.

3.3 Human adaptation

Now we will move on to the second agent of the learning process, the human. Humans can adapt their behavior to achieve a better performance. Ison et al. (2016) studied the human-learning skills and their effects on the final system's performance. Like in every task, the user is able through practice to improve their results with a fixed model (Dyson et al., 2018; Radhakrishnan et al., 2008) and become more stable and consistent in the signal generation. Recently, studies focused on finding the right tools to help the user understand the system's output and interact with it. The comprehension of the system would make the human adaptation process more efficient (Powell et al., 2014). Complex environments where the user does not understand the given feedback

would not allow them to learn and adapt. Because of this, finding the best feedback to exploit the benefits of human adaptation and improving the user experience has gained relevance in recent years.

As expected, the human-learning process seen in prosthesis control follows the stages of a typical motor skill learning for a new task. The first step is to understand the general remit of the task but not necessarily the details. This understanding is achieved through repetition and practice where an appropriate feedback map would play a fundamental role (Dyson et al., 2018, 2020; Jiang et al., 2012; Pistohl et al., 2013). Finally, once the user builds the appropriate internal model, they can perform the task (in this case controlling the prosthesis) readily. At this point, the user has learned and performs significantly better than during the first trials due to the experience gained. Strazzulla et al. (2017) proved the hypothesis of how experienced users outperform amateurs. The difference between the two groups was not in the accuracy metric, both were able to complete the task. The difference was on the time metrics, experienced users completed the target faster than amateurs. Their experience made them aware of the shortest strategies to reach the target so they performed it straight way. Opposite to this, the amateurs that did not have any experience had to search for an optimal strategy before executing the task. Being the completion time, the main difference between both groups' performances (and not the completion ratio) made the researchers set the cause in the human adaptation and not the machine-learning process. The larger experience of more experienced users was translated into a more efficient behavior.

The initial idea of taking advantage of human adaptation was conducting an on-line prosthesis control test (Hwang et al., 2017). The fixed model learned with the user's EMGs is tested in real time, giving the control to the participant. The on-line control with feedback to the human created a closed-loop structure as in Figure 3.3. The feedback of the machine's output could be used by the human to adapt their behavior to the machine improving the system's performance with respect to the previous off-line proposals (Vidovic et al., 2015; Zhu et al., 2017). Human adaptation is able to solve some robustness issues that prostheses users were facing in experimental applications due to the nonstationary EMG signals. Due to the given feedback, the user is able to correct their contraction pattern and compensate potential disturbances. This user real-time reaction was tested by Hahne et al. (2017). They conducted an experiment adding noise to the EMG signals and testing on-line the capability of the user of maintaining a stable control. The results showed that the noise disturbances were countered successfully. Comparing a classification algorithm

against a regression method, the regression had a better performance due to the continuous output. This study proved that with the right feedback, the user can understand the process and adapt properly to unstable situations avoiding degradation in the system's behavior.

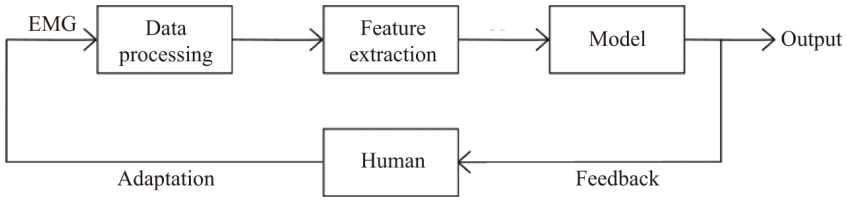

Figure 3.3: Closed-loop structure. The output of the machine generates the input of the human and vice versa.

3.4 Re-calibration

As we have said, sometimes the user is able to counter some undesired effects of the non-stationarities. However, what human adaptation can overcome has its limits and in other occasions the user cannot succeed in dealing with the system's degradation. There can be multiple reasons for a model to stop performing as well as at the beginning: different sensor positioning (Hargrove et al., 2008a), EMG patterns that are not consistent through time (Betthauser et al., 2018; Huang et al., 2017), the user (Amsüss et al., 2013), etc. In these scenarios, the possibility of re-calibrating the model is a suitable solution (Zhu et al., 2017).

The idea of re-calibration is to retrain the model with new data in order to adapt it to the present, and probably new, conditions. The human is in constant adaptation using the system daily, leading to some modifications in their behavior. The patterns the user ends up using could not be the same with the ones used for training the model. After some time, the machine could need to go through an adaptive process if we want the system to stay functional. With re-calibration, what we try to achieve is to adapt the machine to the EMGs that the human is using after some time since the model was trained.

During this period, the user has been adapting, while the machine remained invariant (human adaptation). The user has been the one taking all the responsibilities to overcome the possible degradation effects. The prosthesis user wants an easy control, so at some point the user efforts could not be enough to deal with degradation, or simply generate an undesired user experience

because the great efforts needed. This is the moment when re-calibration should be implemented. We have to be aware that this need could be dependent on the user; if the user is comfortable with the behavior or he prefers to stay with the current model, the re-calibration will not be necessary. The process will teach the machine some part of the adaptation the user has gone through and readjust their behavior to the present EMG spectrum input. The machine will now be aware of the new conditions and release the user of the needs to force their behavior to achieve a desired performance. With this, we will be updating the machine learning including in their training data the new user knowledge generated with the adaptation. Both agents have adapted independently in different occasions, and with the re-calibration we merge both adaptation processes in one common retraining. This could be seen as restarting the process again, but not from scratch. Now the machine and the user have a lot of experience (the initial training data for the machine and all the user adaptation process for the human). Both have gone through a first adaptation process and the cycle would be repeated; the machine will update its learned model and after that the user would re-adapt to it. However, these new adaptation phases will be shorter as the new information or changes are less different compared to the initial step. The active learner will become the frozen one when the other agent goes under their adaptation process. The agents will be switching their roles through time as the re-calibration phases are executed.

The re-calibration process can be executed in a wide range of different protocols (example in Figure 3.4). At the beginning, the first approaches were using a more frequent re-calibration (Sensinger et al., 2009). Trying to reduce these

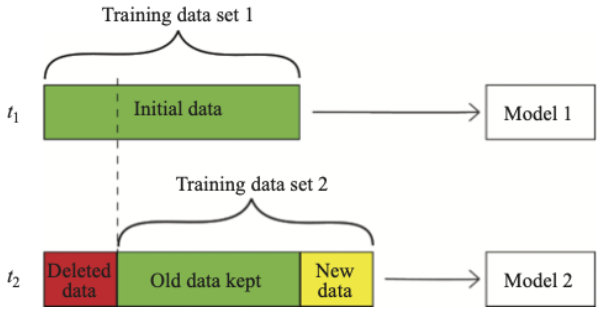

Figure 3.4: Example of a re-calibration protocol. Initial data is recorded in t_1 for training the model 1. After some time, in t_2 new data is recorded (yellow). A new training set is configured with the new data and a high percentage of the old data that is kept (green). The oldest (or outdated) data from t_1 will be deleted (red).

times, researchers kept developing new ideas until they reached more efficient paradigms (Vidovic et al., 2015; Zhu et al., 2017). To represent the untrained conditions and add them to the training set, Chen et al. (2013) proposed a training data set expansion during the test. Once the test data was labeled correctly, it was added to the training data set. This procedure was reinforcing the correct labeled data for each cluster trying to reduce the weight of the data that could be leading to misclassification. Expanding the training set proved to have benefits against shorter data sets, so the idea was to increase it with the test data and re-calibrate the system with the expanded training set. Yeung et al. (2019) proposed a similar method but with a directional paradigm. As newer data was being added to the training set, and older data with similar information was being erased. With this, they reduced the distortion to each region generated by redundant and outdated data while updating the training set. The data erased was obsolete as the newer data represented the same condition in a recent situation. The model was receiving the new data representing something already learned that had undergone some small changes. These small changes could not be a problem yet, but in the long run it could end in a poor performance. With re-calibration, we are looking to update the system to the present and forget about the past representations.

What all methods have in common is the general concept of re-calibration, adding new data to the training set and updating the model to the newest EMG patterns and disturbances. However, it would be ideal that the system does not need re-calibration at all (Hahne et al., 2018). The system should be robust enough to deal with disturbances from the outside and keep their performance stable. The user also does not want to spend their time re-calibrating the system very often. Therefore, the re-calibration process has to be as fast as possible and requires less time as possible to be usable.

While researchers experimented with re-calibration, based on this, the concept of transfer learning emerged (Ameri et al., 2019; Paaßen et al., 2018). The basic concept of transfer learning is that the outdated data (and model) from a task is still usable to update the model to a current state. Because the differences between the past and the present will be small and the basic information carried by the EMG patterns are the same; only a small amount of data will be necessary to update the small changes in the task through time. In this case, we are retraining the model in the same task but in different times succeeding in keeping the high performance. Moreover, researchers found out that the task does not need to be the same to take advantage of previously recorded data. There is underlying information that is shared among similar tasks (Braun et al., 2010). This is similar to the idea of structural learning in the motor control

community. Structural learning advocates that humans can learn the general structures of a task and then generalize it to other tasks that are related in some base level. So instead of re-calibrating for the same function, we could use a similar protocol to learn a new task faster. If there are similar tasks, we could use the data and the model of the previously learned one to learn a new task adding only a small amount of data that represents the differences and updating the previous model. Paaßen et al. (2018) used this concept to adapt an old myoelectric control model to a new situation where the data was completely obsolete.

3.5 Co-adaptive prosthesis control

Now as we studied both learners, we can look for the opportunities to combine their adaptation processes in one. In the on-line tests, the human is able to adapt his behavior with the objective of reducing the difference between the estimated and the desired output. The human has the opportunity to interact with the machine to achieve the best possible performance. However, in this phase the machine is fixed, it is not adapting, and all the adaptation is being performed by the user. The on-line condition during the test gives the user the possibility of adapting, while the machine had adapted during the model training. The first natural approach for co-adaptive systems was to merge both concepts in one, a complete on-line experimentation, training and test (Betthauser et al., 2018; Nishikawa et al., 2001). The model is trained at the same time the data is collected, all executed in real time. This closed-loop learning structure gives the two learners, user and machine, influence over the other's learning. This was the beginning of co-adaptive systems.

Before co-adaptive models, it was obvious that both agents were going through a learning process but separately. Besides, they were learning for their own interest. The data from the other agent was being used as input to adapt and perform as good as possible without considering the other's adaptation process. With the new proposal, the learning becomes cooperative. The co-adaptive training makes both agents focus on the same goal: to optimize the model. However, for that purpose they have to take into account all the variables including the other agent adaptation. Now that both agents adapt at the same time, each of them can react in real time to the other's adaptation and its consequences. So, instead of having one agent learning while the other is off, here both have to adapt to the previously learned situation, as before, but now it also adapts to the new behaviors the other part is adopting. This

procedure allowed simpler algorithms to obtain a higher performance avoiding some problems that are present with off-line training (Hahne et al., 2015).

The co-adaptation inkling is the common goal for both the learners. The essence is making them work together in order to learn the best model (Müller et al., 2017). The novelty relies in that each part does not only adapt to different situations with a prefixed answer. Now the other part adaptation has to be taken into account too. So, for adapting each learner does not only have to think in how it should react to an undesired performance but it also has to consider how the other will echo to your new reaction because its behavior is not fixed. The human learning shapes the machine's behavior and vice versa.

The feedback has a great importance in the human learning (Fang et al., 2017), but it acquires a higher impact in co-adaptive systems. The channels of information between human and machine have to send clear information to the receiver about the transmitter actions. The EMG patterns, which are used by the machine as input, have to be consistent. The same targets need to have similar EMG patterns for the model to be robust. At the same time, the displayed output of the machine has to be clear for the user as it is his/her input data for the adaptive process. If the user does not understand the meaning of the feedback, he/she is not capable to perform consistent EMG patterns or the required correction. His/her misunderstanding of the information would probably lead to a poor model with an undesired behavior. Because of the on-line training and the real-time adaptation of both learners, their inputs would be constantly adapting as well as their outputs. The adaptation of one side will be the input for the adaptation of the other side. This potential continuous adaptation was ignored for a long time in the prostheses control research.

The two-learners problem was modeled by Müller et al. (2017). The model describes that the system has two channels of information as in Figure 3.5. The first one goes from the human to the machine. The human sends the myoelectric signals that the machine takes as representation of the user's intent. This channel (human–machine) was developed widely with the evolution of the machine-learning algorithms as we commented earlier. The objective is to decode the encoded information in the EMGs through the machine-learning process. The second channel goes the other way around, from the machine to the user. Here is where the feedback system plays its part. The human receives information about the machine's output through this channel that represents the machine's estimation of the user's intent. This feedback is meant to provide data to the user to make him aware of the machine's behavior. The user has an expectation of the machine's behavior, so with the feedback they can evaluate whether there is a need for adaptation or not. The understanding

of this data provides the user the knowledge to change his/her own behavior in order to correct the possible undesired actions. In the end, both channels could be represented by learning coefficients that would define the system's performance. Both the adaptation processes have an effect on the general cost function. The first experiments showed promising results for prostheses control (Hahne et al., 2015). With co-adaptive algorithms, the user tries to minimize the error adapting him/herself with the real-time feedback he/she is receiving about what the machine is understanding from his/her attempts. With this information, the user can search for the signals that generate the desired output. At the same time, the machine knows what the target is and which EMGs the user is generating so it adapts its coefficients to get closer to the target with those EMGs. This co-adaptive process continues through the whole training. Once the training is over, the system has converged to a common solution between the two agents. With this paradigm and interaction, when one of the sides is converging to a local minimum, the other side adaptation could force to avoid this situation and keep searching for a better solution. If the user is not contented with the machine model, he/she could keep varying the inputs trying to make the machine react and achieve a better performance. The novelty is that instead of a two-phase process, now those coefficients are updated at the same time in one phase. Therefore, the evolution of the cost function would be different than in a two-step paradigm leading to different solutions.

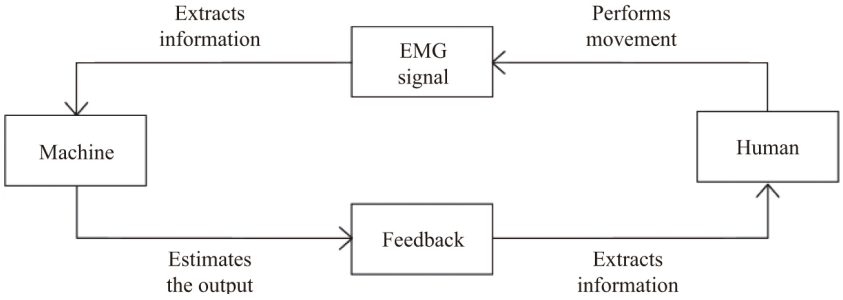

Figure 3.5: Co-adaptation scheme. The human receives the machine's output through some sort of feedback (sensor, visual or a prosthesis) and reacts according to the feedback. He will generate the desired EMG patterns to achieve the target and send them to the machine.

For all these reasons, the experimentation should shift from off-line to on-line. The real-time reactions allowed in on-line experimentation would lead to faster adaptive systems with simpler models performing with high accuracy. In next chapter we introduce an algorithm that is based on this co-adaptive idea.

The co-adaptive system overcame a strong barrier in users with limb deficiencies using more developed algorithms that include multiple DoFs. It is not easy for them to generate combined movements without any kind of feedback that allows them to reproduce the pattern consistently. Also it can be stated that the co-adaptive learning allows a simple regression model to outperform the state-of-the-art regression controls. As a result of co-adaptive learning and the simplicity of the algorithm, the computational time is reduced compared to more complex state-of-the-art methods.

Couraud et al. (2018) also studied the effects of co-adaptation in the field of myoelectric control. They designed a model of human adaptation and performed different levels of co-adaptation. With a gain parameter (setting a value of 1 as fast human adaptation) they controlled the speed of the human model adaptation to the data. Low adaptation gain values generated a model too slow to perform a full adaptation and high values were too unstable to adapt to the added noise. At the end, the best solution was a variable gain system combining the benefits of both.

3.6 Discussion

As we have seen, there are two potential learners in machine-learning-based prosthesis control systems. Depending on the structure defined for the control loop, the adaptation process will differ. The machine-learning process has been exploited since the introduction of it to this field. However, the human–machine adaptation was not as important as it is now. In the most recent studies, the human adaptation has shown significant influence in the system's performance and a great potential to be used as a solution to the most common obstacles. In these scenarios, co-adaptive systems raise as an option to take advantage of maximizing the benefits of both adaptation processes to overcome the difficulties. The co-adaptation idea lies in making the human and the machine learn simultaneously and dependently on the other's learning. These co-adaptive implementations have already allowed simple algorithms to present a robust and high performance against disturbances solving some of the most common problems among prostheses control algorithms. However, the commercial prostheses are still majorly controlled by old non-learning control protocols that do not allow the user to have a natural control of the hand. The reason is that these simple and old paradigms are still the most robust option. The academia has made great advances in the prostheses control algorithms, but the achievements have been only partly transferred into the industry. However, the research has shifted from very controlled environments to more

realistic conditions, which points the future research path. It is clear that the current goal is to improve the user experience. Advanced algorithms have been already developed with high performances. The challenge is to transfer these algorithms into real scenarios, reaching stable conditions in daily life. Here is where co-adaptive models could be a solution to close the gap between the academia and the industry.

The most important element in a real scenario are the users. At the end, they are the ones who will utilize the system, and their interests and opinions have to be taken into account. This is why the research is more focused in reaching the user than before. Having a high accuracy could not be as valuable as having a good user experience. That is one of the reasons why studies shifted to a more realistic experimentation trying to evaluate the real usability. The co-adaptation concept has the advantage that it incorporates the user in the training process and generates a shared experience between user and machine. The theoretical benefits of the co-adaptation systems have been already explained. But there are some qualitative benefits that the user experiences too. The process is now more personal and the user can feel how the machine learns with him. This relation makes the control more natural and intuitive as it is more similar to how humans learn to use their bodies. The idea at the end is to have a prosthesis that feels as similar as possible as a real hand. For this, it seems natural to involve the user as much as the machine during the training of the system. This will help the users to feel the control protocol as theirs and not as an external forced model. There are other reasons for the studies to shift to a more realistic experimentation, other elements that will be relevant for improving the user experience. The robustness of the prosthesis control is a clue element in the future of the field. A prosthesis has to be robust, not just to reach the market but also to have a high acceptance among the users. Users with limb deficiencies would rather not use a prosthesis and overcome their necessities in another way than using a prosthesis that does not make their lives easier. The ideal situation would be where the prosthesis reaction is always the one expected by the user.

The system has to have a robust behavior against the different disturbances the user will face during the time they are using the prosthesis. The electrodes will not be always placed in the same location, the EMG patterns will change for the same movement depending on the arm position, fatigue or other external conditions that will affect the system. The prosthesis cannot have an erratic behavior depending on external states unavoidable for the user. Thus, an optimal system should be usable in almost all common conditions with a high performance and not only in controlled environments. At the same time, the

easy use of the prosthesis is also important. Tedious training protocols and complicated control structures, in order to achieve a robust performance, are not a solution and will lead to rejection. The use of a prosthesis has to be intuitive and natural, and for this a clear communication between the two agents is essential. Here the training paradigms play a key role and researchers will have to give them the attention proportional to their high relevance in the final outcome. For this, it is essential that the training procedures are clear for the user so the learned model is consistent. Co-adaptive models are potential candidates to achieve these requisites. So the model is shaped by the user's learning and therefore by their comprehension of the system. These models will be then more logical for the own user and adapted to their way of understanding the control, increasing the final usability.

Chapter 4

Adaptive auto-regressive proportional myoelectric control

This chapter develops a co-adaptive controller for two-dimensional continuous wrist movement. The novelty lies in the use of adaptive auto-regressive moving average (ARMA) filters, which can in principle smoothly titrate between velocity and position control. The human-machine pairs learn to perform smoother cursor movements with a larger range of motion as compared to our previous efforts with moving-average (MA) filters. Importantly, the novel co-adaptation approach results in faster and more accurate movements with less muscle effort based on a more intuitive velocity control strategy. which is the likely cause of the performance gains.

Chapter based on **Igual, C.**, Igual, J., Hahne, J. M. and Parra, L. C. (2019). Adaptive Auto-Regressive Proportional Myoelectric Control. In *IEEE Trans. Neural Syst. Rehabil. Eng.*, vol. 27, nº. 2, pp. 314-322. JCR Impact factor: 3.34 (Q1).

Contents

4.1 Introduction

Electromyographic (EMG) signals are small electric potentials generated during muscle contractions (Merletti and Parker, 2004). They can be measured non-invasively on the surface of the skin. As their amplitude increases with increasing muscle force, EMG signals can be utilized for proportional control. In rehabilitation this is successfully used to control electrically powered hand and arm prostheses from EMG-signals of the residual muscles (Muzumdar, 2004). In conventional myoprostheses, two bipolar EMG-signals are placed on antagonistic muscle-groups, such as the wrist extensors and flexors, and are used to control the velocity of one degree of freedom (DOF) (Muzumdar, 2004). Extending this concept to more DOFs is usually not directly possible because typically not enough independent control signals are available. In commercially available prostheses, cumbersome switching concepts are used to control multiple functions sequentially.

Research efforts over the past decade have extracted more complex control information of a larger number of EMG-sensors with machine learning techniques (Oskoei and Hu, 2007; Parker et al., 2006; Peerdeman et al., 2011; Scheme and Englehart, 2011). Most work focused on classification-based approaches, which in its original form were still restricted to sequential on/off control of each individual function. Extensions of this work allow for a proportional control (Castellini and Van der Smagt, 2009) and combined activation of multiple functions (Young et al., 2013), but the highest flexibility is obtained by a continuous mapping of EMG features into control signals using regression techniques (Ameri et al., 2014a; Fougner et al., 2012; Hahne et al., 2014, 2018; Jiang et al., 2008; Muceli and Farina, 2012).

A challenge in most mapping algorithms is obtaining reliable labels for supervised training. While in able-bodied individuals the kinematics (Hahne et al., 2014; Muceli and Farina, 2012) or forces (Jiang et al., 2008), of the actual limb can be measured, in prosthetic end-users this is not possible. One approach is to perform bilateral mirrored contractions, but this implies certain errors and is limited to unilateral amputations (Nielsen et al., 2011). Alternatively, one may rely on visual cues given to the participants as targets under the assumption that participants can reliably follow these cues (Ameri et al., 2014a). However, "blindly" generating consistent muscle contractions is difficult and so here we provide real-time visual feedback to help participants follow a desired target movement. In this approach, both the user and the learning algorithm attempt to follow a common target, whereby humans adjusts muscle force in real-time and the machine simultaneously adapts its

control parameters. As a result, the human and the machine can in principle concurrently adapt to converge to a common control strategy.

The new algorithm proposed in this chapter extends the work done by Hahne et al. (2014) developing a more advanced control for continuous movements in 2D environments. We ask able-bodied participants to generate muscle contractions that result in 2D wrist movement (wrist flexion/extension, ulnar/radial deviation). Myoelectric activity is recorded from the forearm by a wearable armband. This activity is then used to predict an intended movement using a virtual target. Previously, it has been used linear regression to predict location from instantaneous EMG-amplitudes. With such linear proportional control, stronger muscle contractions lead to larger cursor displacements, i.e., muscle contractions control the position of the target (Hahne et al., 2014). The regressor was defined as:

$$\mathbf{y}(t) = \mathbf{B}(t)\mathbf{x}(t) \tag{4.1}$$

where $y(t)$ is the target position, $x(t)$ the EMG feature vector and $B(t)$ the linear transformation to be estimated. In position control, the position is maintained as long as the user maintains the muscle contraction. This can be tiring and would quickly cause fatigue when holding objects. Therefore, in most commercial prosthetic devices, the velocity is controlled proportionally to the EMG amplitude instead, i.e., the strength of the contraction controls the speed of movement. If the user relaxes, the prosthesis remains in the current position and an antagonistic contraction is required to revert the movement. However, because it is difficult to visually estimate and replicate the velocity of an object, training of regression algorithms by visual cues are typically done in a position control mode. In the current work we present a novel, more general control concept, that is not restricted to either position control or velocity control. The algorithm is capable of incorporating both control schemes including intermediate combinations of both. The goal is for the control strategy to emerge naturally from a closed-loop interaction of the human and machine, rather than imposing position or velocity control arbitrarily through the design.

4.2 Auto-regressive approach

Our approach is to explicitly use the current position to predict the next intended location. This leads to an auto-regressive predictor that is more flexible than either position or velocity control. To clarify the importance of using an auto-regressive filter consider the following. Denote the 2-dimensional position that we would like to control as $\mathbf{y}(t)$, and the M-dimensional myolectric control signal as $\mathbf{x}(t)$ (typically related to the EMG signal power). In its simplest form, proportional controls implies $\mathbf{y}(t) = \mathbf{B}\mathbf{x}(t)$ (ordinary linear regression), which is what it was implemented in (Hahne et al., 2014). To implement velocity control, the input has to be able to modify the difference of the current from the previous position, $\mathbf{y}(t)-\mathbf{y}(t-1) = \mathbf{B}\mathbf{x}(t)$. In other words, we need an auto-regressive structure: $\mathbf{y}(t) = \mathbf{y}(t-1) + \mathbf{B}\mathbf{x}(t)$. To gradually adjust between position and velocity control we should allow for additional coefficients: $\mathbf{y}(t) = \mathbf{A}\mathbf{y}(t-1) + \mathbf{B}\mathbf{x}(t)$. When $\mathbf{A} = \mathbf{0}$ we have pure position control, when $\mathbf{A} = \mathbf{I}$ we have pure velocity control. More generally, we will allow these coefficients $\mathbf{A}$ and $\mathbf{B}$ to be multi-input multi-output (MIMO) filters: multiple temporal inputs are filtered in time to generate multiple outputs in time (not just instantaneous mapping). In doing so we can filter the input, for instance, to smooth the noisy fluctuations of myographic activity (with q tabs of a moving-average (MA) filter: $\mathbf{B}_k, k = 0 \dots q$). With an auto-regressive (AR) filter we can take a variable history into account for computing velocity or acceleration on a variable time-scale (with p filter tabs: $\mathbf{A}_k, k = 1 \dots p$). The most important aspect here is that these filters are not fixed, but instead, they should be adapted to best match the behavior of the human when presented with the task. In total, we are proposing an adaptive ARMA-MIMO system that attempts to predict the desired locations $\mathbf{y}(t)$ recursively from the myographic signals $\mathbf{x}(t)$:

$$\mathbf{y}(t) = \sum_{k=1}^{p} \mathbf{A}_k(t)\mathbf{y}(t-k) + \sum_{k=0}^{q} \mathbf{B}_k(t)\mathbf{x}(t-k) \tag{4.2}$$

The mathematical derivations that follow are established theory of adaptive IIR filtering (Diniz, 2013; Shynk, 1989; Widrow and Stearns, 1985). We reproduce this theory here to tie it into the context of myographic motor control, to motivate the choices we made among various recursive algorithms, and to provide explicit equations for implementation. Note that during training the filter matrices $\mathbf{A}_k(t)$ and $\mathbf{B}_k(t)$ are themselves dependent on time as they will be adjusted so that $\mathbf{y}(t)$ matches a desired target location $\mathbf{d}(t)$. Generally the user will vary $\mathbf{x}(t)$ on a rapid time scale of less than a second, whereas

the filter parameters are adjusted on a slower time scale of many seconds or minutes. The human learner can also adjust strategy of movement on this slower time scale. The concurrent learning system is expected to converge due to the common training goal (reducing the distance of current position to target) and assuming an appropriate choice of learning constants to prevent instabilities (we touch on this in more detail in Section 4.6).

The feature used as the input vector $\mathbf{x}(t)$ in this case is the moving root mean square (RMS) of the digitized EMG signals $\hat{\mathbf{x}}(t)$:

$$\mathbf{x}(t) = \sqrt{\frac{1}{N}\sum_{k=t_1}^{t} \hat{\mathbf{x}}^2(k)} \tag{4.3}$$

where $t_1 = t - N + 1$, $\hat{\mathbf{x}}(k) \in \mathbb{R}^{M\times 1}$, with M number of sensors (channels) and N the sample size. This is the discrete version counterpart of the continuous moving RMS value:

$$\mathbf{x}(\tau) = \sqrt{\frac{1}{T}\int_{\tau-T}^{\tau} \hat{\mathbf{x}}^2(t)dt} \tag{4.4}$$

where $N = T \cdot f_s$ and f_s is the sampling frequency.

Note that when $p = 0$ in eq. (4.2), the output has a finite impulse response (FIR) and when $p = q = 0$, we obtain the instantaneous linear regressor proposed in eq. 4.1 (Hahne et al., 2014). Here we extend over this prior work by adding the auto-regressive filter $\mathbf{A}_k$, which results in an infinite impulse response (IIR). In all experiments we will compare the performance of the FIR system with the new adaptive IIR filter structure proposed here.

In order to simplify the problem, we will assume that $y_1(t)$ and $y_2(t)$ are independent; this means that the axes that determine the two wrist angles, the flexion-extension axis, and the radial-ulnar axis are independent (Hahne et al., 2014). Assuming this independence, the matrices $\mathbf{A}_k(t)$ are diagonal, and each angle $y_i(t)$ $i = 1, 2$ can be estimated separately from previous positions of the same DOF and input signals:

$$\begin{aligned} y_i(t) = &\sum_{k=1}^{p} a_{i,k}(t) y_i(t-k) \\ &+ \sum_{k=0}^{q} \mathbf{b}_{i,k}^T(t) \mathbf{x}(t-k), \quad i = 1, 2 \end{aligned} \tag{4.5}$$

where $a_{i,k}(t)$ are the corresponding diagonal entries in $\mathbf{A}_k(t)$, and $\mathbf{b}_{i,k}(t)$ are the corresponding rows in the filter matrices $\mathbf{B}_k(t)$.

We can express equation (4.5) in a compact form such as:

$$y_i(t) = \beta_i^T(t) \mathbf{z}_i(t), \quad i = 1, 2 \tag{4.6}$$

with the coefficients vector $\beta_i(t)$ and the data vector $\mathbf{z}_i(t)$, both of which are column vectors of length $p + (q+1)M$, and are defined as:

$$\begin{aligned} \beta_i(t) = &[a_{i,1}(t), a_{i,2}(t), \ldots, a_{i,p}(t), \\ &\mathbf{b}_{i,0}(t), \mathbf{b}_{i,1}(t), \ldots, \mathbf{b}_{i,q}(t)]^T \end{aligned} \tag{4.7}$$

$$\begin{aligned} \mathbf{z}_i(t) = &[y_i(t-1), y_i(t-2), \ldots, y_i(t-p), \\ &\mathbf{x}^T(t), \ldots, \mathbf{x}^T(t-q)]^T \end{aligned} \tag{4.8}$$

The learning task is to find the $\hat{\beta}_i(t)$ that minimizes the mean squared error $\varepsilon_{MSE}(t)$ between the output of the system $\mathbf{y}(t)$ and the desired position $\mathbf{d}(t)$, i.e.:

$$\varepsilon_{MSE}(t) = \sum_{i=1}^{2} E\left\{ \left(d_i(t) - y_i(t) \right)^2 \right\} \tag{4.9}$$

This is called the output-error formulation (Shynk, 1989), since the filters are estimated using the mean squared-error of the output $\mathbf{y}(t)$. Once the filters $\hat{\beta}_i(t)$ are calculated, the estimate of the current position $\hat{\mathbf{y}}(t)$ is obtained using eq. (4.5) and the error can be obtained.

However, notice that with definition (4.8) $\mathbf{z}(t)$ depends on the history of $y(t)$ and thus it itself depends of the parameters $\beta(t)$. Through this recursive dependence the error is a non-linear function of the parameters β_i.

Nevertheless, since eq. (4.6) resembles a linear regression problem, it is called a pseudolinear regression. The nonlinearity implies that the cost function is not a quadratic function, so the linear estimate can be suboptimal.

4.3 Adaptive filtering of the EMG signals

An adaptive approach to the problem is particularly important in the context of closed-loop feedback. The user can in principle change the control strategy in real-time, and so the optimal mapping between EMG signal and target location should be able to adjust to the current control strategy. Our goal is to continuously adapt the coefficient sample by sample, instead of recalculating the coefficients with a batch of training data, and then having the user adjust to the new set of coefficients as in our previous work (Hahne et al., 2015).

The main idea behind the adaptive methods is that the new estimate is obtained from the previous estimate by moving in the direction that minimizes the MSE in eq. (4.9). Since the negative gradient vector points in that direction, we just have to calculate the partial derivatives of the MSE with respect to the coefficients of the system.

The updating rule is:

$$\beta(t+1) = \beta(t) - \mu \nabla \varepsilon_{MSE}(t), \tag{4.10}$$

where $\nabla \varepsilon_{MSE}(t)$ is the gradient and μ the step size. The gradient requires the calculation of the expected values. Since we do not know the distributions, these expectations must be estimated. The simplest solution is to remove the expectation operator; i.e., to use the instantaneous value, obtaining the least mean squares LMS algorithm (Widrow and Stearns, 1985).

Calculating the gradient vector, the updating rules for the coefficients in β_i are:

$$a_{i,k}(t+1) = a_{i,k}(t) + \mu e_i(t) \frac{\partial y_i(t)}{\partial a_{i,k}(t)}, \quad k = 1, \ldots, p \tag{4.11}$$

$$\begin{aligned} b^j_{i,k}(t+1) =& b^j_{i,k}(t) + \mu e_i(t) \frac{\partial y_i(t)}{\partial b^j_{i,k}(t)}, \\ & k = 0, \ldots, q;\ j = 1, \ldots, M \end{aligned} \tag{4.12}$$

where $e_i(t)$ is the instantaneous error at time t, i.e., $e_i(t) = d_i(t) - \beta_i^T(t)\mathbf{z}_i(t)$.

The partial derivatives in the preceding equations are given by:

$$\frac{\partial y_i(t)}{\partial a_{i,k}(t)} = y_i(t-k) + \sum_{l=1}^{p} a_{i,l}(t)\frac{\partial y_i(t-l)}{\partial a_{i,k}(t)}, \quad k = 1, \ldots, p \tag{4.13}$$

$$\frac{\partial y_i(t)}{\partial b_{i,k}^j(t)} = x_j(t-k) + \sum_{l=1}^{p} a_{i,l}(t)\frac{\partial y_i(t-l)}{\partial b_{i,k}^j(t)}, \quad k = 0, \ldots, q;\ j = 1, \ldots, M. \tag{4.14}$$

The second term in the right hand side of eq. (4.13,4.14) is due to the recursion model, since the estimated position at time t depends on the p previous positions, and, each of these depends on the coefficients.

In eq. (4.13,4.14) we have an additional problem. The equations are not recursive; i.e., they depend on the present value of $a_k(t)$ and $b_k(t)$ (do not confuse a recursive system with a recursive algorithm). If we use a small step size μ, we can assume that the coefficients are changing slowly, so:

$$\frac{\partial y_i(t-l)}{\partial a_{i,k}(t)} \simeq \frac{\partial y_i(t-l)}{\partial a_{i,k}(t-l)} \tag{4.15}$$

$$\frac{\partial y_i(t-l)}{\partial b_{i,k}^j(t)} \simeq \frac{\partial y_i(t-l)}{\partial b_{i,k}^j(t-l)} \tag{4.16}$$

Using this approximation in eq. (4.13,4.14), we obtain:

$$\frac{\partial y_i(t)}{\partial a_{i,k}(t)} \simeq y_i(t-k) + \sum_{l=1}^{p} a_{i,l}(t)\frac{\partial y_i(t-l)}{\partial a_{i,k}(t-l)}, \quad k = 1, \ldots, p \tag{4.17}$$

$$\frac{\partial y_i(t)}{\partial b_{i,k}^j(t)} \simeq x_j(t-k) + \sum_{l=1}^{p} a_{i,l}(t)\frac{\partial y_i(t-l)}{\partial b_{i,k}^j(t-l)}, \quad k = 0, \ldots, q;\ j = 1, \ldots, M. \tag{4.18}$$

So we can obtain the approximations of the derivatives $\psi_{a_{i,k}}(t) = \frac{\partial y_i(t)}{\partial a_{i,k}(t)}$ and $\psi_{b^j_{i,k}}(t) = \frac{\partial y_i(t)}{\partial b^j_{i,k}(t)}$ in a recursive calculation:

$$\begin{aligned} \psi_{a_{i,k}}(t) =& y_i(t-k) + \sum_{l=1}^{p} a_{i,l}(t)\psi_{a_{i,k}}(t-l) \\ & k = 1, \ldots, p \end{aligned} \tag{4.19}$$

$$\begin{aligned} \psi_{b^j_{i,k}}(t) =& x_j(t-k) + \sum_{l=1}^{p} a_{i,l}(t)\psi_{b^j_{i,k}}(t-l) \\ & k = 0, \ldots, q;\ j = 1, \ldots, M \end{aligned} \tag{4.20}$$

Note that the derivatives in eq. (4.19,4.20) are delayed versions of $y_i(t)$ and $x_j(t)$ filtered by the time-varying recursive filter $a_{i,k}(t)$.

We call this the IIR LMS algorithm. This algorithm estimates $p + q \times M - 1$ parallel filters at every iteration; this requires a lot of storage and computational resources. With the assumption that the step size μ is small, we can obtain a simplified IIR LMS algorithm. Since the coefficients $a_{i,k}(t)$ do not vary too much in intervals of length p, $a_{i,k}(t) \simeq a_{i,k}(t-1) \simeq, \ldots, \simeq a_{i,k}(t-p)$, we can assume that they are time invariant in that period, and we can exchange the order of filtering and delay operations in eq. (4.19,4.20). It means that we can first filter the input and output signals for $k = 1$ and $k = 0$, respectively,

$$\tilde{y}_i(t) = \psi_{a_{i,1}}(t) \tag{4.21}$$

$$\tilde{x}^j_i(t) = \psi_{b^j_{i,0}}(t) \tag{4.22}$$

and, then, approximate the other elements in the gradient vectors as delayed versions of them. This is called the filtered IIR LMS algorithm. It requires only $M + 1$ filters to approximate the derivatives.

The LMS algorithm updates the parameters according to the gradient of the instantaneous squared-error (a stochastic gradient descent method). Another option is to use the recursive Gauss-Newton RGN algorithm that improves the convergence rate using sample covariance matrices to control the direction during the updating step. The algorithm is more complicated, since in every iteration the inverse of the covariance matrix must be also updated.

Nevertheless, the inversion of the matrix is avoided thanks to the matrix inversion lemma, reducing the computational cost (Diniz, 2013).

The general updating rule for the RGN algorithm for the equation and output error formulations is:

$$\beta_i(t+1) = \beta_i(t) + \mu \mathbf{P}_i(t+1)\tilde{\mathbf{z}}_i(t)e_i(t), \tag{4.23}$$

where $\tilde{\mathbf{z}}_i(t)$ is the filtered version of the data vector, $e_i(t)$ is the error with the current coefficients $e_i(t) = d_i(t) - \beta_i^T(t)\mathbf{z}_i(t)$, and $\mathbf{P}_i^{-1}(t)$ an estimate of the Hessian matrix that is updated by:

$$\mathbf{P}_i^{-1}(t+1) = \lambda \mathbf{P}_i^{-1}(t) + \gamma \tilde{\mathbf{z}}_i(t)\tilde{\mathbf{z}}_i^T(t) \tag{4.24}$$

with λ the forgetting factor that controls the weight of previous values in the current estimate. Typical values (see Shynk (1989)) are $\lambda = 0.9, \ldots, 1$, and $\lambda = 1 - \mu$, $\gamma = 1$.

The inversion of the matrix is avoided using the matrix inversion lemma, and the updating rule becomes:

$$\mathbf{P}_i(t+1) = \lambda^{-1}\left(\mathbf{P}_i(t) - \frac{\mathbf{P}_i(t)\tilde{\mathbf{z}}_i(t)\tilde{\mathbf{z}}_i^T(t)\mathbf{P}_i(t)}{\lambda/\gamma + \tilde{\mathbf{z}}_i^T(t)\mathbf{P}_i(t)\tilde{\mathbf{z}}_i(t)}\right) \tag{4.25}$$

The difference with the LMS algorithm is due to the $\mathbf{P}_i(t)$ matrices. So, if these matrices are equal to the identity matrix, both algorithms are the same and depending on the equation or output-error formulation that is chosen, we get the LMS algorithms explained previously.

The implementation of the filtered IIR RGN algorithm is summarized as follows:

Initialization,

Iteration ($t = 0, 1, \ldots$),

for $i = 1, 2$:

Error estimate:

$$y_i(t) = \beta_i^T \mathbf{z_i}(t) \tag{4.26}$$

$$e_i(t) = d_i(t) - y_i(t) \tag{4.27}$$

Filter signals:

$$\tilde{y}_i(t) = y_i(t) + \sum_{l=1}^{p} a_{i,l}(t)\tilde{y}_i(t-l) \tag{4.28}$$

$$\tilde{x}_i^j(t) = x_j(t) + \sum_{l=1}^{p} a_{i,l}(t)\tilde{x}_i^j(t-l) \tag{4.29}$$

$$\begin{aligned}\tilde{\mathbf{z}}_i(t) =&[\tilde{y}_i(t-1), \tilde{y}_i(t-2), \ldots, \tilde{y}_i(t-p),\\ &\tilde{\mathbf{x}}^T(t), \ldots, \tilde{\mathbf{x}}^T(t-q)]^T\end{aligned} \tag{4.30}$$

Update:

$$\mathbf{P}_i(t+1) = \lambda^{-1}\left(\mathbf{P}_i(t) - \frac{\mathbf{P}_i(t)\tilde{\mathbf{z}}_i(t)\tilde{\mathbf{z}}_i^T(t)\mathbf{P}_i(t)}{\lambda/\gamma + \tilde{\mathbf{z}}_i^T(t)\mathbf{P}_i(t)\tilde{\mathbf{z}}_i(t)}\right) \tag{4.31}$$

$$\beta_i(t+1) = \beta_i(t) + \mu\mathbf{P}_i(t+1)\hat{\mathbf{z}}_i(t)e_i(t) \tag{4.32}$$

Updates of the AR coefficients are only executed if they lead to stable recursion (i.e. the poles of the AR coefficients remain within the unit circle).

Note that if we remove the filtering step, we obtain a pseudolinear regression algorithm. If we substitute the output signal by the observed output, i.e., we follow an equation-error instead of the output-error formulation, $p = q = 0$ (there is no feedback nor memory in the system) and $\mu = \gamma = 1$, the algorithm is the same that the exponentially weighted recursive least squares algorithm. The cost function is a modification of the least-squares cost function, by incorporating a forgetting factor λ so recent samples are weighted more strongly in the error computation:

$$\varepsilon_{ERLS}(T) = \sum_{t=1}^{T} \lambda^{T-t}|d(t) - y(t)|^2 \tag{4.33}$$

Note that eq. (4.33) is the cost function used in Hahne et al. (2015), i.e., the recursive version of the linear regression solution. The algorithm in Hahne et al. (2015) is adaptive, but the system is not recursive, so there is no feedback between the past and present positions, nor between the past EMGs observations and the current position. The exponential factor allows to obtain a weighted covariance matrix in order to accommodate the time varying nature of the signals.

4.4 Experimental paradigm

4.4.1 Data acquisition

We use a Myo Armband from Thalmics to acquire the EMG signals. It has a flexible diameter to fit a forearm circumference between 7.5 to 13 inches. It has eight bipolar EMG electrodes and samples the EMG at 200 Hz at 8 bit resolution. This does not cover the entire EMG-spectrum and would be insufficient for more complex feature-extraction, but is sufficient for extracting simple amplitude features. Signals are transferred to the computer via Bluetooth. A Matlab program is executed in order to acquire and process the data in real-time. We use Matlab 16a 64 bit version running on a 2.6 GHz personal laptop with 8 GB RAM.

We use log-variance of the EMG signals as the input feature vector $\mathbf{x}(t)$, with variance computed in a time window of 200 ms and updated every 40 ms as in Hahne et al. (2014) (t is sampled at 25 Hz). The sensors are placed in the same position and orientation for all participants (upper part of the forearm, close to the elbow with the LED light of the device pointing to the same direction). This experiment targets the muscles from an upper limb with a forearm stump of 3 inches or longer. The targeted muscles are the flexor carpi radialis and ulnaris muscles, extensor carpi radialis longus and the brachioradialis muscle, among other residual EMG measurements. Fifteen able-bodied participants were tested (8 males, 7 females) with ages ranging between 20 to 50 years. We also tested two male individuals and a female with limb deficiency; one amputee (with a 20 cm stump; Figure 4.1) and two congenital (with a 10 cm and a 25 cm stump respectively). All individuals provided written informed consent before the experiment. The experiments were in accordance with the declaration of Helsinki and were approved by the UPV ethics committee, approval number P11-23-03-18.

(a) **(b)**

Figure 4.1: Myoelectric Armband. (a) Amputee participant using the Myo Armband. (b). Able-bodied participant using the Myo Armband.

4.4.2 Study design

Participants sat in a comfortable position in front of a computer screen, with the elbow of the arm resting on the table and flexed by nearly 90 degrees. The able-bodied ones were instructed to relax the hand so that forearm activity was only dedicated to wrist motions as shown in Figure 4.2. After the armband was placed on the forearm of the participant and connected to the computer, the device was initialized. The experiment consisted of a training and testing phase as follows.

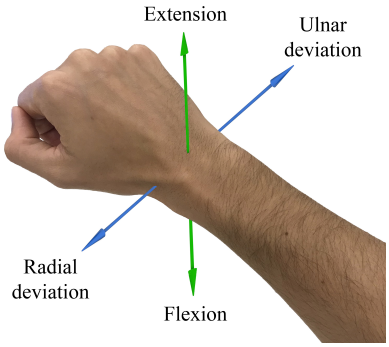

Figure 4.2: Controllable DoFs. Directions of wrist movements allowed to the participant and learned by the model.

Training phase

Figure 4.3(a) shows the user-screen during training. The center of the coordinate system corresponds to the neutral position and the two axes to the two DOFs controlled in this study. The green circle indicates the desired target position $\mathbf{d}(t)$ and the red cross is the current estimated position $\mathbf{y}(t)$. This display is updated at the same 25 Hz rate (40 ms) as the adaptive filter equations. Before the start of the training phase participants are familiarized with the closed-loop user feedback shown in Figure 4.3(a).

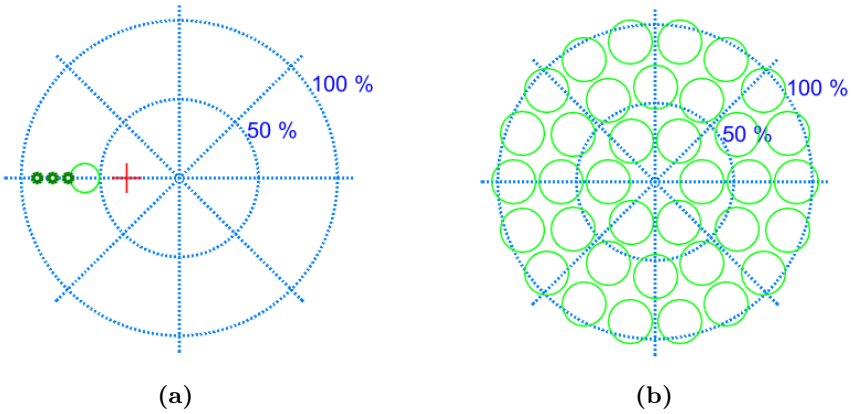

Figure 4.3: User interface. (a) User-feedback screen during training experiment. Red cross: estimated position. Large green circle: current target position. Small green circles anticipate future target positions. (b) The 36 targets placed in 3 different radii (0.3, 0.6, 0.9) for the test experiment. There are 6 targets in the inner circle, 12 in the intermediate and 18 in the outer circle.

Training of the IIR system: The three small circles indicate the direction of movement for the upcoming target positions. This helps the user prepare for the upcoming movement and maintain muscle contractions synchronized with the desired target locations. We defined a set of simple trajectories in the flexion-extension (right-left) and radial-ulnar (up-down) axes that were paced with a constant speed that participants could easily follow without significant delays. The target starts in the center. Then it moves during 6 seconds from center to the right side. Once it reaches the right-most position, it returns back to the center in 6 seconds without stopping at any location. The same is done for the up, left and down directions. This four movement directions defines a lap. The training experiment consists on five consecutive laps, totaling 240 s

of training. The order and time of these target movements are identical across participants. The users were instructed to move their wrist so that the red cursor follows the green circle. For example, in Figure 4.3(a), participant would have to conduct a left movement with his/her wrist. They were instructed not to worry even by larger deviations from the target, but to try their best and remain focused on the task. For the able-bodied individuals it was easy for the experimenter to monitor their effort. During the training phase the $\mathbf{A}_k$ and $\mathbf{B}_k$ parameters are continuously adjusted using the filtered IIR RGN algorithm explained in the previous section. Here we used $p = 1, q = 0$, i.e. we used the immediately preceding position and the instantaneous input (without temporal filtering).

Training of the FIR system: As comparison to the new recursive IIR algorithm we test a FIR structure with the same training procedure as in Hahne et al. (2015). Briefly, a target circle is first shown at the center to start at a neutral position. When the red cross is at the center a target appears at one of the outer-most positions, directly to the right, up, left or down. The participant has to move the forearm till it arrives at this target. The users have 20 seconds to hit the target, after which the next target appears. After reaching the target and maintaining the red cross inside the green circle for 1 s (a hit) the target circle jumps back to the center. If the target is not hit within 20 seconds, it also jumps back to the center. The process repeats with the other three directions. This is considered one lap and total training consists of 5 repeated laps. During the training phase the $\mathbf{B}_k$ parameters of the algorithm are continuously adjusted using the FIR algorithm in Hahne et al. (2015). That algorithm is the same as the one in our model in eq. (4.2) with $p = 0, q = 0$, i.e. no recursive feedback of position is used, but the input is filtered, and an additional post-processing step (an exponential moving average filter) is used to smoothen the output (see Hahne et al. (2015) for the details).

Test phase

The test phase starts after the 5 training runs were completed and is identical for the IIR and FIR systems. During the test-phase the parameters of the algorithm were kept constant. In the test phase, the goal for the participants is to move the red cursor to various target locations (indicated by the green circle) and maintain this location for at least one second. The task was similar as in the training FIR phase, targets were static. If the target was reached in less than 20 seconds and maintained for 1 second it was counted as a hit, otherwise it was counted as a missed target. After each hit or miss, a new

target was shown at a new pseudo-random location. Eventually a total of 36 uniformly distributed target positions were presented with no repetition (Figure 4.3(b)). The targets were shown in the same pseudo-random order for all participants. Note that the targets include regions that have not been explored during training. Therefore, we are also testing the ability of the algorithm to generalize and to avoid over-fitting.

To control the effects of fatigue and practice, we divided participants into two groups. One group first trains and tests with the FIR system and after that with the IIR system. The other group does the opposite. We set the learning constants to $\mu = 1$ and $\lambda = 1$ during training so the algorithm is effectively integrating across all samples.

4.4.3 Performance metrics

To quantify the performance during the online test phase, we measured four quantitative metrics. The completion rate (CR) was defined as the number of hits H over the total amount of targets N expressed in a percentage scale %:

$$CR(\%) = 100 \cdot \frac{H}{N} \tag{4.34}$$

We defined previously a hit such as reaching the target and staying inside for one second, everything in less than 20 seconds.

To evaluate the efficiency and ease-of-use we also calculated the traveled distance (TD) during the entire test session, including hits and misses:

$$TD = \sum_{i=1}^{N} \sum_{j=1}^{J_i} \|\mathbf{y}_i(j) - \mathbf{y}_i(j-1)\| \tag{4.35}$$

where N is the number of targets and J_i is the number of samples to get from target i to target $i+1$. For the first target $i = 1$, we assumed that $\mathbf{d}_0 = (0, 0)$ and $\mathbf{y}_1(0) = (0, 0)$ (the starting point for all the test experiments was the origin of coordinates). The starting point for the next segment was equal to the final position of the actual one, i.e., $\mathbf{y}_{i+1}(0) = \mathbf{y}_i(J_i)$.

The path efficiency (PE) indicated if the distance traveled by the participant during the experiment was close to the optimal path, i.e., the shortest one.

The PE was defined as the ratio in % of the sum of distances between targets and the real distance traveled by the subject:

$$PE(\%) = 100 \cdot \frac{\sum_{i=1}^{N} \|\mathbf{d}_i - \mathbf{d}_{i-1}\|}{TD} \tag{4.36}$$

A larger value of PE implies a more linear trajectory in the 2D space. Linear trajectories in the 2D space are directly correlated with the activation of combined DoFs movements. Therefore, the PE can be used also as an indirect measurement of the simultaneous multiple degree of freedom control.

The completion time (CT) metric measured the efficiency in the time domain. It was calculated as the time average in seconds to reach a target:

$$CT(s) = \frac{\sum_{i=1}^{N} t_i}{N} \tag{4.37}$$

where t_i is the time in seconds to travel from target $i-1$ to target i. For the missed targets (the subject was not able to reach the target before 20 seconds and kept into the target for at least one second), $t_i = 20$ in Equation 4.37.

To measure the stability of the system to accomplish the targets hit condition, we defined the attempt ratio (AR). It was defined as the average ratio between the number of times the subject enters the hit targets E and the number of hits H.

$$AR = \frac{E}{H} \tag{4.38}$$

By definition, $AR \geq 1$; the lower the AR value, the lower the attempts needed to hit the targets. A value close to 1 means that the system was very stable, since the first time that he got into the target he was able to stay for the required second to be considered a hit.

4.5 Results

4.5.1 Real-time adaptation during training

To gain a sense for the speed of adaptation of the system during closed-loop training, we first show the learning process for one user in Figure 4.4. The panels show the FIR and IIR coefficients (b_i and a_1) for the flexion-extension direction as they adapt in time. In this example, the FIR coefficients start to converge after the first lap (48 seconds), while the IIR coefficient is learned in just 15 seconds.

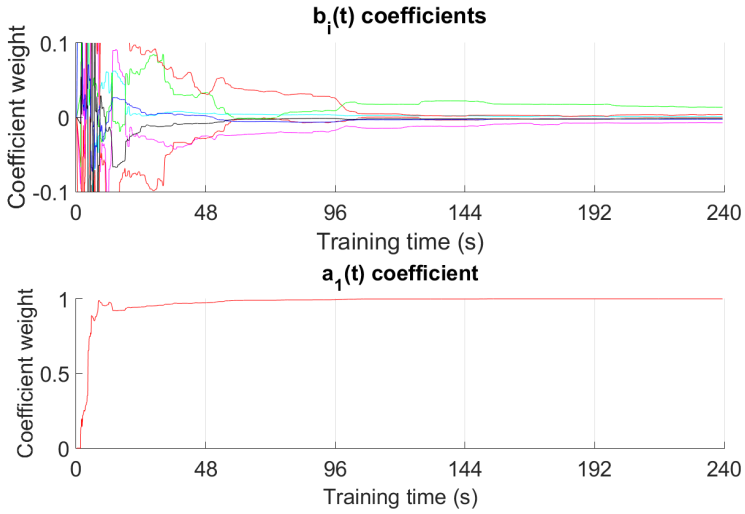

Figure 4.4: Parameter adaptation during training. This is a representative sample from the training. The behavior presented in this plot is common among all users. The first row shows the eight FIR coefficients b_i as they develop in time during training for one representative able-bodied participant. The second row is the IIR coefficient a_1 in that same time period. Coefficients are shown here for the flexion-extension direction only. Note that the IIR coefficient converges almost immediately to $a_1 = 1$, which corresponds to velocity control. Results are similar for other participants and in radial-ulnar direction. Gray vertical lines indicate start/end of the five repeated training laps with identical target trajectories.

In Figure 4.5 we show the position and error during training. The first two panels show the moving target (black) and the cursor position (color) generated by two users during training. The position error increases whenever the target moves ahead of the user's response, but decays over the total duration of the training session.

The same trend is observed for the instantaneous error averaged over the 15 participants as shown in the third panel. A repeated measures ANOVA on the mean position error of the five repeated training laps shows that position error is reduced over time ($F(14) = 32.9$, $p = 3 \cdot 10^{-7}$, with time coded as a continuous predictor variable). In particular, there is a reduction of error between the last two laps (paired t-test, $t(14) = 3.2$, $p = 0.007$).

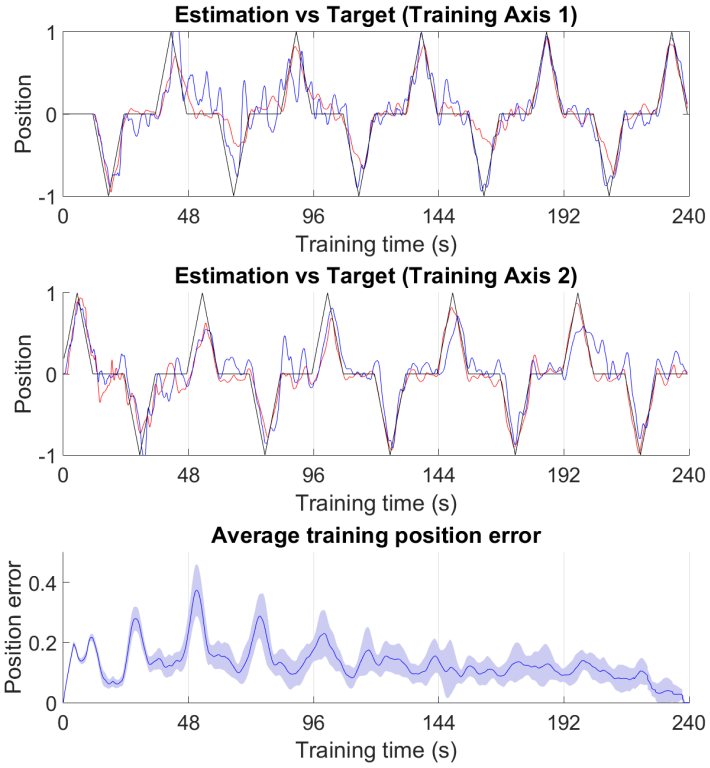

Figure 4.5: Performance during training. This is a representative sample from the training. The behavior presented in the first two rows of this plot is common among all users. First and second row indicate the instantaneous position of the user-machine system during training for both axes. Able-bodied participant (red), a participant with limb deficiency (blue) and target (black). The third row shows the instantaneous error during training averaged over all 15 able-bodied participants. Shaded area indicates standard error of the mean across participants. Gray vertical lines indicate start/end of the five repeated training laps with identical target trajectories.

4.5.2 Performance gains of IIR system during the test phase

We observed during the test phase that participants produced smoother trajectories and wider range of movement when using the IIR system. In contrast, the FIR system required more force and some participants had a limited range of movement in some directions.

Test phase performance of the closed-loop learning algorithm was evaluated for all participants with both FIR and IIR algorithms. Figure 4.6 shows that the rate of targets hit increases in all but one participant by addition of the auto-regressive filter structure (IIR). At the same time, the length of the path to reach the targets is reduced for all participants. A Wilcoxon signed rank test shows that difference in rate of hits as well as in path length are statistically significant ($p = 0.005$ and $p = 0.00006$, respectively with $N = 15$).

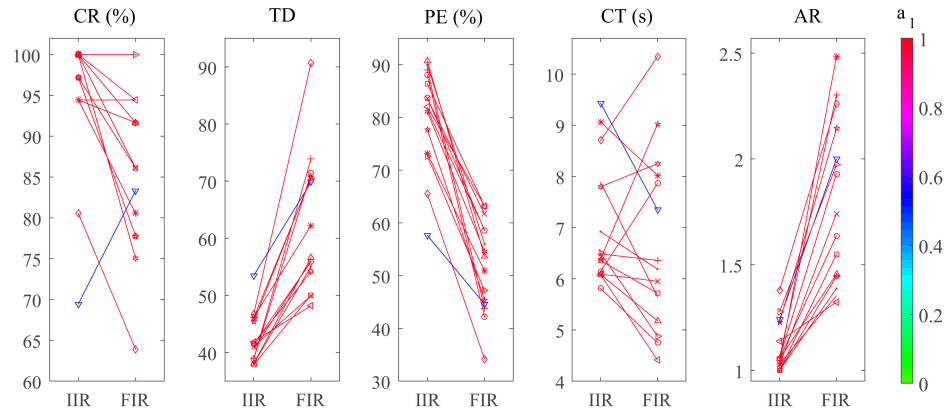

Figure 4.6: Test phase metrics for able-bodied individuals. Each line is a participant. Completion rate increases or stays the same for IIR structure. Average path length to reach a target is shortened for all 15 participants when using the IIR structure. This method also improved the path efficiency and reduced the number of attempts needed to hit a target for all users. Completion time does give mixed results. Line color indicates the value a_1 learned by the IIR filter (in the IIR condition) for one axis. Evidently almost all participants learned velocity control, i.e. $a_1 \approx 1$. There is a single exception with $a_1 = 0.54$ (the blue line).

With the IIR method, 95% of the targets were hit, with perfect performance for half the users (no targets were missed). Of the 5% that were missed, 90% were missed due to the 20 seconds time limitation. A color map of the interface is shown in Figure 4.7. Only one position was missed by three out of fifteen participants (orange circle) while many targets were hit by everyone (electric green circles) and some of them were missed by one or two participants (clear

green circles). For the FIR algorithm, hit rate was around 85% and there are targets that were missed by 3 people (orange), 4 (light red) and 5 or more times (dark red). Only one participant got a perfect score. The FIR errors were located in the outer positions indicating the FIR learning algorithm is limited in gain. This could be the result of a non-linear relation between EMG and displacement, whereby the linear gain $\mathbf{b_0}$ is suitable in the inner range, but not for larger displacements. In contrast, the IIR system has no range limitation as the cursor can in principle continue moving if the user/machine pair learned velocity control, i.e., $a_1 = 1$.

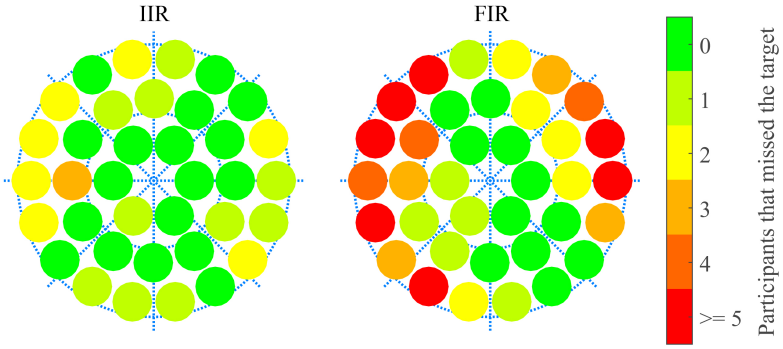

Figure 4.7: Test accuracy. Number of missed targets over all 15 able-bodied participants during the test phase.

The other metrics are also shown in Figure 4.6. Path efficiency is improved similarly to overall path-length, as it is the same measure except that it is normalized by the shortest length to reach a target. Completion time is faster for most participants when using the IIR system (11 out of 15). In general, movement was slower and better controlled, which explains why some participants did not gain in speed despite improving on all other measures. Attempt ratio captures the ability to reach and maintain the target for the prerequisite 1 second. A ratio of 1 indicates that the participant never exited the target area prematurely. Evidently, the IIR system allows significantly better control to hold the position, despite velocity control.

To visualize the difference in path efficiency, we plot in Figure 4.8 the trajectories of one participant for both algorithms. This figure also compares the paths from an inner to an outer target achieved with both methods (blue: IIR, red: FIR). With both algorithms, the user was able to hit the outer target, but the FIR path is much more erratic and clearly shows the effort that was required. As an example of the user experience, we show the last seconds of

the testing phase for the FIR and IIR algorithms for the same participant in the video (*User experience video* 2018).

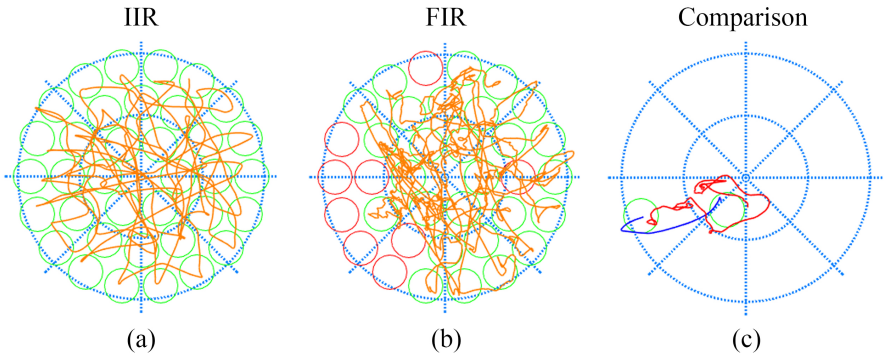

Figure 4.8: Trajectories following the 36 targets during the test phase for one user. These are representative samples for common behaviors during the test. The IIR trajectories are smoother and shorter than for the FIR filter. This participant does not reach some areas in the FIR case. The right panel compares the trajectory from one target to the next for another participant. The blue line is the IIR method; the red line is the FIR algorithm. The IIR trajectory (blue curve) is smoother than the FIR trajectory (red curve) and takes less time and effort.

4.5.3 Results on participants with limb deficiency

Able-bodied individual rely on actual wrists movements during training and testing. To demonstrate that this is not required with the closed-loop feedback, we recruited three individuals with limb deficiency (Figure 4.1). The identical training and testing was used as before. These individuals relied purely on visual feedback on the screen to guide their muscle contractions. Performance is numerically lower in these individuals, as compared to able-bodied participants. We ascribe this to the lower EMG signal strength we observed in these participants, in particular for the individual with a shorter stump.

All performance metrics showed a performance benefit with the IIR system (Figure 4.9). The number of hits increases, the total path length, is reduced almost by 40% and the efficiency of the trajectories increases accordingly. The attempt ratio is improved in all participants and is close to 1 with the IIR. This indicates that when the target was reached, it was easy to maintain the position. When inspecting the coefficients found by the IIR algorithm we find

again that the $a_1 \approx 1$, meaning that this human-machine pair again learned velocity control.

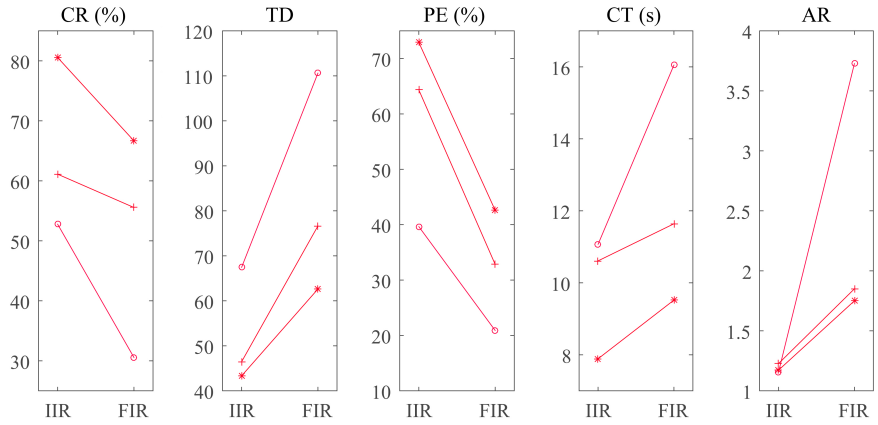

Figure 4.9: Performance metrics for the participants with limb deficiencies. Same metrics as in Figure 4.6. Same color map is used also for a_1 values, in this case all are $a_1 \approx 1$.

4.6 Discussion

We have demonstrated here the benefits of learning recursive filters for proportional myographic control. The recursive filter allowed us to seamlessly titrate between position and velocity control. Given these options, the human-machine system naturally converged to a velocity-control strategy. Velocity-control is known to have a number of benefits in practice (Engeberg et al., 2008) such as less overall effort for the user and no limitations of the range of motion (e.g. due to fatigue) . However, to our knowledge no adaptive strategy has yet been proposed to directly learn proportional velocity control, and our own previous efforts had been limited to position control (Hahne et al., 2015). By introducing a recursive structure we were able to readily incorporate more general control strategies into a closed-loop learning mechanism. To do this we leverage established theory of adaptive IIR filtering (Diniz, 2013; Shynk, 1989; Widrow and Stearns, 1985). The novelty lies in relating this theory to myoelectric control, which allows for a gradual transition between position and velocity control and an efficient closed-loop training procedure without the need for manual parameter adjustments.

In the case of the FIR filter, the controller only learns instantaneous regression coefficients $\mathbf{b_0}$ as in eq. 4.1. Afterwards a post-processing filter can be used to smooth the output signals, following Hahne et al. (2015). In the IIR approach proposed in this paper, this post-processing is not necessary since it is implicitly implemented in the output recursion. In addition, the human-machine pair naturally learned a velocity control strategy. Since we are using a model with only one recursion and instantaneous input coefficients, this limited number of free parameters allowed us to learn the coefficients with relatively short training session of a few minutes.

Another practical benefit is that velocity or gain-factors do not need to be adjusted manually as in other approaches Hahne et al. (2018), since all factors are learned during the process of real-time, closed-loop adaptation.

An important caveat of this work is that we have tested the system on a somewhat artificial 2D cursor movement task and that we have focused mostly on able-bodied individuals. The preliminary results with limb deficient participants are nevertheless encouraging. In these individuals, myographic signals are typically weaker and electrodes more difficult to place. Despite overall lower performance we find that the adaptive IIR filter still shows an improvement in this target group over to the FIR filter. A larger number of participants have to be tested to determine if these results can be replicated across the more diverse physiology in this group. This work will be later introduce in Chapter 5. Similarly, the proposed strategy should be tested on a realistic motor control task, ideally using an actual prosthetic device, e.g. Amsuess et al. (2015a) and Hahne et al. (2018). This work is part of the continuation of this thesis (future post doctoral work); we show some preliminary results in Chapter 7.

Here we used a closed-loop learning system where in principle the human and machine can simultaneously adapt. In contrast to Hahne et al. (2015), parameter adaptation is ongoing during the entire closed-loop training period. The learning rules proved stable in practice despite concerns that such concurrent adaptations can become unstable (Rupp and Sayed, 1996). The issue of stability of co-adaptive learning has been studied previously on a theoretical level (Müller et al., 2017). The main observation of that work is that stable co-adaptation may be achieved as long as one learner adapts slower than the other. In the example shown in Figure 4.4, adaptation of the controller happened relatively quickly (15-50 seconds). This is evidently slower than the time constant of human motion control (<1 second), but faster than the time constant a human may use for adapting movement strategy. This means that the machine is slow enough to allow the participants to control the

specific movement trajectory, yet fast enough to adapt to the strategy the user is trying to implement. From the controller's standpoint, the human is quasi-stationary, and from the human's standpoint, the controller is quasi-stationary as well (since it stabilizes so fast). The net result is a stable system despite the closed-loop interaction of the human-machine controllers. For this stability it is necessary that the user generates consistent muscle contractions on the time scale of parameter adaptation (approximately 120 seconds here). We believe that providing clear instructions to the users at the beginning is important in this regard, as well as the game-like interface which keeps participant motivated to follow those instructions. The most important aspect of this interface is the real-time feedback coupled with a consistent goal, namely, the machine and human continuously attempt to reduce the same error.

Note that the guidance to the user can be suggestive of position control ("to move further out, try to make a larger effort") or it can suggest velocity control ("to move in a given direction, flex the muscle and just wait for the cursor to move"). We could think about envision controlling wrist rotation, which is common in prosthetic devices. In that case we anticipate that participants will require more careful instructions in order to consistently perform muscle contractions that were not previously associated with wrist rotation. Future work may explore this and other training protocols with concurrent human-machine learning (Hahne et al., 2015; Müller et al., 2017). The next chapter introduces a new training protocol that already benefits from the co-adaptation process.

Finally, we note that nothing about the proposed approach is specific for myoelectric control. The method could be used equally well for motion control using high-dimensional signals from re-innervated muscles (Kuiken et al., 2009) as these behave similarly to conventional myographic signals where signal amplitude increases with effort. The approach could also be used in brain-machine interfaces (Hochberg et al., 2006; Velliste et al., 2008). These capture neuronal firing directly from the motor cortex, which is known to encode both position and velocity of movement (Paninski et al., 2004).

Chapter 5

Optimal training for myoelectric regression control

The training paradigms for regression-based controllers commonly follow a training protocol based on the classification approach, where only a finite set of movements are trained. Along with this, the training is usually the same for all users, not considering that prostheses control is highly dependent on the patient condition and abilities. In this chapter we present a novel training protocol for regression based solutions that, instead of using only a finite predefined set of movements, it explores the whole set of the output space and exploits in real time the previous performance of the patient to automatically adapt the training session to his skills. As a consequence, the algorithm distributes the training time efficiently, focusing on the movements where the performance is worse and optimizing the training for each user. The results prove that this novel training procedure autonomously produces a better training session, since the completion rate is significantly increased for able-bodied and subjects with limb deficiencies.

Chapter based on **Igual, C.**, Castillo, A. and Igual, J. (2020). Optimal training for myoelectric regression control. Paper submitted.

Contents

5.1 Introduction

As we have seen in previous chapters, looking to improve the prosthesis control behavior and its robustness, researchers have been exploring deeply the four parts of the prostheses control loop: the EMG signal acquisition, the feature extraction, the models and the feedback channel to the user from the prosthesis behavior. As a reminder, the model algorithms are mostly divided into two groups: classification and regression. This chapter will focus its attention into the regressors modeling part, specially the training phase, which plays a critical role in the system final performance.

The training paradigms that were employed with the first classification based models basically consisted in generating data for each cluster, clustering different arm positions or functionalities (Fang et al., 2017; Young et al., 2013). More recently, understanding the relevance of a correct training, a study analyzed different training protocols for a classification controller; concluding that a dynamic environment is the optimal one (Yang et al., 2017). With the introduction of the regression based models, the conventional classification training protocol was reproduced with a positional target representation of the prosthesis state (Ameri et al., 2019; Hahne et al., 2015). This training consisted in showing the patient a desired target in a specific location (related to a prosthesis position) while the user generates the appropriate EMG pattern. The target varies from a predefined list while the user adapts the input EMG pattern to the new targets. During this process the machine learns the relation between the input and the desired output so that, when the training has finished, it is able to map EMG patterns to a continuous spectrum of prosthesis positions.

However, this positional training goes against the usual velocity control of the prostheses, where the system's output is the velocity of movement and not the prostheses position. This led to a transformation into a velocity control model after the learning phase (Hahne et al., 2015), shifting the meaning of the learned positional targets from prosthesis positions to directions of movement. Despite of this, the model kept being trained in a position based environment. Some studies tried to reduce this gap with mobile targets (Hahne et al., 2017) or directional feedback (Shehata et al., 2018a,b); however the model remained mapping the EMG input patterns into estimated positions.

In addition, the traditional positional training contains two inherent drawbacks. The first one is that it only trains in a discrete space (finite number of targets) while the final use is in a continuous one. This works under the assumption that, for linear models, any (non-trained) movement would be given

by a linear interpolation of the learned ones. However, the linear assumption is far from the human behavior and, consequently, the interpolation to non-trained targets may contain significant errors.

The second issue is that it is implicitly assumed that the skills of *any* user are almost the same. In fact, since all users run the same training protocol, it is implicitly considered that their ability to generate EMG signals and learning procedure are almost the same; i.e. one-size-fits-all approach. This also considers that, for the same target at different times, the generated EMG signals will be approximately equal. All these assumptions may fail, specialy for the real final patients with limb deficiencies, who present a wide range of different anatomies that may degrade their EMG pattern generation/recognition. A potential solution to these problems goes through designing a personalized training (Montalivet et al., 2020), with the goal of giving the best possible training to each user. However, generating personalized trainings has to be developed carefully as it could require large quantities of time and resources, something that can be non-acceptable from a clinical/commercial point of view.

The chapter introduces a novel training protocol that is automatically customized for each patient without increasing the training length, generating an optimal training for each particular individual. The basic idea is that, in order to enhance the training efficiency, the user should spend more time at the directions that have shown poor performance, evaluating it in real time. As stated before, the poor performance of the algorithm can be due to the skills of the user and due to the variance of the EMG input signals for the same target. In both cases, a natural solution is that the subject spends more time in the directions that showed significant errors in the past. In this way, the user is forced to keep training the directions that have exhibited errors (no matter which is the cause). To achieve this goal, an output feedback training algorithm is proposed, where the previous performance of the user is taken into account in real time in order to determine the next training target.

This training protocol is independent of the regression based model used by the controller as it only uses the error and the training target list; in other words, it can be integrated with other regression based learning algorithms. In this paper, for providing experimental results and continuing the previous work, we will apply the proposed training paradigm to our previously developed regression based model seen in Chapter 4 (Igual et al., 2019a).

5.2 Prostheses control problem

The user generates, at each time instant, internal muscular contractions used to control related prosthesis movements. These measurement of this electric potentials through M EMG sensors is transformed to an input feature vector $\mathbf{x}(t) \triangleq [x_1(t), ..., x_M(t)]^T$. The prosthesis control learning problem consists on inferring the user intentions from this generated EMG pattern and map them into the desired prosthesis movement.

This problem can be mathematically formulated as follows: find a mapping $f(\mathbf{x}(t))$ as introduced in Chapter 4, so that:

$$\mathbf{u}(t) = f(\mathbf{x}(t)) \tag{5.1}$$

where $\mathbf{u}(t) \in \mathbb{R}^Q$ represents the control signal for a prosthesis with Q DoF. For the linear regression case, the problem can be stated as:

$$f(\mathbf{x}(t)) = \mathbf{B}(t)\mathbf{x}(t), \tag{5.2}$$

where the rows of the $\mathbf{B}(t) \in \mathbb{R}^{Q \times M}$ matrix represent the regression coefficients for the corresponding DoF.

The matrix $\mathbf{B}(t)$ is estimated during some time (the training period) under controlled conditions, e.g., in a supervised experiment, and then validated in order to measure its performance (the test period).

During the training period, the EMG sensors are installed in the upper limb (forearm) of the participant to record the generated muscular contraction data. Once the training process starts, a target signal $\mathbf{d}(t) \in \mathbb{R}^Q$ is shown. Then, the user generates the related EMG pattern altering the input signal $\mathbf{x}(t)$ as the target $\mathbf{d}(t)$ changes. These input-output signals (supervised learning) are used to obtain the model coefficients $\mathbf{B}(t)$ so that $\mathbf{d}(t) \approx \mathbf{B}(t)\mathbf{x}(t)$.

After training, the learned controller $\mathbf{B}(t)$ is used to move the prosthesis in a real scenario. If the training was correct, the obtained output should be close to the intended one by the user: $\mathbf{u}(t) = \mathbf{B}(t)\mathbf{x}(t) \approx \mathbf{d}(t)$, where $\mathbf{u}(t)$ is no more restricted to the specific set of targets used during the training (now, it is a continuous Q dimensional space).

This training-test procedure must be repeated when performance is deteriorated (for example, due to electrode shifting (Prahm et al., 2019; Young et al.,

2011) or time degradation (Amsüss et al., 2013)). The goal is to shorten the re-training sessions and, at the same time, to obtain a robust enough matrix $\mathbf{B}(t)$ so that it can maintain a good performance as long as possible to guarantee that the user experience is satisfactory; otherwise the user will reject the prosthesis.

5.3 Traditional position based controller open-loop training paradigm

The standard training paradigm is composed of three steps. First, a set of I targets are defined $D = \{\mathbf{d}_1, \mathbf{d}_2, \ldots, \mathbf{d}_I\}$. Second, a target $\mathbf{d}_i$ is selected from the list and shown to the participant during some time T_i by using a computer visual interface, $\mathbf{d}(t) = \mathbf{d}_i$, $t_i < t \leq t_i + T_i$. During this time, the corresponding EMG pattern $\mathbf{x}(t) \simeq \mathbf{x}_i$ generated by the participant is recorded. It is common that the duration of each target is the same, i.e., $T_i = T$, and to repeat the whole procedure L times so the targets are shown several times to the participant. Third, the supervised learning $\mathbf{u}(t) = \mathbf{B}(t)\mathbf{x}(t)$ is carried out using the input-outpout pairs $(\mathbf{x}(t), \mathbf{d}(t))$, $t = 1, \ldots, T'$, with $T' = L \cdot T \cdot I$.

The least squares criterion is the most common cost function used to learn the coefficients:

$$\begin{aligned} \mathbf{B}(t) &= \arg\min \sum_{t=1}^{T'} \|\mathbf{d}(t) - \mathbf{u}(t)\|^2 , \\ &= \arg\min \sum_{l=1}^{L} \sum_{i=1}^{I} \sum_{t=1}^{T} \|\mathbf{d}_i - \mathbf{u}(t)\|^2 \end{aligned} \tag{5.3}$$

The $\mathbf{B}(t)$ matrix is usually estimated iteratively and sometimes the cost function is modified by including a forgetting factor: $\sum_{k=1}^{t} \lambda^{t-k} \|\mathbf{d}(k) - \mathbf{u}(k)\|^2$, being $\lambda \leq 1$.

A block diagram of this procedure is shown in Fig. 5.1. Note that this diagram only represents the controller learning loop (open-loop in this case) and not the human-machine loop which is a closed-loop structure due to the visual feedback.

Many papers follow this learning methodology (Ameri et al., 2014a,b,c; Hahne et al., 2014, 2015, 2012b; Huang et al., 2017; Hwang et al., 2017; Jiang et al.,

2008); although we can find differences in the used cost function or details in the specific training set up, they can all be grouped under the same training paradigm: the open-loop controller training model. Afterwards, some of them include a post-processing stage where the position training algorithm is used to obtain a velocity controller for the prosthesis (directions of the movement).

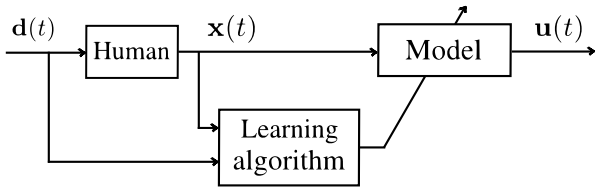

Figure 5.1: Block diagram of the controller learning process. A desired positional target, $d(t)$, is shown to the human; who generates EMG signals, $\mathbf{x}(t)$, to reach this desired position. The signals $\mathbf{x}(t)$ and $d(t)$ are sent to the learning algorithm, which finds the best regression coefficients, $B(t)$, so that $d(t) \approx u(t)$.

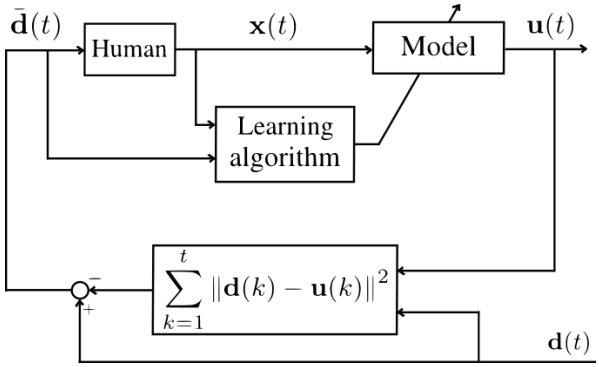

Figure 5.2: Block diagram of the proposed controller closed-loop learning process. If there exists a persistent error $e(t) = u(t) - d(t)$ between the theoretical direction computed with the current regression coefficients $u(t) = B(t)x(t)$ and the desired direction $d(t)$, the feedback term reinforces the learning in such direction. If the learning is correct, then $e(t) \approx 0$ and it reduces to the open-loop training in Fig. 5.1.

Some issues about this controller learning method

As mentioned in Section 5.1, it is clear that one underlying drawback in this kind of models is that the untrained values $\hat{\mathbf{u}}(t)$, $\hat{\mathbf{u}}(t) \notin D$, will be interpolated using the trained observed outputs. This relies on the assumption that, for linear models, any (non-trained) movement would be given by a linear interpolation of the learned ones. However, in practice, this interpolation may lead to errors as there is no real knowledge about the signals $\mathbf{x}(t)$ that the patient will generate in those unknown conditions. To mitigate these errors, the set D of training positions should be made larger in order to include as much targets as possible. In the ideal case where there were no limitations for the duration of the training, an optimal learning process should include *all* possible prosthesis movements. For a typical 2 DoF velocity control prosthesis, this is a continuous space; thus, it may require a lot of time and consistency from the user to generate a reliable set of EMG signals, $\mathbf{x}(t)$, for all the possible targets. Obviously, this optimal training makes no sense from a practical point of view as it will take an excessive amount of time; therefore, a trade off between the accuracy of the model and the duration of the training must be chosen in advance by the experiment designer.

On the other hand, since the target-input $\mathbf{d}(t)$ does not depend on the estimated output $\mathbf{u}(t)$, this training strategy is clearly an open-loop process for the controller (Fig. 5.1). As a consequence, the training procedure remains static (i.e. any participant will always see the same targets unless they are manually changed by the experiment designer). This implies that the training it is neither adapted to the specificity of each participant nor to the unintentionally errors (outliers) that the participant could have introduced (for example due to distractions or fatigue), resulting in a learning procedure whose accuracy mainly depends on the consistency of the input data generated by the patient. The effects of these errors can be also mitigated by increasing the duration of the experiment with the purpose of extending and diversifying the training data set. But, in addition to the associated disadvantages of increasing the training duration, it is not optimal to extend the duration for all the I targets when the outliers are just generated during a short period of time that may only affect to one or two of them.

In conclusion, this training procedure does not detect outliers in the input data in real time and adapt the training accordingly. Also, as the target list is just a finite set of points, additional errors may appear due to interpolation. As a potential *a posteriori* solution the algorithms can be prepared to deal with the robustness problems caused by these caveats (Lin et al., 2018). We propose a

parallel potential *a priori* solution focused on optimizing the training protocol itself.

5.4 A novel velocity based controller closed-loop training paradigm

Here we propose a novel controller closed-loop training strategy for mitigating the previously discussed caveats. The main idea is simple: the learning algorithm makes use of the real time knowledge about the previous performance of the user in order to modify adaptively the current target that the user sees. In order words, it introduces a closed-loop term that modify the current target, $\mathbf{d}(t)$, based on the previous errors $\mathbf{d}(t') - \mathbf{u}(t')$, $t' < t$. A block diagram of this new controller learning paradigm is depicted in Fig. 5.2.

The targets are modified according to the next rule:

$$\bar{\mathbf{d}}(t) = \mathbf{d}(t) - \sum_{t'=1}^{t-1} \left\| \mathbf{d}(t') - \mathbf{u}(t') \right\|^2 \tag{5.4}$$

The second term in Eq. 5.4 adapts the training, reinforcing the learning in the directions that have caused errors. This term updates the final target $\bar{\mathbf{d}}(t)$ increasing the training time in those movements where the algorithm performs poorly and reducing the time spent in the directions where the model is already working well. This effect persists until the error is corrected; i.e., if the next target is the same as the previous one, it means that the algorithm did not learn anything and it must continue the training repeating the same movements until it finally learns how to perform that movement (exploitation learning phase). The model learns by itself how to generate the training movements starting from an universal set of targets, the predefined $\mathbf{d}(t)$, designed to guarantee the exploration learning phase by introducing movements in different directions.

With the proposed controller training strategy, we ensure that the input data to the controller learning algorithm is customized to the particular behavior of the corresponding user. This is very important, specially for real patients, where we find a large diversity in physiological characteristics, e.g., the ability to generate some myoelectric signals depends strongly on the kind of amputation and active muscles. So it is vital that the training session is able to detect those difficult movements and over-train them until the user-controller system

performs well and under-train those movements that are already learned by the algorithm.

In the next section we show how this new paradigm can be effective in order to obtain better training sessions compared to the uniform non adaptive controller open-loop traditional mode.

5.5 Experimental paradigm

5.5.1 Data acquisition

The same hardware explained in Chapter 4 was used. As usual, the armband is placed in the upper part of the forearm. However, this experiment is independent of the muscles source, therefore reproducible with other EMG signals from different origins. Previous works (Igual et al., 2020, 2019a) have used these specifications for the data acquisition protocol with successful results.

In this case, the experiment was performed by 20 able bodied participants (13 males and 7 females) and 4 with limb deficiencies (2 males and 2 females) with ages ranging between 20 to 60 years. All participants provided written informed consent before the experiment. The experiments were in accordance with the declaration of Helsinki and were approved by the UPV ethics committee, approval number P11-23-03-18.

5.5.2 Controller

The proposed new controller training paradigm is designed based on the general definition of regression-based algorithms; therefore, it is adaptable to different controllers.

In this chapter we use the same velocity controller introduce in Chapter 4 (Igual et al., 2019a) based on the one pole IIR linear filter:

$$\mathbf{u}(t) = \mathbf{y}(t) - \mathbf{A}(t)\mathbf{y}(t-1) = \mathbf{B}(t)\mathbf{x}(t) \tag{5.5}$$

where $\mathbf{u}(t)$ is the controlled output (direction of movement), $\mathbf{y}(t)$ is the current estimated position, $\mathbf{A}(t)$ the IIR matrix to be estimated, $\mathbf{B}(t)$ the FIR part of the filter that must also be estimated and $\mathbf{x}(t)$ is the input features (in this

case, the root mean squared (RMS) vector of the EMG raw signal). The IIR filter is reduced to a velocity control of independent DoFs, i.e., $\mathbf{A}(t) = \mathbf{I}$ (see Chapter 4 for details).

It is important to emphasize that the proposed procedure is independent of the regression model used. For example, an alternative can be found in Hahne et al. (2015), where they use a position control based model without the IIR filter part. The goal is to show the benefits of the proposed closed loop controller training scheme, not to compare different controllers. Also note the difference between the novel closed-loop structure used in the controller training that we propose in this chapter which is not related to the commonly used closed-loop structure for the human-machine feedback channel with sensory cues as both co-exist in this system.

5.5.3 Study design

Training phase design

Participants are asked to sit in a comfortable position with the elbow flexed 90 degrees and the forearm pointing forward. After the armband is placed and the Bluetooth connection is opened, the experiment starts. The whole process is divided in two controller training phases: traditional open-loop paradigm (Fig. 5.1) and the novel proposed closed-loop paradigm (Fig. 5.2). The participants are divided equally in two groups: half of them perform first the open loop training and later the closed loop one; the other half perform the reverse trainings order. The number of controllable DoFs is 2, so $\mathbf{B}(t) \in \mathbb{R}^{2\times 8}$.

Open-loop training: Figure 5.3(a) shows the user-screen interface that represents the open-loop structure from Figure 5.1. Similarly to the one used in Chapter 4, the center of the coordinate system corresponds to the rest position and the two controlled DoFs are mapped in the vertical and horizontal axis. The vertical axis corresponds to wrist flexion/extension movements and the horizontal axis to wrist radial/ulnar deviation. The positional target $\mathbf{d}(t) = \mathbf{y}_d(t)$ is displayed as a green circle and the user current estimated output $\mathbf{u}(t) = \mathbf{y}(t)$ is prompted as a red cursor after each iteration of the algorithm. Participants get familiarized with all the interface elements and their meaning before starting the experiment. The training protocol consists of 5 laps, i.e., $L = 5$ in Eq. 5.3. Each lap is divided in 4 active targets (up, left, down, right) and 4 rest targets alternated with the active ones. For each target the user has to perform the related EMG pattern $\mathbf{x}(t)$. The user has ten seconds to reach the target and maintain the cursor within the target for one

second. If this happens, the target is hit and the next target appears. If after the ten seconds this requirement is not fulfilled, the target is missed and the next target appears. During this phase the model updates the $\mathbf{B}(t)$ coefficients in real time (eq. 5.5).

Closed-loop training: Figure 5.3(b) shows the user-screen interface for the closed-loop training paradigm (Figure 5.2). In this case, the targets $\bar{\mathbf{d}}(t)$ are a modified version of the predefined trajectory $\mathbf{d}(t) = \mathbf{y}_d(t) - \mathbf{y}_d(t-1)$, where $\mathbf{y}_d(t)$ is the previously defined position. The interface presents the target $\bar{\mathbf{d}}(t)$ as a yellow arrow centered in the origin of the coordinate system and rotates over it. The modified directional target $\bar{\mathbf{d}}(t)$ (eq. (5.4)) is represented with the arrow. The user performs the related EMG pattern $\mathbf{x}(t)$ to the arrow's direction. In this case the targets are directional (m dimensional vectors pointing to the direction of movement), instead of positional targets (desired positions) as in the open-loop training case; this directional representation has a more similar behavior to a real prostheses since they are usually based on velocity commands and not position. As for the DoFs, wrist flexion/extension and wrist ulnar/radial deviation are used as in the position control paradigm mapping them to vertical and horizontal movements respectively. The main novelty takes place in the background, with a hidden evaluation process the target generation takes into account the user performance to adapt the target (the bottom of the closed-loop in Figure 5.2) exploring directions that might not be considered in the initial target list D.

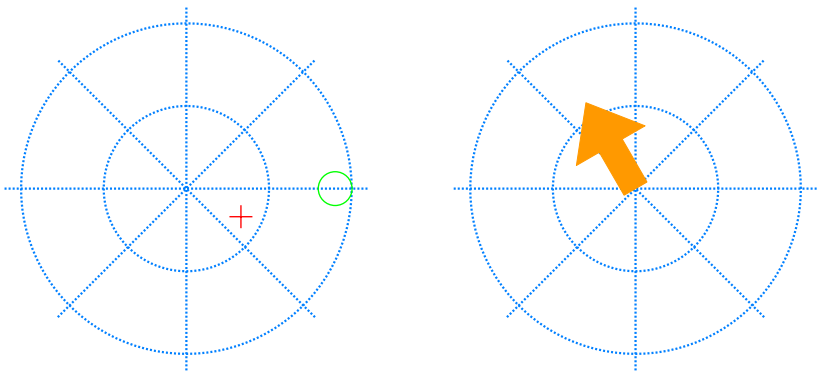

Figure 5.3: User interfaces. (a) User interface adapted to the traditional open-loop controller training paradigm. Red cross: estimated output $\mathbf{u}(t)$. Green circle: current target $\mathbf{d}(t)$. (b) User interface adapted to the novel closed-loop controller training paradigm. Yellow arrow: Desired target $\bar{\mathbf{d}}(t)$.

A lap is initiated at the center and starts moving in the up direction for 6 seconds with constant speed, i.e., $\mathbf{d}(t) = [0, 1]$, $0 < t < 6$, and bounces back to the center for the next 6 seconds, i.e., $\mathbf{d}(t) = [0, -1]$, $6 < t < 12$. After those 12 seconds, the target generates the same kind of trajectory but for the other three semiaxis in a counterclockwise direction (left-right, bottom-up and right-left). A lap consists on this four movements. The whole training process consists of 5 laps totaling 240 seconds. The user estimated output, $\mathbf{u}(t) = \mathbf{y}(t) - \mathbf{A}(t)\mathbf{y}(t-1)$, is estimated with the velocity control model (eq. 5.5). The $\mathbf{A}(t)$ and $\mathbf{B}(t)$ coefficients are updated in real time creating the closed-loop structure proposed above and updating the user estimate. The target is modified, as mentioned previously, feeding the resulting direction to the user through the arrow in the interface. Therefore the target generation depends on the user performance while the user is only aware about the trained direction at each time period. To make the results comparable, note that both paradigms start with the same initial target list, which includes only 1 DoF activation targets. However, the closed-loop model is able to generate new training directions while the open-loop paradigm is constrained to the predefined set ($\mathbf{d}(t)$ is not modified before it is shown to the user, no matter the previous performance).

Test phase design

After each training, the participants perform the same test phase from Chapter 4 but in this case with only 10 seconds to reach the target and remain inside for 1 second. As before, the model for the test is frozen and the targets are prompted in a pseudo-random order (the same for every participant). The test ends when the participant goes trough the 36 targets that cover the complete output space.

To quantify performance we used several metrics described in Chapter 4: the completion rate (CR) defined as the number of hit targets over the total, the path efficiency (PE) as the shortest path between targets over the path followed by the user, the completion time (CT) as the time to complete a target (or 10 seconds in case of a missed target) and the attempt ratio (AR) as the number of entrances in a target per complete targets.

5.6 Results

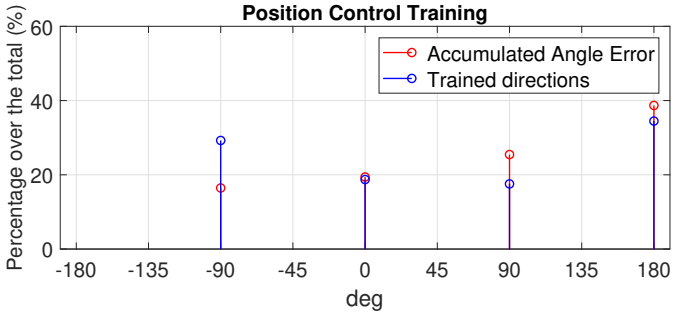

(a)

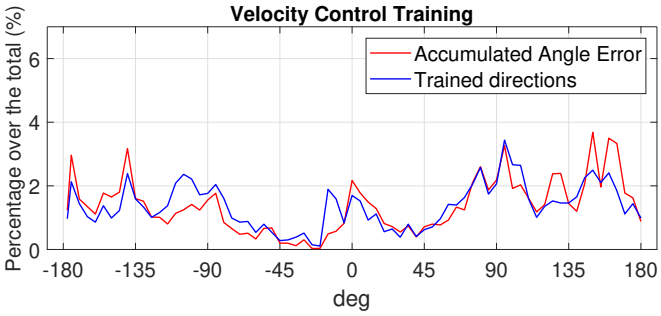

(b)

Figure 5.4: Training time and error distribution. (a) Controller open-loop training paradigm. (b) Controller closed-loop training paradigm. The two plots show the training metrics for a specific able-bodied participant. The blue lines represent the percentage of time used to train a specific direction over the total training. The red lines represent the percentage of the accumulated error in a specific direction (eq. 5.6) over the total of the complete training. Note how the case a) generates a discrete distribution while at b) one is continuous with a high correlation with the accumulated error (i.e. it spends more time training the directions that showed errors). In plot b) the data is sampled for visual purposes, generating a data point every 5 degrees with a value equal to the sum of the interval values.

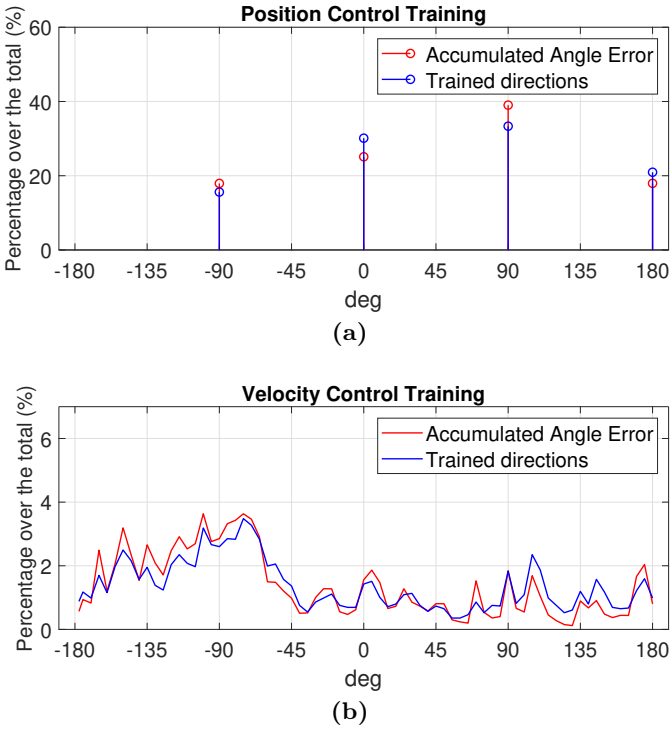

Figure 5.5: Training time and error distribution. Same plot as in Fig. 5.4. This time with the results of a limb-deficient participant.

5.6.1 Training analysis

The first result is the different target distribution generated by the two paradigms. While in a controller open-loop training paradigm (see Section 5.3) this distribution is finite and limited to a predefined target list with cardinality $|D| = 4$, the novel controller closed-loop training paradigm (see Section 5.4) searches in a continuous $[-\pi, \pi]$ range of values.

In Figure 5.4 we show the time spent in each angle (percentage) during a training session by an able bodied participant (the blue lines). While the controller open-loop training paradigm results in a discrete learning of only the four principal directions (predefined targets), the controller closed-loop training protocol trains all directions exploring outside the principal directions (predefined targets). We show in Figure 5.5 the same case for an amputee, obtaining the same conclusion.

The second experimental result is related to the target generation process. While in a open-loop protocol the targets are listed in advance and fixed, this does not occur in the closed-loop version. In this last case, the target generation, as stated in Eq. 5.4, depends on the accumulated error. The paradigm autonomously emphasizes the training in those directions that generate errors, aiming to minimize them. As the targets depend on the error, the larger the error in one direction, the longer the time to learn and minimize that error, i.e., the algorithm by itself is able to allocate smartly the training time dynamically depending on the performance. This error over the final system input $\bar{\mathbf{d}}(t)$ is computed as:

$$\mathbf{e}(t) = \bar{\mathbf{d}}(t) - \mathbf{u}(t) \tag{5.6}$$

with $-\pi < e(t) \leq \pi$. The relation between this error and the trained directions in the closed-loop structure is shown (red lines) in Figure 5.4 (b) and 5.5 (b) for able-bodies and amputees respectively. We can see how the peaks and valleys of the error and the trained directions have a similar pattern. We obtain that the able bodied participants have an average correlation value between error and trained directions of $\rho = 0.799 \pm 0.108$ while in the amputees group the average correlation value is even higher, $\rho = 0.863 \pm 0.052$ ($p = 0.27 > 0.05$ for a two-sample t-test, so we can not reject the null hypothesis that the average correlation of the able bodied and amputees populations are equal). As an example, in Fig. 5.6 we show the Pearson correlation for one able bodied case ($\rho = 0.79$) and an amputee case ($\rho = 0.93$).

As a consequence of this high correlation, both paradigms also differ in the user customization of the training session. While a open-loop protocol is fixed and does not depend on the user, we observed that the closed-loop paradigm generates targets dependent on the accumulated error and therefore on the user performance. This difference in the trained direction distributions leads to a customized training in the controller closed-loop training version. With this method, each participant training is focused on the regions with the worst performance, which differ among users. Figure 5.7 illustrates this result comparing the trained directions histograms of two participants from the same group for both groups. The histograms show that in each case participant 1 and 2 perform a completely different training. In the case of Figure 5.7 (a) we can see how able-bodied 1 (blue) trained considerably the directions between -45º and 0º. However, able bodied 2 found the control in this range relatively easy but hard to learn the range from 90º to 180º.

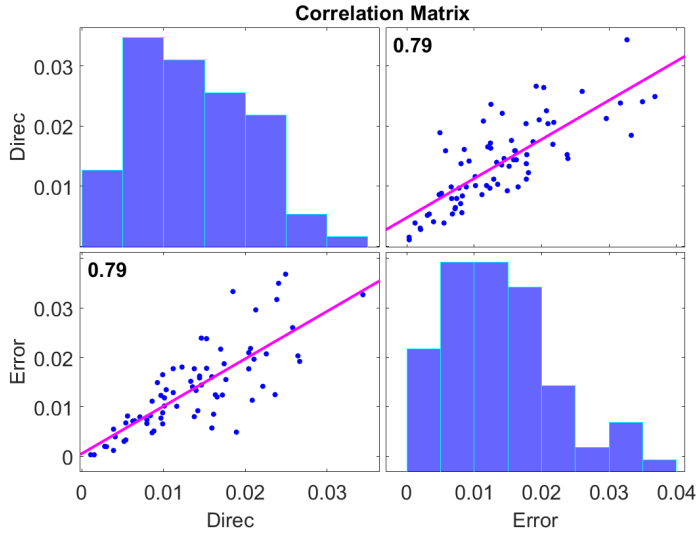

(a)

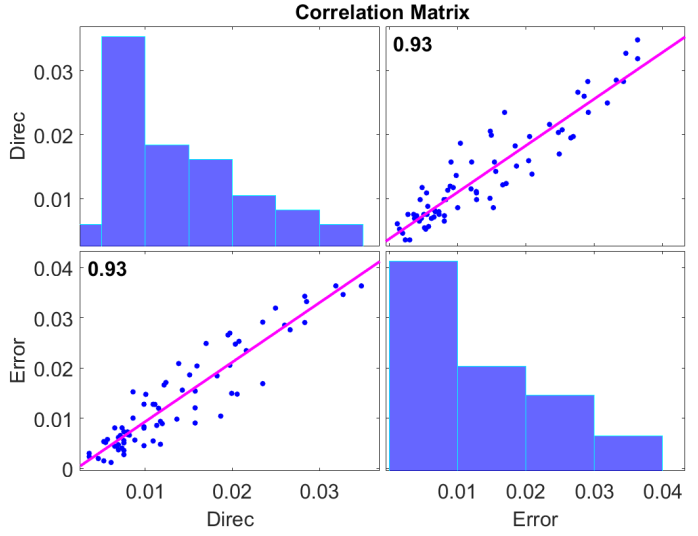

(b)

Figure 5.6: Correlation analysis. (a) Able bodied participant. (b) Participant with limb deficiency. Pearson correlation test with two variables: the trained directions (Direc) and the accumulated error (Error) for the controller closed-loop training paradigm (eq. 5.6). Both participants show a high correlation value between the two variables as shown in Figures 5.4 and 5.5.

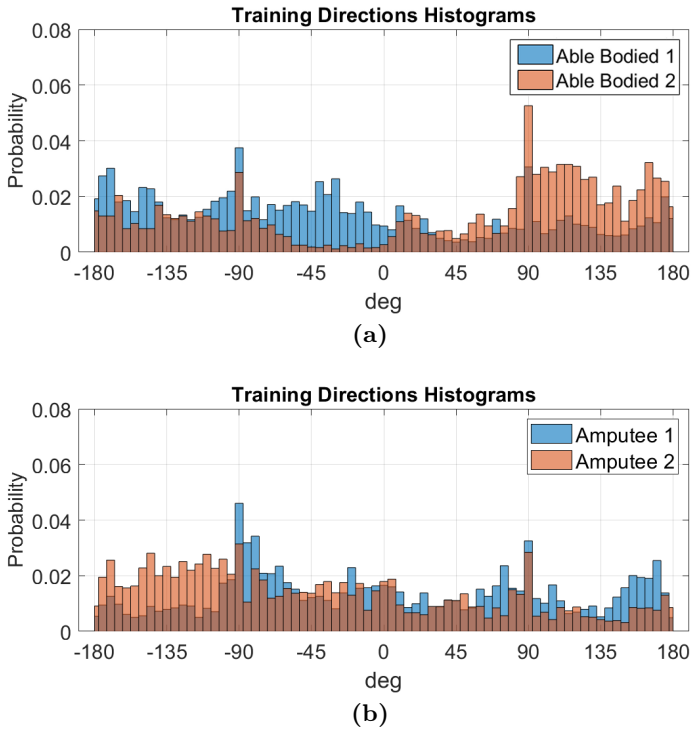

Figure 5.7: Comparison of training time histograms. (a) Able bodied participants. (b) Participants with limb deficiencies. The plots show the trained direction probability histogram for two participants in each case (blue and orange). Note how the histograms are different due to the adaptation to each patient performance.

5.6.2 Test analysis

The analysis of the metrics during the test phase (Table 5.1) shows a significant improvement in the system performance with the novel closed-loop training strategy. As we can see, the completion rate metrics increases about a 10% in both groups while the path efficiency metric is more than doubled in both cases. The stability is also improved significantly as we can see with the decay of the attempt ratio, close to 1 in both groups with the closed-loop strategy, indicating that once the targets were hit the participants had the control to stay inside.

	Able Bodied		Limb Deficient	
	Open-Loop	Closed-Loop	Open-Loop	Closed-Loop
CR (%)	86.25	95.83	58.33	69.44
PE (%)	39.55	83.74	24.83	56.55
CT (s)	4.81	6.79	6.76	7.32
AR	1.67	1.08	2.27	1.17

Table 5.1: Test metrics. Average metrics (Completion Rate (CR), Path Efficiency (PE), Completion Time (CT) and Attempt Ratio (AR)) among all participants divided by groups for the test phase.

5.7 Discussion

We have demonstrated the differences and benefits of a novel controller closed-loop training paradigm against the classical open-loop version for a regression based myoelectric prosthesis control.

The first practical benefit is the continuity in the generated target list. The continuity of the output in regression-based algorithms was the main advantage against the classical classification-based algorithms. However, this characteristic has only been exploited for the test phase, maintaining a discrete training paradigm based on the traditional classification protocols. In this sense, the controller closed-loop structure introduces a changing control input signal that achieves the exploration of continuous set of possible outputs during the training, generating a diverse and complete training data set. In the case of the open-loop paradigm, the trained targets are immutable, belonging to a finite predefined list.

The second benefit is related with the following question: can we detect the most difficult movements for each user in real time during the training in order to reinforce the learning of these movements?. With the proposed closed-loop strategy, the learning starts with a predefined target-list; but the target is modified in real time depending on the accumulated error (which is related to the user performance and the difficulties that he/she may have in some directions). In this sense, the learning is reinforced in the directions that have shown accumulative errors in the past; which generates an autonomous customization of the training for each individual. In contrast, the open-loop version does not adapt the training autonomously, being the same for all participants and relying on the capability of the user in generating the correct data.

As a consequence, the participants have improved the completion rate and the path efficiency by +10% and +50%, respectively.

Finally, we want to highlight that these two benefits arise from the controller closed-loop training structure (Fig. 5.2) and not to the specific target-modification rule (Eq. (5.4)). In addition, this closed-loop learning structure could be applied to other machine-learning problems that are not strictly related with EMG prothesis control but whose learning principles are similar.

Summarizing, we have presented a novel controller closed-loop training paradigm that enhances the qualities of the regression based models compared to the classical controller open-loop training paradigm. While the second ones try to minimize the training session relying on the capability of the algorithm to generalize to unknown movements, the novel paradigm follows an efficient training time distribution focusing the training on the worst targets. At the same time, this novel strategy explores the whole input spectrum generating a continuous input target list, opposite to the discrete training in an open-loop version. This is a characteristic of any regression model versus the classification approach that has been overseen till now in the proposed regression based prostheses controllers. As an additional advantage, we accomplished to autonomously create a personal training for each participant depending on his/her needs and performance. All this lead to a significant improvement of the system performance, mainly of the path efficiency. These findings make the novel controller training protocol a potential solution to improve the performance of the current state of the art myoelectric prosthesis control by improving the training data set generation and learning process.

Chapter 6

Robustness analysis

One reason to explain the reluctance to deploy more advanced controllers in the commercial prostheses is robustness. Traditional controllers are validated by many years and users, so open the door to another controller paradigm requires a lot of evidence. In this chapter we approach the robustness against donning/doffing and arm position for recently proposed linear filter adaptive controllers based on myoelectric signals. We show that the model learned during the initial training is robust enough to different scenarios. It means that the adaptive linear regression approach can be one candidate for future real world controllers. The adaptive approach allows to introduce some feedback in a natural way in real time in the human-machine collaboration, so it is not so sensitive to input signals changes due to donning/doffing and arm movements.

Chapter based on **Igual, C.**, Camacho, A., Bernabeu, E. J. and Igual, J. (2020). Donning/Doffing and Arm Positioning Influence in Upper Limb Adaptive Prostheses Control. In *Applied Sciences*, vol. 10, nº 8: 2892. JCR Impact factor: 2.47 (Q2).

Contents

6.1 Introduction

In the last years the upper limb prostheses control has become a growing research field (Igual et al., 2019b). The prosthetic industry has been developing new prostheses to mitigate the effects of losing a limb. However, despite of all the research and efforts carried out, there is a gap between the newer developments in the academia and the available commercial prostheses. The main problems the research faced have been a low user satisfaction and high prosthesis rejection due to a non-functional use (Biddiss and Chau, 2007a; Biddiss and Chau, 2007b; Datta et al., 2004; Davidson, 2002; Vujaklija et al., 2016). Because of that, nowadays a primary goal in this field is to find prostheses control protocols robust enough to be used in real life.

As seen in previous chapters, there have been several developments in all the areas of the prosthesis control systems, including new prostheses technologies (Pasquina et al., 2015b). Nevertheless, most of these improvements have never been implemented in real life devices. One of the reasons is the lack of usability in real world scenarios. Thus, although these new systems have a high performance in controlled environments, they exhibited a lack of robustness when tested in daily life situations on realistic environments (Igual et al., 2019b; Jiang and Farina, 2014; Scheme et al., 2011). Several factors could generate non-stationarities in the EMG signals that fed the system limiting a robust performance. The most common problems are: limitations of EMG signal acquisition process (Beck et al., 2008; Lendaro et al., 2017; Mastinu et al., 2015; Pasquina et al., 2015a), arm positioning (Fougner et al., 2011; Hwang et al., 2017), electrode shifting (Hwang et al., 2017; Prahm et al., 2019; Young et al., 2011), skin conditions (Jiang et al., 2012), fatigue (Cipriani et al., 2011) or time degradation (Amsüss et al., 2013). These factors affected the reliability of modern prosthesis control methods over time and conditions of use. A lot of work is being done in this direction in order to obtain controllers that behave in a more natural and robust way (Dohnálek et al., 2013; Marasco et al., 2018; Mastinu et al., 2017; Scheme and Englehart, 2011; Scheme et al., 2010).

We have previously proposed an adaptive auto-regressive proportional myoelectric control system (see Chapter 4), which showed a much effective performance in controlled environments, such as laboratory experiments, than the today state of the art regression models. The goal in this new work is to analyze whether this higher performance is maintained under real life "noisy" conditions, i.e., to study the robustness of the system against external disturbances while performing the virtual task. Firstly, we analyze the effect of time

degradation and small electrode shifting; to do this, the participants simulate the real life use of prostheses by a donning/doffing experiment during a four-day period. Secondly, we study the robustness and generalization of the model for different configuration environments; to do this, the participants carried out a consecutive series of tasks while the arm position is changing. Our results demonstrate the algorithm capabilities to overcome non-stationary inputs without any re-adjustment. These capabilities are essential for a comfortable real prosthesis control and open the possibility that the proposed method could be implemented in the future in a test stage with real patients in a clinically supervised experiment.

6.2 Materials and methods

See Chapter 4 for details about the methods and data acquisition process.

The two disturbances effect studies were conducted independently with different participants so we can guarantee that there was no learning contamination from one experiment to the other; 8 able-bodied participants (5 males and 3 females) executed the donning/doffing experiment and 4 participants (2 males and 2 female) the arm position experiment. Participants were in between 20-50 years old. All individuals provided written informed consent before the experiment. The experiments were performed in accordance with the declaration of Helsinki and were approved by the UPV ethics committee, approval number P11-23-03-18.

6.2.1 Study design

All participants were asked to sit in a pleasant position so that they could perform the entire experiment in a comfortable way, minimizing the movement of different parts of the body other than the desired arm movements. Two wrist DoFs were used in this study: wrist flexion/extension and radial/ulnar deviation measuring the forearm EMG activity of those movements. The flexion/extension movements were mapped into the vertical axis and radial/ulnar deviation into the horizontal axis of the 2D interface explained in Chapter 5 (see Figure 5.3 (b)). To guarantee that the participant run the experiment naturally, no more instructions were given about how to move. Few additional instructions regarding the experiment and the user interface used were given. In this way, we ensured that the subject knew the objective function and understood the procedure to achieve the goal. Henceforth, the device was initialized and the experiment started.

Experimentation had two procedures: training and testing. Depending on the experiment purpose, the protocol of the procedure execution was different.

Training phase

During the training, the machine and the user collaborated to achieve a common goal: minimize the error between estimation and target. The proposed co-adaptive system set both agents (machine and user) as active learners. The machine learning algorithm obtained the model coefficients grouped in the $\beta_i(t)$ vector for each direction, while the user adapted his behavior to the estimated machine output. As feedback, a visual interface was prompted to represent the machine's performance in a natural and understandable environment for the user (see Figure 5.3 (b)).

The training process consisted in 4 laps as in Chapter 5. One lap was 32 seconds long, 8 seconds each movement. Therefore, the complete training (4 laps) lasted 128 seconds. The training phase was equal for every participant independently of the experiment. The purpose of the training was to generate the model coefficients for each participant. They were requested to try to follow the target with the cursor controlled by their wrist movements.

Test phase

The test phase evaluates the performance of the coefficients learned during the training. With a fixed model, the participants controlled a cursor in a visual interface used as feedback (the same as in the experiments in previous chapters).

The test consisted in a total of 36 targets that covered the full space. Targets in every direction were displayed testing in untrained positions and the ability to avoid over-fitting. The participant had to reach and stay in a target for two consecutive seconds before a 10 seconds timer expired. Once accomplished the task, the next target was displayed and a new 10 seconds timer started. If the user did not achieve the task, it was considered a miss and a new target was prompted with the corresponding new timer. The 36 targets were shown in the same random order for all participants. The user was requested to reach each target as fast and straight as possible.

6.2.2 Experimental paradigm

Donning and doffing protocol

Eight participants were used to analyze the effects of donning and doffing the armband on the system performance. The right arm was set in the same position for all sessions, with the elbow flexed 90 degrees, to do not add more variables. All participants executed the experimental protocol shown in Figure 6.1 (testing and resting days) in the same schedule to obtain comparable results.

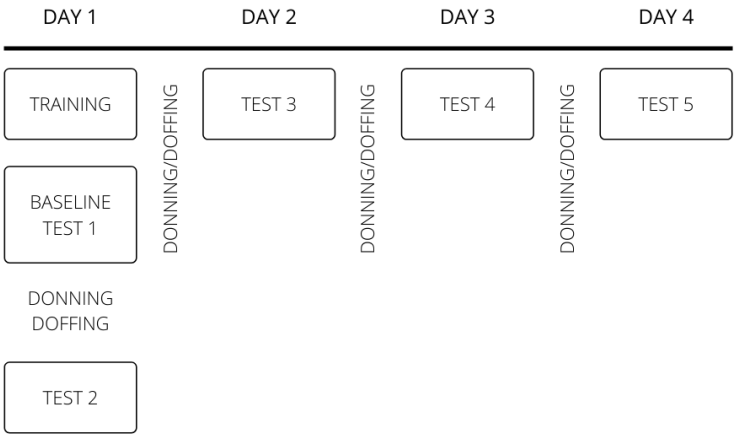

Figure 6.1: Donning/Doffing experimental protocol scheme. All test sessions used the same model learned on day 1 training session. Five tests were performed after the training session. First, a baseline test is executed immediately after completing the training, so the differences between testing and training conditions are minimal. Afterwards, starting at the same day, one test per day is performed. The donning and doffing of the Myo Armband was carried out on the first day between the baseline test 1 and test 2 and between experimental days.

The first day the participants completed a training phase. The model learned during the training was used in all the tests sessions in order to study its degradation through time and donning/doffing. The first test after the training was performed without any electrode shifting and without removing the sensor. This was considered the baseline test. Once the first test was completed, the Myo Armband was removed and the participant had a 5-minute break. Afterwards, a second test phase was performed relocating the Myo Armband.

The positioning was done in realistic and manual conditions without any technical procedures. The researcher photographed the initial position to place the sensor as similar as possible in further sessions. No other re-positioning considerations were taken into account trying to reproduce a realistic environment where a daily-based prosthesis user places it without absolute precision.

The following days the participants performed one test phase per day, with the same trained model, completing three more tests. At the end of the entire process each participant had carried out one training session and five test sessions.

Arm position protocol

Three arm positions were adopted to analyze the effects of arm postures variation: straight arm pointing aligned with the torso (P1), elbow flexed 90 degrees (P2), and straight arm at a 90 degree angle to the torso (P3) (see Figure 6.2).

Figure 6.2: Training arm positions. Each position involves different muscle activation and has different effects from gravity and fatigue. P1: Arm fully extended pointing down with the wrist. P2: Arm pointing front with the wrist and elbow flexed 90 degrees. P3: Arm fully extended pointing front.

The experiment protocol was divided in three sessions conducted in one day. A single session had one training and four tests. First, the training was carried out in one of the three arm positions P1, P2 and P3, and then tested in all of them. The fourth test evaluates the robustness in a less controlled environment. During this test (P4), the participant was requested to variate the arm posture at his will after three consecutive targets without constrains. This was repeated

two more times, until all the arm postures (P1, P2 and P3) were used as the training arm position. The test in each session using the trained position was considered the baseline to compare with the results of the other positions. The order of the training position was permuted between patients to cover all combinations.

6.2.3 Performance metrics

To quantify performance we used several metrics described in 4: the completion rate (CR) defined as the number of hit targets over the total, the path efficiency (PE) as the shortest path between targets over the path followed by the user, the completion time (CT) as the time to complete a target (or 10 seconds in case of a missed target) and the attempt ratio (AR) as the number of entrances in a target per complete targets.

6.3 Results

6.3.1 Donning and doffing experiment

The obtained metrics (mean and variance) of the five donning/doffing experiments for each subject are shown in Table 6.1. They are shown graphically in a box and whisker plot in Figure 6.3.

Figure 6.3 shows that the completion rate metric had a consistent high value for all subjects. In our previous work at Chapter 4 (Igual et al., 2019a) we showed that the IIR adaptive algorithm had a 95% CR when the training and test armband position were the same. In this study it was observed that the high completion rate was not diminished by the donning/doffing effect. Three participants achieved a median 100% accuracy and the worst result was a value of 90% for subject #3 one day. Figure 6.3 also shows that the variance is small for all participants and metrics. It means that after training the first day, the system was robust enough to maintain the same performance the next days both in space and time efficiency.

Only one participant showed a wider variance in path efficiency, subject #6. Looking into the time evolution of the results for that subject, we discovered a continuous learning trend during the experiment. This was the only patient that showed an accentuated learning behavior as the others kept a more robust performance.

Participant	CR (%)	PE (%)	CT (s)	AR
1	99.44 ± 1.24	90.75 ± 1.86	5.338 ± 0.387	1.017 ± 0.025
2	97.78 ± 3.62	87.20 ± 1.95	5.554 ± 0.230	1.046 ± 0.034
3	95.00 ± 2.32	75.32 ± 4.00	6.153 ± 0.321	1.212 ± 0.076
4	98.33 ± 2.49	92.28 ± 2.40	6.151 ± 0.230	1.049 ± 0.066
5	92.22 ± 3.62	73.42 ± 3.07	5.673 ± 0.388	1.151 ± 0.087
6	95.55 ± 4.65	82.56 ± 7.85	5.740 ± 0.499	1.121 ± 0.116
7	95.00 ± 3.62	79.90 ± 4.03	5.568 ± 0.257	1.070 ± 0.060
8	93.33 ± 2.48	92.14 ± 1.98	5.994 ± 0.217	1.053 ± 0.047
Avg	95.83 ± 3.00	84.19 ± 3.39	5.771 ± 0.316	1.090 ± 0.064

Table 6.1: Performance metrics for the eight participants in the donning/doffing experiment. The metrics tabled are completion rate (CR) as the completed targets over the total targets, path efficiency (PE) as the shortest distance over the total distance traveled, the completion time (CT) as seconds per target and the attempt ratio (AR) as number of attempts to hit a target. Each row presents the results for one participant showing the value and the variance for each metric. Last row is the average of all subjects.

Analyzing our results in deep, Figure 6.4 shows the PE for subject #6 (blue line) compared to the average value of all participants (black line) vs. the test number. It reveals that the PE performance of subject #6 improved during the training sessions, while the other participants had a steady performance, with an approximately 84% PE value. Thus, his higher variance in the PE metric is not due to a lack of robustness but to a learning process.

A repeated measures ANOVA ($p < 0.05$) confirms that no-one metric was changing with time, reassuring the robustness of the initial training: CR $p = 0.8397$, PE $p = 0.3152$, AR $p = 0.8096$, and CT $p = 0.5311$. To confirm the robust behavior, we run a MANOVA test that restates the results obtained with the previous ANOVA analysis: there was not statistically sufficient evidence to reject the hypothesis that all metrics come from the same distribution ($p < 0.05$).

The values in Figure 6.3 and Table 6.1 provide a visual and quantitative performance analysis of the adaptive filtering algorithm in donning/doffing experiments, but do not show the dynamics of the experiments, i.e., the user experience.

To show this behavior in a more intuitive and visual way, we included some videos where the dynamics of the system are appreciated. We show the trajectories for each test for the five tests for the first seven participants:

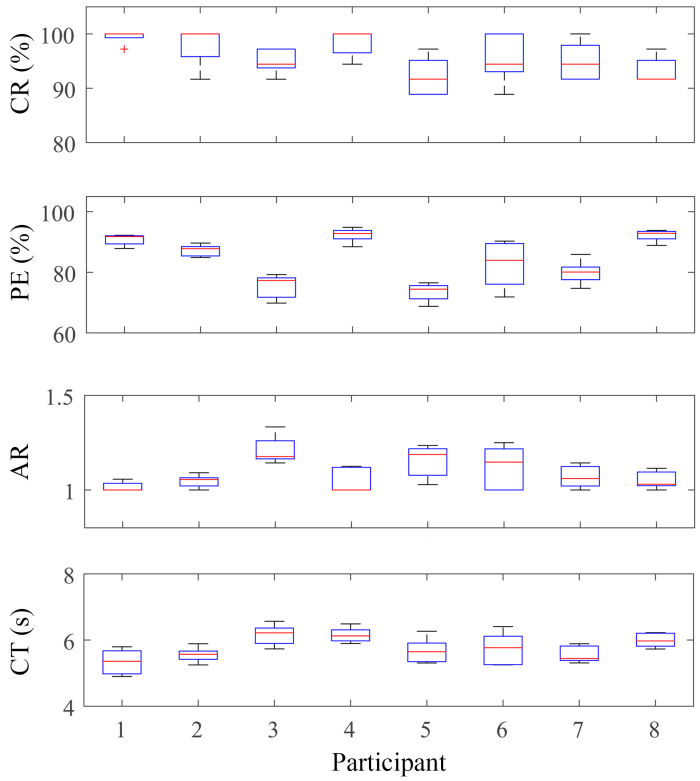

Figure 6.3: Robustness analysis. Box and whisker plot for the Completion Rate (CR), Path Efficiency (PE), Attempt Ratio (AR) and Completion Time (CT) for each participant. Except for patient 6's PE value, the rest of the boxes show a small variance. This is a proof of a consistent behavior through time.

participant 1 [1], participant 2 [2], participant 3 [3], participant 4 [4], participant 5 [5], participant 6 [6] and participant 7 [7]. In the videos every test is represented by a different color: red, green, blue, cyan and magenta for test 1,2,3,4 and 5 respectively. The next target for a corresponding test is displayed with the same color code at any given time. For a visual purpose targets are plotted

[1] https://youtu.be/whB_6Ci76oM
[2] https://youtu.be/2GKl48cotCI
[3] https://youtu.be/iFlcD628Wnw
[4] https://youtu.be/DzmafnQnKcQ
[5] https://youtu.be/5T5EtZtTOWA
[6] https://youtu.be/DE5Tv4Euikc
[7] https://youtu.be/Yj2aICLStlO

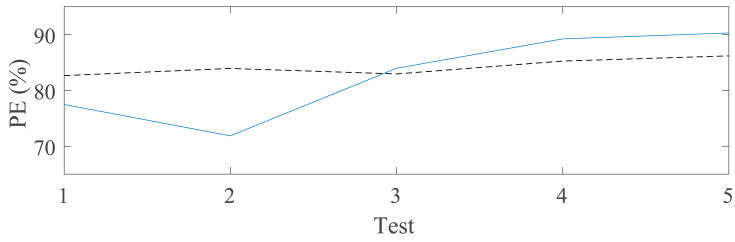

Figure 6.4: Path efficiency case. PE for subject #6 (blue line) and average PE value between all participants (black line) vs. the day of experiment. This figure explains that the larger variance of the PE value for that participant is not due to instability problems of the algorithm, but to his learning process (his performance improved significantly from test 1 to 5). Once the learning saturates (as we can see in the last two tests) the behavior started to be more stable like the other participants results.

as circles with different diameters. Note that in the real experiments all the circles (targets) had the same size. In addition, to avoid that the plots become too cumbersome because cross crossing trajectories, only a few samples are plotted. Analyzing the videos, if lines are far away, it means that some target was missed or the path efficiency was changing from test to test. The way to check the simplicity from the user point of view is to check if the trajectories are close to the straight lines joining the previous and next target. A curve that is moving around a target means that the attempt ratio was poor (AR much greater than 1), since it means that the user was entering and leaving the target in an unstable way. This behavior of the system will be translated from the user point of view, first, as an insecure experience, and later, if he finds out that this instability is persistent in time, in a disaffection to the system.

In order to show a visual interpretation of some trajectory patterns examples that determine the global PE values, Figure 6.5a shows the paths traveled by two users: participant #1 (red curve) and participant #5 (green curve) for targets 1 to 5. It is clear that the path between targets 2 and 3 was smoother for subject #1. The longer path traveled by subject #5 translated into a lower PE compared to subject #1 PE. There were other trajectory behaviors in this timespan that were related to the path efficiency. Note that the red trajectory was smoother not only between targets, but also in the transition (when one target was achieved and the next one was shown to the user). On the contrary, the green line is slightly advanced than the red line; the user chose between a faster movement with the risk of a potential instability or at least more attention since muscle activity translates into more erratic trajectories,

and a smooth movement where inertia can be sometimes an annoying issue depending on the subject perception.

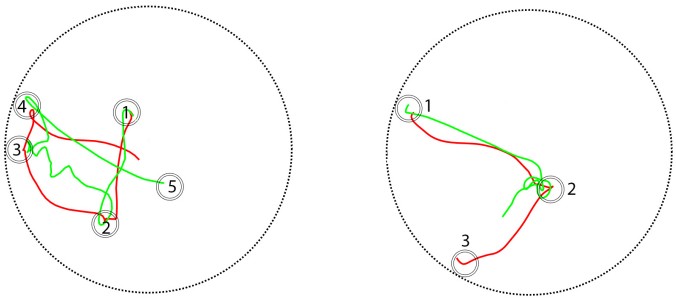

Figure 6.5: Example trajectories. (a) Path for test 5 for subjects 1 (red) and 5 (green) for the first five targets. This is a comparison between a high PE and a lower PE value. Green path shows a more erratic behavior reaching a lower PE value as the red path follows an almost straight trajectory from target to target with a high PE value. (b) This is an attempt ratio value example showing the stability of the controller to maintain a position. Red line corresponds to subject 1; green line corresponds to subject 3. The subject 1 entered the target 2 and remained inside at the first try. Opposed to this, subject 3 entered and left the target two times until the target was missed. The participant, in this occasion, was not able to maintain the position having a less stable control measured by the attempt ratio value. This is a representative sample from the training. The behavior presented in this plot is common among all users.

In Figure 6.5b we show the trajectories for subjects #1 (red line) and #3 (green line) moving from target 1 to 2 and then to target 3 on test 5. The performance in this timespan gives us a visual example of the AR metric values. It is clear that subject #3 had difficulty maintaining the position in target 2. He achieved target 2 easily from target 1, but could not remain into the circle for two consecutive seconds. He left and entered the circle several times. As a consequence, the attempt ratio was increased indicating a less stable position control, also the completion time metric was increased, i.e., it was delayed with respect the path defined by subject #1. As we can see in the Figure 6.5, subject #1 was able to arrive to the third target while subject #3 was still in between. This effect seems to be repeated occasionally as we can see in Table 6.1 comparing the AR and CT values for both participants.

Analyzing statistical relationships between the different performance metrics, we found a positive correlation between the CR and PE and a negative correlation between the CR and AR. This is in accordance with the expected

values. A high CR means that few targets were missed so the subject was accomplishing the task; i.e., the path efficiency must be high and the attempt ratio must be low in those cases. We also obtained a negative correlation between the path efficiency and the attempt ratio. However, the time required to complete the experiments is independent of the other metrics.

6.3.2 Arm position experiment

The arm position experiment was developed to test the robustness of a model in unknown arm positions (different to the trained one) and also to study if any of the training positions obtains better results. The mean values for each metric, training and testing position are shown in Figure 6.6. The free arm positioning was called P4 to simplify the notation.

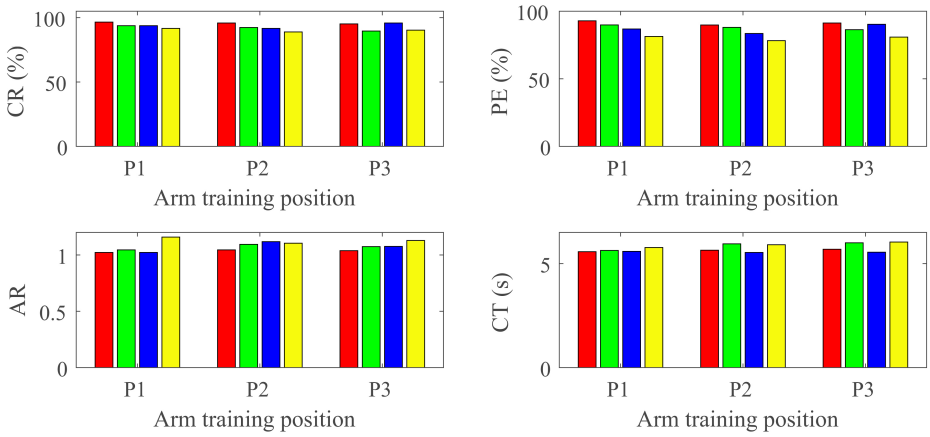

Figure 6.6: Arm position experiment metrics. Mean CR (top-left), PE (top-right), AR (bottom-left) and CT (bottom-right). The horizontal axes are the training positions. The color bar represent the arm position during the test: P1 for the red bars, P2 for the green bars, P3 for the blue bars and yellow when there were no restriction in the arm position (P4). The height of the bar indicate the corresponding metric average value between all participants.

The exact mean values are shown in Tables 6.2, 6.3, 6.4 and 6.5.

Figure 6.6 plots the data for every test. Our results clearly show that the performance is high regardless the learning position or the training position. The minimum CR= 89.58% is obtained for the model trained in P3 when tested in P2; the rest of the CR values are above 91%. The PE values are also high independently of the combination, with PE$\geq$ 83%. The system was

Training	Test P1	Test P2	Test P3	Test P4
P1	96.53	93.75	93.75	91.67
P2	95.83	92.36	91.67	88.89
P3	95.14	89.58	95.84	90.28

Table 6.2: Completion Rate metric analysis. Average Completion Rate (%) metric among all users for different training and test arm positions. Each row indicates the arm position used to train the model. Each column indicates the arm position used to test the model.

Training	Test P1	Test P2	Test P3	Test P4
P1	92.91	89.85	86.87	81.32
P2	89.78	88.06	83.50	78.22
P3	91.30	86.34	90.31	80.84

Table 6.3: Path Efficiency metric analysis. Average Path Efficiency (%) metric among all users for different training and test arm positions. Each row indicates the arm position used to train the model. Each column indicates the arm position used to test the model.

robust against arm positioning variations. Figure 6.6 also shows that the trend inside each training arm position is consistent with all the different training options, i.e., the bars follow a similar pattern for all the training arm positions. This confirms that the results were independent of the training position.

The results in Figure 6.6 indicate that P1 was the best testing position. Position P1 (red bars) performed slightly better than P2 (green bars) and P3 (blue bars) in almost all metrics, independently of the training arm position.

We applied the non parametric Friedman test for repeated measures to each training position. The results revealed a statistically significant difference for the PE metric with values of $p = 0.0112, 0.0129, 0.0194$ for the three different training positions. A posterior multiple comparison test indicated that the difference was between testing in P1 and testing in P4 (free movements) in all cases. After ranking the PE for the different training positions, P1 was always ranked in the first place and P4 in the last position in all experiments except one.

We also observed qualitative results related to the effect of fatigue and usability. All the patients reported ending up very tired after performing the test in P3. Holding the arm straight generated shoulder fatigue that did not allow the patients to keep a consistent performance. Some participants even stopped at

Training	Test P1	Test P2	Test P3	Test P4
P1	1.022	1.045	1.022	1.159
P2	1.045	1.094	1.118	1.104
P3	1.038	1.074	1.076	1.128

Table 6.4: Attempt Ratio metric analysis. Average Attempt Ratio metric among all users for different training and test arm positions. Each row indicates the arm position used to train the model. Each column indicates the arm position used to test the model.

Training	Test P1	Test P2	Test P3	Test P4
P1	5.573	5.632	5.590	5.776
P2	5.643	5.950	5.536	5.908
P3	5.690	6.001	5.549	6.037

Table 6.5: Completion Time metric analysis. Average Completion Time (s) metric among all users for different training and test arm positions. Each row indicates the arm position used to train the model. Each column indicates the arm position used to test the model.

some point to relax the arm. This observation is related to the quantitative results seen before, where P3 tests have lower PE values training in P1 an P2. This effect was mitigated when P3 was the training arm position because the fatigue was included in the training information.

The yellow bars in Figure 6.6 give information about the system robustness against arm position changes within short periods of time (P4). These tests were performed allowing the users to move the arm with no restrictions at all becoming every test unique, therefore not comparable with other test. In any case, the results showed that all the metrics had an expected drop in this dynamic and uncertain scenario. The user adaptation was proven to be essential in this case. The participants managed to maintain a high performance (CR=90.28% and PE=80.13% on average). However, the system and the user needed a moment after changing the arm position to adapt to the EMG variations of it. Changing the arm position generated a transitory state in the EMG where the muscle activation was the result of changing the arm position and not due to the controller. Added to this effect, because of having a new arm position, the EMG patterns differ from one position to the other, so the user has to find again the correct activation patterns for the control. This process would take a small amount of time, but enough to generate an

unavoidable decay of the metrics. After this, the users performed consistently again until the next arm change.

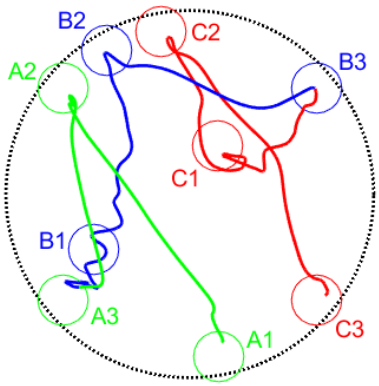

Figure 6.7: Trajectories in arm position experiment. Trajectories during free arm position test. During this test the participants were asked to change the arm position every three targets. Each color represents the estimations for the period of time (three targets) that one arm position was hold. Three sets of three targets and the trajectories followed between them are plotted: Set A (green), Set B (blue) and Set C (red). Starting from A1, after reaching the last target of each set, A3 and B3 (which means changing the arm position), the plot shows how the trajectories became more erratic. Once the user adapted to the new position the behavior returned to a smooth control. This is a representative sample from the training. The behavior presented in this plot is common among all users.

An example of this is illustrated in Figure 6.7. In order to prove the robustness against the disturbance we can analyze the behavior in these situations. Figure 6.7 demonstrates how the participant presents a high PE before changing the arm position (before reaching A3 and B3). After moving the arm to the new position, there was a drop in the PE (after leaving A3 and B3) followed by the user reaction against the drop, successfully recovering the high PE.

6.4 Discussion

An important handicap of the current myoelectric prostheses controls is the performance degradation suffered facing daily EMG pattern alterations. These effects emerge as a result of "noisy" factors that alter the input data. An ideal control should overcome these disturbances and lasts for a long time under different real-life scenarios before the performance starts to degrade and a re-calibration is necessary. In this chapter, we have analyzed whether the adaptive IIR linear filtering control previously described in Chapter 4

(Igual et al., 2019a) satisfies these robustness requirements for an optimal prostheses control. The results demonstrate that the performance of this recently proposed method was not affected by the time elapsed since training or the small electrode shifting deviations due to donning/doffing the armband in consecutive days that alter the EMG patterns. Moreover, we also show that the models trained in a specific arm position kept the high performance in other arm positions and that this position can be changed at any time. Thus, the important novelty of this work relies on the capabilities of the algorithm to stay stable through different disturbances without any re-adjustment. In spite of the encouraging results, a larger number of subjects must be tested in order to enhance the statistical confidence in the results reported in this paper. In addition, we have to experiment with limb deficiency subjects in order to analyze if the robustness is maintained in real patients.

It has to be noted that in this study, and along the whole manuscript, we used wrist movements to control the active DoFs. This is not a restrictive choice. As far as there are enough independent patterns, any muscle activation could be used as input. For some patients, such as amputees, the limitation in the EMG signals that they can generate will limit the number of DoFs and the pattern selection. At the end, EMG patterns will be mapped to the available movements in the prosthesis no matter which is the biological origin. If desired, the EMG patterns could be selected to match the prosthesis functions. In summary, the algorithm performance relies only on the independence of the EMG signal patterns. Of course, the larger the signal to noise ratio, the better the system will be able to map the EMG signals into the desired movements.

In order to exploit the benefits of the algorithm, the training protocol was implemented as a co-adaptive task in real-time. Due to the IIR adaptive algorithm characteristics (the previous estimated output is used to estimate the next output in addition to the new EMG signals), the system was able to learn the dynamics of the user-computer interaction in real time avoiding any post processing, allowing to obtain a velocity controller in a natural way. If one of the agents does not operate properly, the other part will become confused, affecting its learning and performance. In practice, it means that user must try to generate similar EMG patterns for a given movement. This is the main advantage of using an adaptive filtering approach: the learning of a continuous and dynamic environment enhances the capability to overcome small variances in the input data.

A first approach focused on the effect of small electrode shifting and time that alters the EMG patterns. The donning/doffing experiment proved that the models learned in a short training (128 seconds) are usable for

at least four days, keeping a high performance. Neither the removal of the sensor nor the long-term use affected the system behavior. In some ongoing tests, some patients have been using the same model for months without significant degradation. These observations strongly support that the model is robust enough to overcome these two real life disturbances. Previously, the FIR version of the model (Hahne et al., 2015) was tested against similar disturbances in Hwang et al. (2017) being significantly affected by the donning/doffing of the electrodes. Overcoming these disturbances is another benefit of the novel IIR version.

Another important aspect of the study is the analysis of the influence of arm position. Modifying the arm posture introduces other disturbance sources as gravity, fatigue or EMG offsets that alter the initial EMG patterns. The results proved that the model was able to generalize from single arm positions to unknown situations keeping a high and stable performance. This is essential for a natural prosthesis control where the user has to be able to control the hand movement with similar EMG patterns no matter the position of the arm.

Other interesting observations came out from this experiment. Note that P1 position gave better results regardless of the training position used to learn the controller. Initially, one could expect that the best results during the test would be achieved by the same position used while training. One possible reason for these results is the effect that external conditions as fatigue or other muscle activity can generate in the system performance. In P1 position the arm is completely relaxed except for the active muscles used to perform the desired movement. Other positions (P2 and P3) require strength to hold the arm position, involving phenomena like gravity, fatigue or tension. These factors will generate and offset in the EMG patterns, non-related to the control task. The absence of this needless information and effort in P1 would be evidenced in a slight improvement on the performance metrics. Our findings also show that the algorithm is robust and efficient even in dynamic situations as the test P4, where participants reproduced a more realistic use. The change of the arm position every three targets generated a transient period where control became erratic since the signal to noise ratio became very low. However, this was quickly overcame by user adaptation, recovering the control and the high performance in a short time. On the other hand, none of the tested training positions seemed to be significantly better for training the model as we could have expected. This makes us think that the clue is again the consistency of the EMG patterns. As far as this is accomplished, this algorithm will learn a high performance model. This is possible thanks to the natural way in which the system learns that a velocity control is the best strategy. Note

that in a system where the learning procedure is based on position control and during post-processing the velocity control is enforced, the system lacks the ability to respond in real time to changes in the input signal patterns. The observations proved that the model was robust enough against the EMG variations generated by different arm positions. This is strictly necessary for a natural prosthesis control where the users arm movements should not affect the prosthesis behavior.

In summary the new model has a high and robust performance in all the real life conditions presented for our able-bodied participants. After facing different types of disturbances that alter the EMG signals, we found out a general benefit of the new model applied to all of them. Since the robustness of the adaptive system is increased with respect to other controllers, it is also remarkable that the model does not need any adaptation or special training further than a basic and short initial training. This helps the user to understand and to increase the acceptance of this controller. The capability to overcome daily disturbances without re-calibrating or re-training the model is a great advantage for the user.

Our future work will replicate and extend in time these experiments in real patients to test if the system is also robust for end users with limb deficiencies in real life scenarios and to increase the number of participants. This future work is initially supported by the results shown in this study for healthy subjects in real conditions and the fact that in Chapter 4 (Igual et al., 2019a) the behavior of the adaptive algorithm was similar for healthy and real patients in controlled conditions.

Chapter 7

Future work

The development of a novel co-adaptive regression based control combined with the new training paradigm allows to perform robustly in non-controlled scenarios with 2 controllable DoFs. These results open the door to more complex applications and the introduction of newer technologies such as extending the control to 3 DoFs, using Virtual Reality (VR) interfaces or deploying the model in real prosthesis. This work is in a preliminary stage, however some promising results indicate its potential as future post doctoral research activities.

Contents

7.1 3 DoFs control

After the success of controlling 2 DoFs, the idea is to extend the regressor to a larger space, 3 controllable DoFs. To the best of the author's knowledge, this task has not been achieved so far with a fully proportional and simultaneous control. In this case we keep the two previously defined degrees of freedom, flexion/extension and radial/ulnar deviation, and introduce a third dimension: opening/closing the hand.

7.1.1 Material and methods

The idea is to extend the controller from Chapter 4 adding a third dimension. Since we are assuming independent movements, the theoretical model is the same; the only difference is that we have to estimate the filter coefficients of the new DoF. From a implementation point of view, it means that eq. 4.5 is extended to the case $i = 1..3$.

As a baseline, we started with a preliminary study setting $p = q = 0$ as it is easier to develop a clear UI and generate a more static training in order to achieve consistent EMG patterns from the users. Later on, with further modifications in the UI, we are capable of switching the environment to the case $p = 1$. In any case, the data acquisition process stays the same as in Chapter 4 while the training and testing are adapted to the new three-dimensional space. The test phase stays very similar testing the complete output space in a uniform distribution and the results are evaluated with the same metrics defined in Chapter 4.

So far we conducted the experiment with ten able-bodied participants (6 males, 4 females) with ages ranging between 20 to 50 years. We also tested two male individuals and a female with limb deficiencies. All participants provided written informed consent before the experiment. The experiments were in accordance with the declaration of Helsinki and were approved by the UPV ethics committee, approval number P11-23-03-18.

Training paradigm

The user interface was modified to represent a three-dimensional environment. The three controllable DoFs are the 2-D position of the mobile object and its size. As in previous experiments, the vertical and horizontal axes are related to the flexion/extension and radial/ulnar deviation movements of the wrist respectively, while the opening and closing of the hand controls the size (larger or smaller) of the object.

During the training, the targets are labeled depending on their number of active DoFs. The target values on each DoF are set to: -1, 0 or 1 (-1 or 1 would be an active DoF value while 0 would set the DoF to an inactive condition, see Figure 7.1).

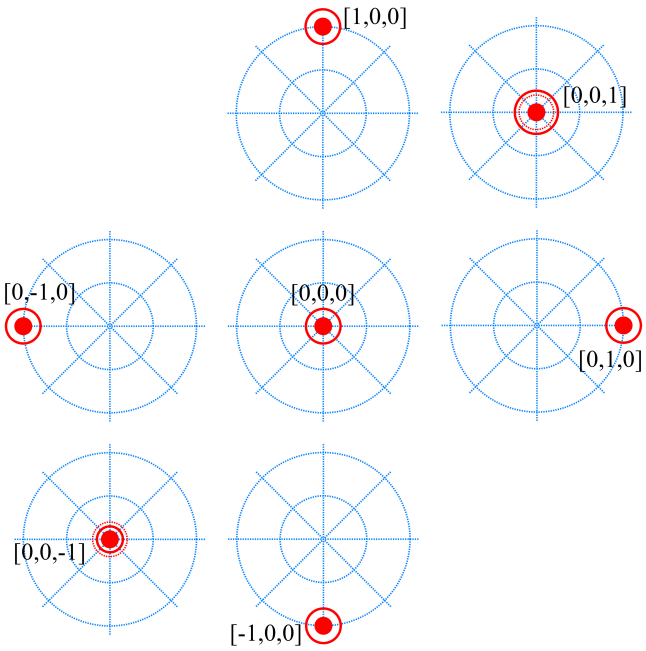

Figure 7.1: Blind training 1 active DoFs targets. The controllable dimensions are the x and y axes and the size of the target. The first two dimensions are represented by a solid circle located at the exact position. The third dimension is represented by a solid ring that increases or decreases its size. To give feedback of the neutral position in the third dimension the target element has a dashed ring in the 0 value of the third dimension.

This distribution generates 27 possible targets combining the three possible values at each DoF: rest position, 1 active DoF (6 possible targets shown in Figure 7.1), 2 active DoFs (12 possible targets) and all 3 DoFs active (8 possible targets).

From here we design three different training protocols and compare them to find out which one reinforces more the benefits of the controller and achieves a more optimal 3-DoF model:

- **Protocol 1**: A blind training with no user feedback about the system's performance. A lap is defined as going once through all the possible 1 active DoF targets with a rest target after each of them. The training is completed after five of these laps.
- **Protocol 2**: A blind training with no user feedback about the system's performance. It develops one first lap as defined in Protocol 1. Afterwards, it goes once through all the possible combined targets (2 and 3 active DoFs) with a rest target after each of them. The difference with respect to Protocol 1 is that here the training goes through combined DoFs targets to reduce the non-trained regions.
- **Protocol 3**: It develops 1 first blind lap as defined in Protocol 1. Afterwards, we activate the user feedback channel showing the controller output with another mobile element (Figure 7.2). The training continues going once through all the possible combined targets (2 and 3 active DoFs) with a rest target after each of them. The difference with respect to Protocol 2 is that here the user has feedback during the combined DoFs targets.

Test paradigm

After each training the participants performed a test where they had to fit the cursor into a positional target. By controlling the 3D cursor they had 20 seconds to reach each target's 3D position with less than a 10% error. If they are capable of reaching and holding this position for 1 second within the 20 seconds the target is considered a hit. If this requirement is not fulfilled the next target is prompted.

The test targets are all the possible combinations of the different DoFs with the three possible values (27 targets) covering the complete output space.

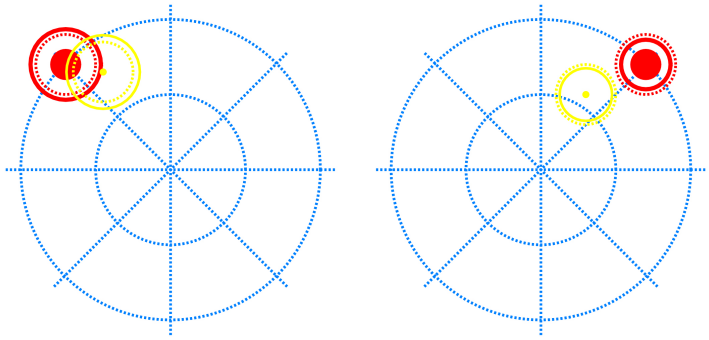

Figure 7.2: Feedback training at 3 DoFs experiment. The targets follow the same representation as in Figure 7.1. The user estimate is represented by a yellow object that follows the same principles. In this case there is a pointer that marks the location of the two first dimensions and should be fit into the solid area of the target. The controllable object also has a ring which size should match the target's one.

	Able Bodied			Limb Deficient		
	CR (%)	PE (%)	AR	CR (%)	PE (%)	AR
P I	64.31	37.75	2.292	16.67	24.67	3.185
P II	71.53	47.71	1.999	28.24	29.71	4.571
P III	76.25	45.97	1.655	43.52	30.35	1.8

Table 7.1: Metric analysis. Average metrics among all participants divided by groups and training protocols (P I, P II and P III) for the test phase.

7.1.2 Preliminary results

Figures 7.3 and 7.4 show the different metrics for both groups depending on the type of target and the training protocol.

The results show an improvement in all metrics from Protocol I to Protocol II (except at the AR for amputees) as a consequence of introducing the combined targets in the blind training. Protocol III achieves the best results globally for each type of target and subject and in average (Table 7.1), proving the utility of the co-adaptive approach.

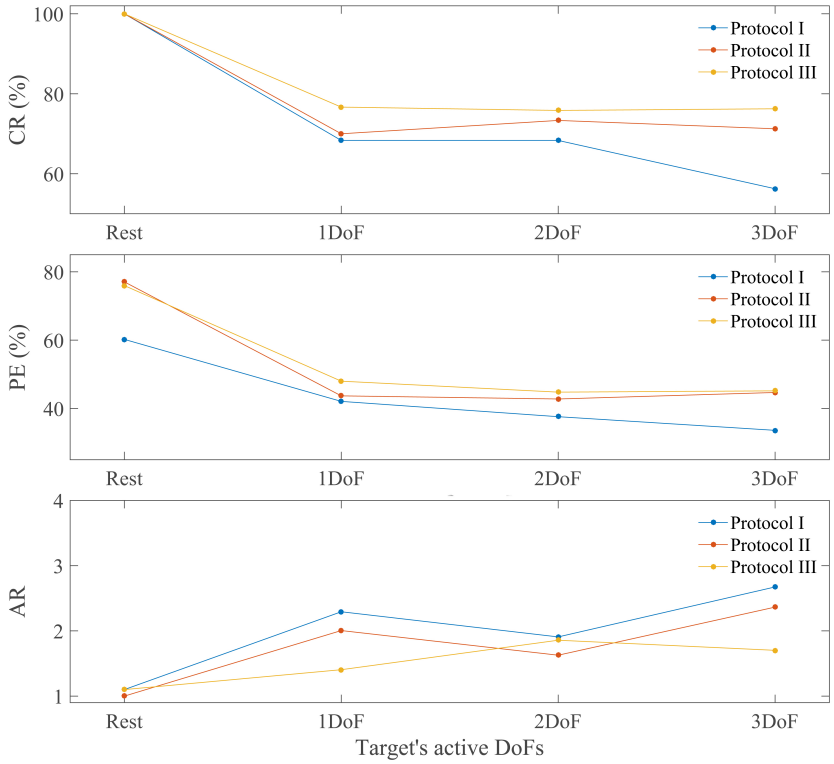

Figure 7.3: Able bodied metrics. Each panel shows the results for each metric depending on the type of target and the training protocol used.

A non-parametric Friedman test followed by a Bonferroni test for each possible pair, revealed that the improvement from training with 3 active DoF targets vs 1 active DoF targets (protocol I vs. II), was statistically significant only for path efficiency (Figure 7.5). However, the co-adaptive training (protocol III) was statistical significant better than protocol I for all three metrics. and in the case of PE the significance was extended to 2 active DoFs targets. This proves how Protocol III is significantly better than Protocol I for the goal of controlling simultaneously the 3 DoFs while none of them remains inactive.

This results could variate with the continuation of the experiments as it is still on going and the number of participants should increase.

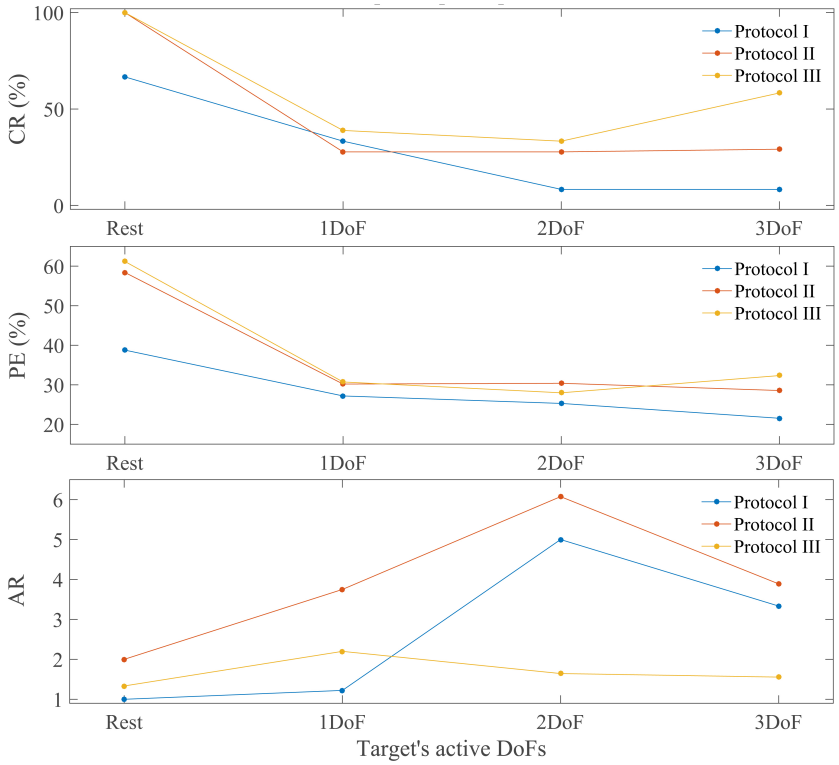

Figure 7.4: Participants with limb deficiencies metrics. Each panel shows the results for each metric depending on the type of target and the training protocol used.

The introduction of co-adaptation did not generate a significant statistical difference between the other training protocol that used combined targets (Protocol II and III). However, we find the key difference between I and III showing a significant improvement in all metrics related to 3 active DoFs (see Figure 7.5), and in the case of PE the significance was extended to rest and 2 active DoFs targets. This proves how Protocol III is significantly better than Protocol I for the goal of controlling simultaneously the 3 DoFs while none of them remains inactive.

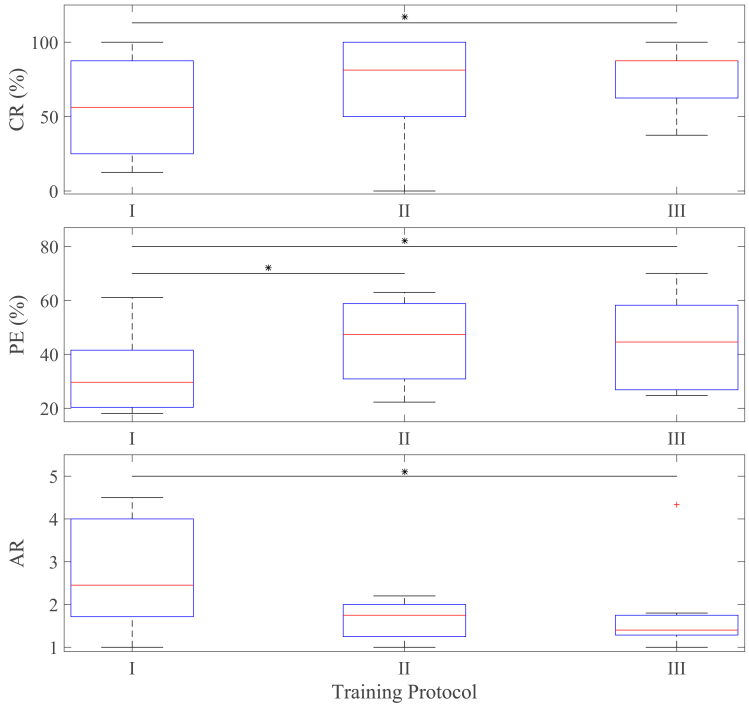

Figure 7.5: Statistical test. Each panel shows the boxplots for each metric in the case of 3 active DoFs targets (only with able bodied participants as the number of participants with limb deficiency is not large enough for an statistical test). The cases with significant difference are indicated with an asterisk.

In Figure 7.6 we focus on the Completion Rate metric. For able bodied participants there is a positive trend as we progress on the training protocols. We can see how the orange targets (missed by the 60% of the participants) become greener with the third protocol as more targets are achieved reaching a 70% of success among participants. In the case of amputees the results are less accurate, but nevertheless we can observe the same trend. At Protocol I almost all targets are missed by all the participants while in the last stage (Protocol III) there is a larger amount of orange targets and some green ones.

All these results prove how the introduction of multiple active DoFs targets combined with a co-adaptive learning allow the model to improve the learning of a fully simultaneous and proportional 3D control for able bodied. In the case of participants with limb deficiencies the algorithm reached the best accuracy in the literature so far to the best of the author's knowledge.

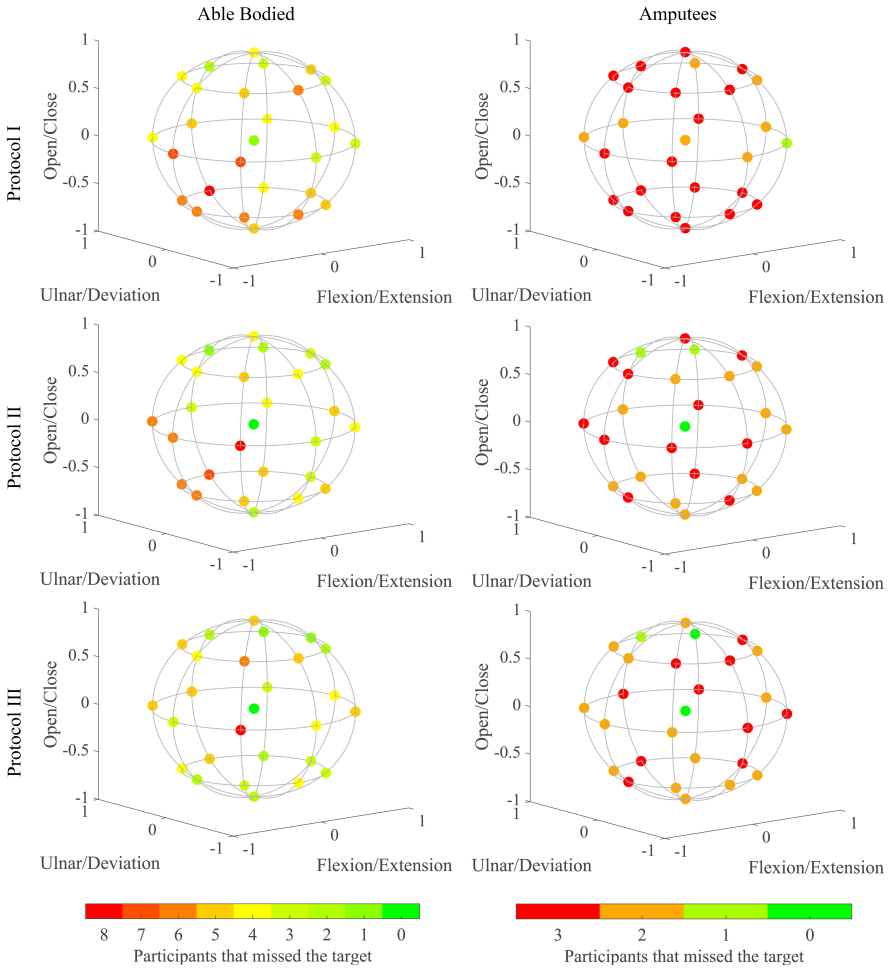

Figure 7.6: Completed targets. The plot is divided depending on the participant group and the training protocol used. Each target is colored depending on the number of participants that missed it.

Adding only one of the two attributes to the training did not generate a significant improvement, while the combination of both proved to be the key to a useful control. So far 3D control has been solved by controlling the 3DoFs in pairs always leaving one inactive and switching the combined pair. The novelty here relies on the capability to fully control the 3DoFs at the same time achieving a consistent performance.

7.2 Virtual reality interface

With the introduction of a third DoF and the complexity of representing a three dimensional space in a two dimension interface we found the need to search for more suitable options to give the user a proper target representation that improved the understanding and therefore the EMG pattern generation.

The UI is the key to a good learning, even more important in the participants with limb deficiencies, as it tells the participant the EMG pattern to perform. The information has to be clear and precise to avoid any type of misunderstanding.

In the last decades the Virtual Reality technology has suffered a major development. This technology offers the perfect qualities for an efficient UI as it directly represents the final use without any misconception. An example with different targets is presented in Figure 7.7.

Figure 7.7: VR interface. Each picture shows the desired target in the VR interface and a smaller image of the wrist movement performed by the user while wearing the Myo armband.

Switching to a VR representation generates a more immersive experience to the user. The need of the user to translate the interface information to arm movements is erased. With the VR interface the user is already controlling the final *product*, an external hand as the prosthesis. Here there is no doubt about the EMG pattern requested as the participants see the hand moving and know which is the desired muscle contraction.

For participants with limb deficiencies this is a great improvement as sometimes visual targets can be hard to correlate to muscle contractions that are not easy to perform consistently. With hand movements the user is more capable of reproduce the same movement each time as it is a straight related target.

The software used to develop the new interface was Unity with version 2019.3.7f1.

7.3 Prosthesis experimentation

A final step to conclude the validation of the proposed controller in this thesis was the deployment of the controller into a real prosthesis. During the stay at the *ART-Lab*[1] in Göttingen we had access to a Michelangelo Hand (Figure 7.8) from *Ottobock*[2] to test the developed system in a real device. However, the limited time access did not allow for a properly designed experiment, but was enough to run some validation experiments.

The development of a prototype to test the model was set as the next goal. In this direction we recently started the manufacturing of our own prosthesis with 3D printing technology. This will allow us to test the controller in the last of the product design stages.

The preliminary test was a success as the user was capable of robustly and accurately control the prosthesis for several manipulative tasks as grasping objects with different shapes or the clothespins relocation test. Figure 7.9 shows snapshots of different prosthesis positions and the interaction with objects fulfilling the user's intentions using the model trained in Chapter 4.

[1] `http://cuop-umg.de/forschung/forschungsthemen/artlab`
[2] `http://ottobock.com`

Figure 7.8: The Michelangelo Hand from Ottobock. The picture shows the prosthesis and the adapter for able bodied users manufactured by the ART-Lab.

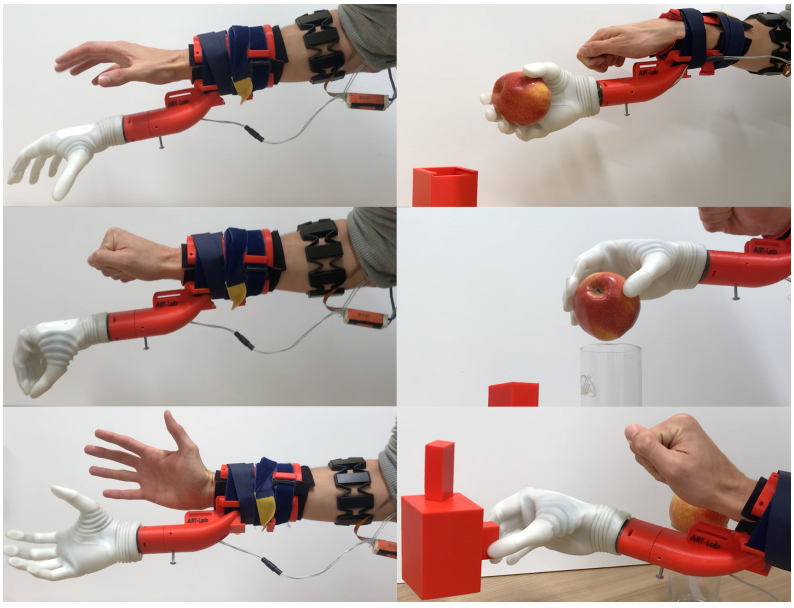

Figure 7.9: Prosthesis experiments. Different snapshots from the test process showing prosthesis positions (left column) and the manipulation of several elements with different shapes and objectives (right column).

Chapter 8

Conclusion

The myoelectric prosthesis control field suffered during the last decades from the gap between the academia and the industry not allowing the latest developments to reach the market. For this reason, in Chapter 2, the state of the art of upper limb prosthesis control and the most relevant caveats the field is facing were introduced.

Firstly, the different input signals for upper limb prosthesis were explored, focusing on EMG signals as an option characterized by its easy access and low signal processing cost without compromising the high performance. Secondly, the next element of the control loop, the learning process, was presented. Nowadays there are two main control models: classification and regression. Classification solutions were the first approaches used for this application. However, this kind of control has an inherent discrete component that generates a rather artificial user experience resembling the typical robotic movement. In pursue of a more natural movement, regressor models allow to map the muscle activity into a continuous output space. Despite of this, regressors did not present enough robustness to overcome some of the real world daily disturbances. As a consequence, the older paradigm based on classification remains the standard controller in today commercial devices. These prostheses are based on a switch that allows to change from one DoF to another and are trained based on the EMG-target patterns (classification approach).

Hitherto, the major interest in the literature has been over the learning algorithm, not paying enough attention to the training paradigms, which play a critical role at reaching the full algorithms' potential. While training technologies and feedback channels have grabbed all the attention in the last decade, there has been a lack of transformation and analysis in the relationship between the two agents, machine and human, during the training phase. Focusing on this element of the system, this manuscript introduced the co-adaptive concept in Chapter 3. So far, the two learning agents (machine and human) were trained independently and in different learning stages in time. However, the integration of a co-adaptive training proved to be an important capability for future algorithms. Making both learners interact and influence each other offers the possibility to solve, in real time, stability problems and escape from local minimum solutions.

This implementation allows the machine and human to learn simultaneously maximizing the benefits of both learners leading to a consistent and robust controller. The model is learned based on the interaction between machine and human and generated from their understanding. This interaction saves future problems that raised when both agents, trained independently, interact for the first time with an already frozen model during the test stage without the capability to adapt simultaneously. With past methodologies the adaptation relies completely on the human once the machine is trained and some times the gap between them is too wide. With co-adaptive strategies these problems are minimized from a consensual solution.

Although this strategy requires a much more amount of time and thinking to carry out the experiments (note that the co-adaptive approach only allows real time online learning experiments, since the training is different for each participant and even for the same participant is different for each iteration of the same experiment), we show the advantages of this approach with respect to fixed target based training paradigms and offline learning (the previously recorded EMG signals are used to train the controller).

To the best of the author's knowledge, regression based prostheses faced a problem achieving high performances and efficient control in real life scenarios. Taking advantage from the benefits of the co-adaptive strategy, the development and implementation of a novel regression based algorithm is presented in this thesis (see Chapter 4). This model overcomes some of the state of the art regression problems for prosthesis control, including current regressors as special cases of the proposed models.

The model is based on a recursive filter used for myographic control. The new closed-loop system merges different control strategies titrating between them depending on the user's intention during the training. The novelty of the system relies on the possibility to train directly a proportional velocity control. This option resulted as the most natural model converged by the users. Moreover, this was not only the most natural option, it also achieved the highest performance compared to other state of the art methods. The hypothesis is that this control represents a more natural, comfortable and intuitive behavior for the user. The controller managed to improve the performance of state of the art regressor in a 2 controllable DoF environment. Additionally, preliminary studies proved the consolidation of this results extending it to a 3DoF environment. This utility has not been achieved before with a fully proportional and simultaneous control to the best of the author's knowledge. This manuscript presents the first results of a 3 DoFs simultaneous and proportional control which integrates all the novel training strategies introduced through the thesis. Since experiments require a lot of time and people, due to the special circumstances (COVID-19 pandemic) in which this new experiments must be carried out, we decided to separate them from this thesis (future post doc work).

As another conclusion from the analysis on the training process, the implementation of this algorithm and the co-adaptive system open the possibility to other kinds of training, which have proved to be more optimal. The velocity control strategy has been present as a final layer in some state of the art proposals that used it to overcome the limitations of a positional based control. This was necessary and beneficial due to the functionality of a real prosthesis, usually controlled by velocity commands. However, the training remained in a positional environment. Chapter 5 detailed a novel co-adaptive training protocol that directly trains a velocity control, without the need to implement it afterwards, offering several benefits. This novel closed-loop controller training generated an autonomously personalized training that distributed optimally the training time at each target depending on the user performance while exploring the continuous output space. As this training covers the complete output space, there are no unknown values which makes the algorithm more robust for future disturbances at the same time that the performance increases with the optimization of the training time distribution.

The robustness problem against external disturbances has been a trending topic in the field literature, therefore the last part of this thesis gives an special attention to the experimentation in non-controlled environments. Chapter 6 proves the robustness of the novel regression based algorithm against small

electrode shifting, arm movements and time. These disturbances that alter the EMGs could alter the output of the system translated into an undesired behavior. The results proved the new model to be consistent in time without measuring significant degradation in any of the performance metrics. One remarkable benefit of the new model is that with a short initial training it does not need any kind of re-training or re-calibration in the medium term to stay robust. The time the user spends on learning how to use the device is significantly decreased and therefore resulting in a simpler system what helps the user to embrace it.

The development of an optimal training along with the new algorithm lead to the possibility of including a third DoF. Preliminary results show the significant improvement compared to a classical blind training achieving the best results with regression control to the best of the author's knowledge in this scenario. At the same time, with the purpose of exploiting all the new algorithm's potential, a new interface was developed using VR to strength the bond between machine and user through a more immersive experience and training. Finally, the algorithm was deployed into a real prosthesis showing the capability of use for several manipulative tasks.

In future works, the great results obtained in all the previously exposed experiments and at the preliminary tests with real prosthesis motivate to continue the project and develop a new prosthesis prototype where the system presented in this manuscript could be deployed.

In summary, this thesis presented a novel adaptive controller for multi-dimensional (up to 3 DoFs) continuous wrist movement. The algorithm is based on adaptive auto-regressive moving average (ARMA) filters, developing a system that can learn directly velocity and position control. The integration of this algorithm with a co-adaptive training allows users to create a velocity control strategy, which results in a smoother and more natural prosthesis control with a larger range of motion. The performance is improved compared to previous state of the art systems at the same time that the muscle effort is reduced. The key of these results relies both in the algorithm and the novel training protocol. By setting both agents as active learners they influence each other and generate a shared learning experience that will take into account both learners at the same time. Along with this, the new training protocol is capable of detecting which areas of the continuous output space need more time diverting more resources to train those low performance areas. Therefore, as the training depends on the low performance areas, the system is autonomously generating a personalized training optimizing the training time distribution while keeping it significantly shorter than other state of the art training. The

resultant controllers of the combination of this novel algorithm and training approaches showed a robust high performance capable of overcoming the daily life disturbances without needing major changes over time. New technologies like VR and 3D printing, open the doors to keep improving the system's capabilities and results,

Merits

Journal papers

Igual, C., Igual, J., Hahne, J. M. and Parra, L. C. (2019). "Adaptive Auto-Regressive Proportional Myoelectric Control". In: *IEEE Trans. Neural Syst. Rehabil. Eng.*, vol. 27, nº. 2, pp. 314-322. JCR Impact factor: 3.34 (Q1).

Igual, C., Pardo, L. A., Hahne, J. M. and Igual, J. (2019). "Myoelectric Control for Upper Limb Prostheses". In: *Electronics*, vol. 8, nº 11: 1244. JCR Impact factor: 2.41 (Q2).

Igual, C., Camacho, A., Bernabeu, E. J. and Igual, J. (2020). "Donning/Doffing and Arm Positioning Influence in Upper Limb Adaptive Prostheses Control". In: *Applied Sciences*, vol. 10, nº 8: 2892. JCR Impact factor: 2.47 (Q2).

Igual, C., Castillo, A. and Igual, J. (2020). "Optimal training for myoelectric regression control". Paper submitted.

Book Chapters

Igual, C., Igual, J., Hahne, J. M. and Nazarpour, K. (2021). "User-prosthesis coadaptation" in Nazarpour, K. (ed.) 'Control of Prosthetic Hands: Challenges and Emerging Avenues (Healthcare Technologies)'. London: *Institution of Engineering & Technology*, pp. 159-174.

Bibliography

A., KuikenT., Dumanian, G. A., Lipschutz, R. D., Miller, L. A., and Stubblefield, K. A. (2004). "The use of targeted muscle reinnervation for improved myoelectric prosthesis control in a bilateral shoulder disarticulation amputee". In: *Prosthetics and Orthotics International* 28.3, pp. 245–253 (cit. on p. 16).

Ajiboye, A. B. and Weir, R. F. (2005). "A heuristic fuzzy logic approach to EMG pattern recognition for multifunctional prosthesis control". In: *IEEE Transactions on Neural Systems and Rehabilitation Engineering* 13.3, pp. 280–291 (cit. on p. 17).

Alkan, A. and Günay, M. (2012). "Identification of EMG signals using discriminant analysis and SVM classifier". In: *Expert Systems with Applications* 39.1, pp. 44–47 (cit. on p. 21).

Almström, C., Herberts, P., and Körner, L. (1981). "Experience with Swedish multifunctional prosthetic hands controlled by pattern recognition of multiple myoelectric signals". In: *International orthopaedics* 5.1, pp. 15–21 (cit. on p. 21).

Ameri, A., Akhaee, M. A., Scheme, E., and Englehart, K. (2019). "Regression convolutional neural network for improved simultaneous EMG control". In: *Journal of Neural Engineering* 16.3, p. 036015 (cit. on pp. 13, 19, 23, 28, 30, 42, 77).

Ameri, A., Englehart, K. B., and Parker, P. A. (2012). "A comparison between force and position control strategies in myoelectric prostheses". In: *2012 Annual International Conference of the IEEE Engineering in Medicine and Biology Society*, pp. 1342–1345 (cit. on p. 24).

Ameri, A., Kamavuako, E. N., Scheme, E. J., Englehart, K. B., and Parker, P. A. (2014a). "Real-time, simultaneous myoelectric control using visual target-based training paradigm". In: *Biomedical Signal Processing and Control* 13, pp. 8–14 (cit. on pp. 22, 24, 25, 35, 51, 80).

— (2014b). "Support Vector Regression for Improved Real-Time, Simultaneous Myoelectric Control". In: *IEEE Transactions on Neural Systems and Rehabilitation Engineering* 22.6, pp. 1198–1209 (cit. on pp. 22, 25, 30, 80).

Ameri, A., Scheme, E.J., Kamavuako, E.N., Englehart, K.B., and Parker, P.A. (2014c). "Real-Time, Simultaneous Myoelectric Control Using Force and Position-Based Training Paradigms". In: *Biomedical Engineering, IEEE Transactions on* 61.2, pp. 279–287 (cit. on pp. 22, 24, 25, 37, 80).

Amsuess, S., Goebel, P., Graimann, B., and Farina, D. (2015a). "A multi-class proportional myocontrol algorithm for upper limb prosthesis control: Validation in real-life scenarios on amputees". In: *IEEE Transactions on Neural Systems and Rehabilitation Engineering* 23.5, pp. 827–836 (cit. on p. 73).

Amsuess, S., Vujaklija, I., Goebel, P., Roche, A. D., Graimann, B., Aszmann, O. C., and Farina, D. (2015b). "Context-dependent upper limb prosthesis control for natural and robust use". In: *IEEE Transactions on Neural Systems and Rehabilitation Engineering* 24.7, pp. 744–753 (cit. on p. 29).

Amsüss, S., Paredes, L. P., Rudigkeit, N., Graimann, B., Herrmann, M. J., and Farina, D. (2013). "Long term stability of surface EMG pattern classification for prosthetic control". In: *2013 35th Annual International Conference of the IEEE Engineering in Medicine and Biology Society (EMBC)*. IEEE, pp. 3622–3625 (cit. on pp. 13, 21, 40, 80, 97).

Beck, T. W., Housh, T. J., Cramer, J. T., Malek, M. H., Mielke, M., Hendrix, R., and Weir, J. P. (2008). "Electrode shift and normalization reduce the innervation zone's influence on EMG". In: *Medicine and science in sports and exercise* 40.7, pp. 1314–1322 (cit. on p. 97).

Betthauser, J. L., Hunt, C. L., Osborn, L. E., Masters, M. R., Lévay, G., Kaliki, R. R., and Thakor, N. V. (2018). "Limb Position Tolerant Pattern Recognition for Myoelectric Prosthesis Control with Adaptive Sparse Representations From Extreme Learning". In: *IEEE Transactions on Biomedical Engineering* 65.4, pp. 770–778 (cit. on pp. 27, 40, 43).

Biddiss, E. and Chau, T. (2007a). "Upper-limb prosthetics: critical factors in device abandonment". In: *American journal of physical medicine & rehabilitation* 86.12, pp. 977–987 (cit. on pp. 3, 11, 97).

Biddiss, E. A. and Chau, T. T. (2007b). "Upper limb prosthesis use and abandonment: a survey of the last 25 years". In: *Prosthetics and orthotics international* 31.3, pp. 236–257 (cit. on pp. 3, 11, 97).

Braun, D. A., Waldert, S., Aertsen, A., Wolpert, D. M., and Mehring, C. (2010). "Structure learning in a sensorimotor association task". In: *PloS one* 5.1, e8973 (cit. on pp. 28, 42).

Buchthal, F. and Schmalbruch, H. (1980). "Motor unit of mammalian muscle." In: *Physiological reviews* 60.1, pp. 90–142 (cit. on p. 14).

Castellini, C. and Van der Smagt, P. (2009). "Surface EMG in advanced hand prosthetics". In: *Biological cybernetics* 100.1, pp. 35–47 (cit. on pp. 20, 22, 28, 35, 37, 51).

Chan, A. D. C. and Englehart, K. B. (2004). "Continuous myoelectric control for powered prostheses using hidden Markov models". In: *IEEE Transactions on Biomedical Engineering* 52.1, pp. 121–124 (cit. on p. 21).

Chen, X., Zhang, D., and Zhu, X. (2013). "Application of a self-enhancing classification method to electromyography pattern recognition for multifunctional prosthesis control". In: *Journal of NeuroEngineering and Rehabilitation* 10.1, p. 44 (cit. on pp. 17, 27, 42).

Childress, D. S. (1985). "Historical aspects of powered limb prostheses". In: *Clin Prosthet Orthot* 9.1, pp. 2–13 (cit. on p. 15).

Chu, J. U., Moon, I., and Mun, M. S. (2006). "A real-time EMG pattern recognition system based on linear-nonlinear feature projection for a

multifunction myoelectric hand". In: *IEEE Transactions on biomedical engineering* 53.11, pp. 2232–2239 (cit. on p. 17).

Cipriani, C., Sassu, R., Controzzi, M., and Carrozza, M. C. (2011). "Influence of the weight actions of the hand prosthesis on the performance of pattern recognition based myoelectric control: Preliminary study". In: *2011 Annual International Conference of the IEEE Engineering in Medicine and Biology Society*. IEEE, pp. 1620–1623 (cit. on pp. 13, 21, 97).

Clancy, E. A., Morin, E. L., and Merletti, R. (2002). "Sampling, noise-reduction and amplitude estimation issues in surface electromyography". In: *Journal of electromyography and kinesiology* 12.1, pp. 1–16 (cit. on p. 17).

Coapt Engineering Website (2020). `https://www.coaptengineering.com`. Accessed: 2020-11-24 (cit. on p. 27).

Cordella, F., Ciancio, A. L., Sacchetti, R., Davalli, A., Cutti, A. G., Guglielmelli, E., and Zollo, L. (2016). "Literature review on needs of upper limb prosthesis users". In: *Frontiers in neuroscience* 10, p. 209 (cit. on pp. 31, 38).

Couraud, M., Cattaert, D., Paclet, F., Oudeyer, P. Y., and Rugy, A. (2018). "Model and experiments to optimize co-adaptation in a simplified myoelectric control system". In: *Journal of Neural Engineering* 15.2, p. 026006 (cit. on p. 46).

Dargazany, A. R., Abtahi, M., and Mankodiya, K. (2019). "An end-to-end (deep) neural network applied to raw EEG, fNIRs and body motion data for data fusion and BCI classification task without any pre-/post-processing". In: *arXiv preprint arXiv:1907.09523* (cit. on p. 30).

Datta, D., Selvarajah, K., and Davey, N. (2004). "Functional outcome of patients with proximal upper limb deficiency–acquired and congenital". In: *Clinical rehabilitation* 18.2, pp. 172–177 (cit. on pp. 3, 11, 97).

Davidson, J. (2002). "A survey of the satisfaction of upper limb amputees with their prostheses, their lifestyles, and their abilities". In: *Journal of Hand Therapy* 15.1, pp. 62–70 (cit. on pp. 3, 11, 97).

Despopoulos, A. (2003). *Color Atlas of Physiology Completely Revised and Expanded 5th edition*. Thieme Stuttgart (cit. on p. 14).

Dillingham, T. R., Pezzin, L. E., and MacKenzie, E. J. (2002). "Limb amputation and limb deficiency: epidemiology and recent trends in the United States". In: *Southern medical journal* 95.8, pp. 875–884 (cit. on p. 11).

Diniz, P. S. R. (2013). *Adaptive Filtering: Algorithms and Practical Implementation*. Springer (cit. on pp. 53, 59, 72).

Dohnálek, P., Gajdoš, P., and Peterek, T. (2013). "Human activity recognition on raw sensor data via sparse approximation". In: *2013 36th International Conference on Telecommunications and Signal Processing (TSP)*. IEEE, pp. 700–703 (cit. on pp. 3, 11, 97).

Dumanian, G. A. et al. (2019). "Targeted muscle reinnervation treats neuroma and phantom pain in major limb amputees: a randomized clinical trial". In: *Annals of surgery* 270.2, pp. 238–246 (cit. on p. 16).

Dyson, M., Barnes, J., and Nazarpour, K. (2018). "Myoelectric control with abstract decoders". In: *Journal of neural engineering* 15.5, p. 056003 (cit. on pp. 36, 38, 39).

Dyson, M., Dupan, S., Jones, H., and Nazarpour, K. (2020). "Learning, Generalization, and Scalability of Abstract Myoelectric Control". In: *IEEE Transactions on Neural Systems and Rehabilitation Engineering* 28.7, pp. 1539–1547 (cit. on pp. 36, 39).

Engeberg, E. D., Meek, S. G., and Minor, M. A. (2008). "Hybrid force–velocity sliding mode control of a prosthetic hand". In: *IEEE Transactions on Biomedical Engineering* 55.5, pp. 1572–1581 (cit. on pp. 23, 72).

Englehart, K. and Hudgins, B. et al. (2003). "A robust, real-time control scheme for multifunction myoelectric control". In: *IEEE transactions on biomedical engineering* 50.7, pp. 848–854 (cit. on pp. 15, 20, 35).

Al-Faiz, M. Z. and Al-Mashhadany, Y. I. (2009). "Human Arm Movements Recognition Based on EMG Signal". In: *Citeseer* (cit. on p. 14).

Fang, Y., Zhou, D., Li, K., and Liu, H. (2017). "Interface Prostheses With Classifier-Feedback-Based User Training". In: *IEEE Transactions on Biomedical Engineering* 64.11, pp. 2575–2583 (cit. on pp. 25, 37, 44, 77).

Farahani, B., Firouzi, F., Chang, V., Badaroglu, M., Constant, N., and Mankodiya, K. (2018). "Towards fog-driven IoT eHealth: Promises and challenges of IoT in medicine and healthcare". In: *Future Generation Computer Systems* 78, pp. 659–676 (cit. on p. 30).

Farina, D., Jiang, N., Rehbaum, H., Holobar, A., Graimann, B., Dietl, H., and Aszmann, O. C. (2014). "The extraction of neural information from the surface EMG for the control of upper-limb prostheses: emerging avenues and challenges". In: *IEEE Transactions on Neural Systems and Rehabilitation Engineering* 22.4, pp. 797–809 (cit. on p. 21).

Farina, D., Merletti, R., and Enoka, R. M. (2004). "The extraction of neural strategies from the surface EMG". In: *Journal of applied physiology* 96.4, pp. 1486–1495 (cit. on p. 17).

Farrell, T. R. and Weir, R. F. (2007). "The Optimal Controller Delay for Myoelectric Prostheses". In: *IEEE Transactions on Neural Systems and Rehabilitation Engineering* 15.1, pp. 111–118 (cit. on p. 17).

Fougner, A., Scheme, E., Chan, A. D. C., Englehart, K., and Stavdahl, O. (2011). "Resolving the Limb Position Effect in Myoelectric Pattern Recognition". In: *IEEE Transactions on Neural Systems and Rehabilitation Engineering* 19.6, pp. 644–651 (cit. on pp. 13, 21, 27, 97).

Fougner, A., Stavdahl, Ø., Kyberd, P. J., Losier, Y. G., and Parker, P. A. (2012). "Control of upper limb prostheses: Terminology and proportional myoelectric control—A review". In: *IEEE Transactions on neural systems and rehabilitation engineering* 20.5, pp. 663–677 (cit. on pp. 15, 22, 51).

Frisoli, A., Loconsole, C., Leonardis, D., Banno, F., Barsotti, M., Chisari, C., and Bergamasco, M. (2012). "A New Gaze-BCI-Driven Control of an Upper Limb Exoskeleton for Rehabilitation in Real-World Tasks". In: *IEEE Transactions on Systems, Man, and Cybernetics, Part C (Applications and Reviews)* 42.6, pp. 1169–1179 (cit. on p. 15).

Galán, F., Nuttin, M., Lew, E., Ferrez, P. W., Vanacker, G., Philips, J., and R., Millán J. D. (2008). "A brain-actuated wheelchair: Asynchronous and non-invasive Brain–computer interfaces for continuous control of robots". In: *Clinical Neurophysiology* 119.9, pp. 2159–2169 (cit. on p. 15).

Ganguly, K. and Carmena, J. M. (2009). "Emergence of a Stable Cortical Map for Neuroprosthetic Control". In: *PLOS Biology* 7.7, pp. 1–13 (cit. on p. 15).

Ghazaei, G., Alameer, A., Degenaar, P., Morgan, G., and Nazarpour, K. (2017). "Deep learning-based artificial vision for grasp classification in myoelectric hands". In: *Journal of neural engineering* 14.3, p. 036025 (cit. on p. 36).

Graupe, D. and Cline, W. K. (1975). "Functional separation of EMG signals via ARMA identification methods for prosthesis control purposes". In: *IEEE Transactions on Systems, Man, and Cybernetics* 1.2, pp. 252–259 (cit. on p. 20).

Guémann, M., Bouvier, S., Halgand, C., Borrini, L., Paclet, F., Lapeyre, E., Ricard, D., Cattaert, D., and Rugy, A. de (2018). "Sensory and motor parameter estimation for elbow myoelectric control with vibrotactile feedback". In: *Annals of Physical and Rehabilitation Medicine* 61, e467 (cit. on pp. 26, 37).

Hahne, J. M., Biessmann, F., Jiang, N., Rehbaum, H., Farina, D., Meinecke, F. C., Muller, K. R., and Parra, L. C. (2014). "Linear and nonlinear regression techniques for simultaneous and proportional myoelectric control". In: *IEEE Transactions on Neural Systems and Rehabilitation Engineering* 22.2, pp. 269–279 (cit. on pp. 6, 17, 22, 51–54, 61, 80).

Hahne, J. M., Dähne, S., Hwang, H. J., Müller, K. R., and Parra, L. C. (2015). "Concurrent adaptation of human and machine improves simultaneous and proportional myoelectric control". In: *IEEE Transactions on Neural Systems and Rehabilitation Engineering* 23.4, pp. 618–627 (cit. on pp. 13, 22, 23, 25, 36, 44, 45, 56, 61, 64, 72–74, 77, 80, 85, 112).

Hahne, J. M., Graimann, B., and Muller, K. R. (2012a). "Spatial filtering for robust myoelectric control". In: *IEEE Transactions on Biomedical Engineering* 59.5, pp. 1436–1443 (cit. on p. 21).

Hahne, J. M., Markovic, M., and Farina, D. (2017). "User adaptation in Myoelectric Man-Machine Interfaces". In: *Scientific Reports* 7.1, p. 4437 (cit. on pp. 22, 23, 26, 36, 39, 77).

Hahne, J. M., Rehbaum, H., Biessmann, F., Meinecke, F. C., Müller, K. R., Jiang, N., Farina, D., and Parra, L. C. (2012b). "Simultaneous and proportional control of 2D wrist movements with myoelectric signals". In: *2012 IEEE International Workshop on Machine Learning for Signal Processing*, pp. 1–6 (cit. on pp. 17, 22, 35, 80).

Hahne, J. M., Schweisfurth, M. A., Koppe, M., and Farina, D. (2018). "Simultaneous control of multiple functions of bionic hand prostheses: Performance and robustness in end users". In: *Science Robotics* 3.19 (cit. on pp. 28, 30, 42, 51, 73).

Hargrove, L., Englehart, K., and Hudgins, B. (2008a). "A training strategy to reduce classification degradation due to electrode displacements in pattern recognition based myoelectric control". In: *Biomedical signal processing and control* 3.2, pp. 175–180 (cit. on pp. 21, 40).

Hargrove, L. J., Li, G., Englehart, K. B., and Hudgins, B. S. (2008b). "Principal components analysis preprocessing for improved classification accuracies in pattern-recognition-based myoelectric control". In: *IEEE Transactions on Biomedical Engineering* 56.5, pp. 1407–1414 (cit. on p. 21).

Hargrove, L. J., Miller, L. A., Turner, K., and Kuiken, T. A. (2017). "Myoelectric Pattern Recognition Outperforms Direct Control for Transhumeral Amputees with Targeted Muscle Reinnervation: A Randomized Clinical Trial". In: *Scientific Reports* 7.1, pp. 2045–2322 (cit. on p. 14).

He, J., Zhang, D., Jiang, N., Sheng, X., Farina, D., and Zhu, X. (2015). "User adaptation in long-term, open-loop myoelectric training: implications for EMG pattern recognition in prosthesis control". In: *Journal of neural engineering* 12.4, p. 046005 (cit. on p. 21).

Hiremath, S., Yang, G., and Mankodiya, K. (2014). "Wearable Internet of Things: Concept, architectural components and promises for person-centered healthcare". In: *2014 4th International Conference on Wireless Mobile Communication and Healthcare-Transforming Healthcare Through*

Innovations in Mobile and Wireless Technologies (MOBIHEALTH). IEEE, pp. 304–307 (cit. on p. 30).

Hochberg, L. R. et al. (2006). "Neuronal ensemble control of prosthetic devices by a human with tetraplegia". In: *Nature* 442.7099, p. 164 (cit. on pp. 15, 25, 35, 37, 74).

Huang, H., Zhou, P., Li, G., and Kuiken, T. A. (2008). "An Analysis of EMG Electrode Configuration for Targeted Muscle Reinnervation Based Neural Machine Interface". In: *IEEE Transactions on Neural Systems and Rehabilitation Engineering* 16.1, pp. 37–45 (cit. on p. 16).

Huang, H. P., Liu, Y. H., Liu, L. W., and Wong, C. S. (2003). "EMG classification for prehensile postures using cascaded architecture of neural networks with self-organizing maps". In: *2003 IEEE International Conference on Robotics and Automation (Cat. No. 03CH37422)*. Vol. 1. IEEE, pp. 1497–1502 (cit. on p. 21).

Huang, Q. et al. (2017). "A Novel Unsupervised Adaptive Learning Method for Long-Term Electromyography (EMG) Pattern Recognition". In: *Sensors* 17.6, p. 1370 (cit. on pp. 22, 27, 40, 80).

Huang, Y., Englehart, K. B., Hudgins, B., and Chan, A. D. C. (2005). "A Gaussian mixture model based classification scheme for myoelectric control of powered upper limb prostheses". In: *IEEE Transactions on Biomedical Engineering* 52.11, pp. 1801–1811 (cit. on pp. 20, 35).

Hudgins, B., Parker, P., and Scott, R. N. (1993). "A new strategy for multifunction myoelectric control". In: *IEEE Transactions on Biomedical Engineering* 40.1, pp. 82–94 (cit. on p. 21).

Hwang, H. J., Hahne, J. M., and Mueller, K. R. (2017). "Real-time robustness evaluation of regression based myoelectric control against arm position change and donning/doffing". In: *PLOS ONE* 12.11, e0186318 (cit. on pp. 22, 23, 26, 27, 39, 80, 97, 112).

Igual, C., Camacho, A., Bernabeu, E. J., and Igual, J. (2020). "Donning/Doffing and Arm Positioning Influence in Upper Limb Adaptive Prostheses Control". In: *Applied Sciences* 10.8, p. 2892 (cit. on p. 84).

Igual, C., Igual, J., Hahne, J. M., and Parra, L. C. (2019a). "Adaptive Auto-Regressive Proportional Myoelectric Control". In: *IEEE Transactions on Neural Systems and Rehabilitation Engineering* 27.2, pp. 314–322 (cit. on pp. 78, 84, 102, 111, 113).

Igual, C., Pardo, L. A., Hahne, J. M., and Igual, J. (2019b). "Myoelectric Control for Upper Limb Prostheses". In: *Electronics* 8.11, p. 1244 (cit. on p. 97).

Ison, M., Vujaklija, I., Whitsell, B., Farina, D., and Artemiadis, P. (2016). "High-Density Electromyograph and Motor Skill Learning for Robust Long-Term Control of a 7-DoF Robot Arm". In: *IEEE Transactions on Neural Systems and Rehabilitation Engineering* 24.4, pp. 424–433 (cit. on pp. 13, 17, 25–27, 36, 38).

Jiang, N., Dosen, S., Muller, K., and Farina, D. (2012). "Myoelectric Control of Artificial Limbs - Is There a Need to Change Focus?" In: *IEEE Signal Processing Magazine* 29.5, pp. 152–150 (cit. on pp. 13, 21, 22, 39, 97).

Jiang, N., Englehart, K. B., and Parker, P. A. (2008). "Extracting simultaneous and proportional neural control information for multiple-DOF prostheses from the surface electromyographic signal". In: *IEEE Transactions on Bio-Medical Engineering* 56.4, pp. 1070–1080 (cit. on pp. 22, 35, 51, 80).

Jiang, N. and Farina, D. (2014). "Myoelectric control of upper limb prosthesis: current status, challenges and recent advances". In: *Front. Neuroeng. Conference Abstract: MERIDIAN 30M Workshop. doi: 10.3389/conf. fneng.* Vol. 4 (cit. on pp. 13, 97).

Karlik, B., Tokhi, M. O., and Alci, M. (2003). "A fuzzy clustering neural network architecture for multifunction upper-limb prosthesis". In: *IEEE Transactions on Biomedical Engineering* 50.11, pp. 1255–1261 (cit. on pp. 21, 35).

Kelly, M. F., Parker, P. A., and Scott, R. N. (1990). "The application of neural networks to myoelectric signal analysis: A preliminary study". In: *IEEE Transactions on Biomedical Engineering* 37.3, pp. 221–230 (cit. on pp. 20, 21, 35).

Khushaba, R. N. and Al-Jumaily, A. (2007). "Channel and feature selection in multifunction myoelectric control". In: *2007 29th Annual International Conference of the IEEE Engineering in Medicine and Biology Society*. IEEE, pp. 5182–5185 (cit. on p. 21).

Krasoulis, A. and Nazarpour, K. (2020). "Discrete action control for prosthetic digits". In: *bioRxiv* (cit. on pp. 36, 37).

Krasoulis, A., Vijayakumar, S., and Nazarpour, K. (2019a). "Effect of user adaptation on prosthetic finger control with an intuitive myoelectric decoder". In: *Frontiers in neuroscience* 13, p. 891 (cit. on pp. 36, 37).

— (2019b). "Multi-grip classification-based prosthesis control with two EMG-IMU sensors". In: *IEEE Transactions on Neural Systems and Rehabilitation Engineering* 28.2, pp. 508–518 (cit. on pp. 36, 37).

Kuiken, T. A., Li, G., Lock, B. A., Lipschutz, R. D., Miller, L. A., Stubblefield, K. A., and Englehart, K. B. (2009). "Targeted muscle reinnervation for real-time myoelectric control of multifunction artificial arms". In: *Jama* 301.6, pp. 619–628 (cit. on pp. 16, 74).

Kuiken, T. A., Miller, L. A., Turner, K., and Hargrove, L. J. (2016). "A comparison of pattern recognition control and direct control of a multiple degree-of-freedom transradial prosthesis". In: *IEEE journal of translational engineering in health and medicine* 4, pp. 1–8 (cit. on pp. 29, 30).

LeMoyne, R. (2016). "Future and advanced concepts for the powered prosthesis". In: *Advances for Prosthetic Technology*. Springer, pp. 127–130 (cit. on p. 30).

Lendaro, E., Mastinu, E., Håkansson, B., and Ortiz-Catalan, M. (2017). "Real-time Classification of Non-Weight Bearing Lower-Limb Movements Using EMG to Facilitate Phantom Motor Execution: Engineering and Case Study Application on Phantom Limb Pain". In: *Frontiers in Neurology* 8, p. 470 (cit. on p. 97).

Li, G., Li, Y., Yu, L., and Geng, Y. (2011). "Conditioning and Sampling Issues of EMG Signals in Motion Recognition of Multifunctional Myoelectric Prostheses". In: *Annals of Biomedical Engineering* 39.6, pp. 1779–1787 (cit. on p. 17).

Li, G., Zhang, L., Sun, Y., and Kong, J. (2019). "Towards the sEMG hand: internet of things sensors and haptic feedback application". In: *Multimedia Tools and Applications* 78.21, pp. 29765–29782 (cit. on p. 30).

Li, X., Samuel, O. W., Zhang, X., Wang, H., Fang, P., and Li, G. (2017). "A motion-classification strategy based on sEMG-EEG signal combination for upper-limb amputees". In: *Journal of neuroengineering and rehabilitation* 14.1, p. 2 (cit. on p. 21).

Lin, C., Wang, B., Jiang, N., and Farina, D. (2018). "Robust extraction of basis functions for simultaneous and proportional myoelectric control via sparse non-negative matrix factorization". In: *Journal of neural engineering* 15.2, p. 026017 (cit. on p. 82).

Lorrain, T., Jiang, N., and Farina, D. (2011). "Influence of the training set on the accuracy of surface EMG classification in dynamic contractions for the control of multifunction prostheses". In: *Journal of neuroengineering and rehabilitation* 8.1, p. 25 (cit. on p. 21).

Marasco, P. D., Hebert, J. S., Sensinger, J. W., Shell, C. E., Schofield, J. S., Thumser, Z. C., and Nataraj, R. et al. (2018). "Illusory movement perception improves motor control for prosthetic hands". In: *Science Translational Medicine* 10.432 (cit. on pp. 3, 11, 97).

Markovic, M., Schweisfurth, M. A., Engels, L. F., Bentz, T., Wüstefeld, D., Farina, D., and Dosen, S. (2018a). "The clinical relevance of advanced artificial feedback in the control of a multi-functional myoelectric prosthesis". In: *Journal of neuroengineering and rehabilitation* 15.1, p. 28 (cit. on p. 30).

Markovic, M., Schweisfurth, M. A., Engels, L. F., Farina, D., and Dosen, S. (2018b). "Myocontrol is closed-loop control: incidental feedback is sufficient for scaling the prosthesis force in routine grasping". In: *Journal of neuroengineering and rehabilitation* 15.1, p. 81 (cit. on pp. 26, 37).

Marquardt, E. (1965). "The Heidelberg pneumatic arm prosthesis". In: *The Journal of Bone and Joint Surgery. British volume* 47.3, pp. 425–434 (cit. on p. 15).

Mastinu, E., Doguet, P., Botquin, Y., Håkansson, B., and Ortiz-Catalan, M. (2017). "Embedded System for Prosthetic Control Using Implanted Neuromuscular Interfaces Accessed Via an Osseointegrated Implant". In: *IEEE Transactions on Biomedical Circuits and Systems* 11.4, pp. 867–877 (cit. on p. 97).

Mastinu, E., Ortiz-Catalan, M., and Håkansson, B. (2015). "Analog front-ends comparison in the way of a portable, low-power and low-cost EMG controller based on pattern recognition". In: *2015 37th Annual International Conference of the IEEE Engineering in Medicine and Biology Society (EMBC)*. IEEE, pp. 2111–2114 (cit. on p. 97).

McMullen, D. P. et al. (2014). "Demonstration of a Semi-Autonomous Hybrid Brain–Machine Interface Using Human Intracranial EEG, Eye Tracking, and Computer Vision to Control a Robotic Upper Limb Prosthetic". In: *IEEE Transactions on Neural Systems and Rehabilitation Engineering* 22.4, pp. 784–796 (cit. on p. 15).

Merletti, R. and Parker, P. A. (2004). *Electromyography: physiology, engineering, and non-invasive applications*. Vol. 11. John Wiley & Sons (cit. on p. 51).

Miller, L. A., Lipschutz, R. D., Stubblefield, K. A., Lock, B. A., Huang, H., Williams, T. W., Weir, R. F., and Kuiken, T. A. (2008). "Control of a Six Degree of Freedom Prosthetic Arm After Targeted Muscle Reinnervation Surgery". In: *Archives of Physical Medicine and Rehabilitation* 89.11, pp. 2057–2065 (cit. on p. 16).

Mioton, L. M. and Dumanian, G. A. (2018). "Targeted muscle reinnervation and prosthetic rehabilitation after limb loss". In: *Journal of surgical oncology* 118.5, pp. 807–814 (cit. on p. 16).

Montalivet, É. de, Bailly, K., Touillet, A., Martinet, N., Paysant, J., and Jarrasse, N. (2020). "Guiding the Training of Users With a Pattern Similarity Biofeedback to Improve the Performance of Myoelectric Pattern Recognition". In: *IEEE Transactions on Neural Systems and Rehabilitation Engineering* 28.8, pp. 1731–1741 (cit. on p. 78).

Muceli, S. and Farina, D. (2012). "Simultaneous and Proportional Estimation of HandKinematics From EMG During Mirrored Movements at

MultipleDegrees-of-Freedom". In: *Neural Systems and Rehabilitation Engineering, IEEE Transactions on* 20.3, pp. 371–378 (cit. on pp. 24, 51).

Müller, J. S., Vidaurre, C., Schreuder, M., Meinecke, F. C., Von Bünau, P., and Müller, K. R. (2017). "A mathematical model for the two-learners problem". In: *Journal of neural engineering* 14.3, p. 036005 (cit. on pp. 44, 73, 74).

Muzumdar, A. (2004). *Powered upper limb prostheses: control, implementation and clinical application*. Springer (cit. on p. 51).

Nazarpour, K., Cipriani, C., Farina, D., and Kuiken, T. (2014). "Advances in control of multi-functional powered upper-limb prostheses". In: *IEEE Trans. Neural Syst. Rehabil. Eng* 22, pp. 711–15 (cit. on p. 35).

Nazarpour, K., Sharafat, A. R., and Firoozabadi, S. M. P. (2007). "Application of higher order statistics to surface electromyogram signal classification". In: *IEEE Transactions on Biomedical Engineering* 54.10, pp. 1762–1769 (cit. on p. 35).

Nielsen, J. L. G., Holmgaard, S., Ning, J., Englehart, K. B., Farina, D., and Parker, P. A. (2011). "Simultaneous and Proportional Force Estimation for Multifunction Myoelectric Prostheses Using Mirrored Bilateral Training". In: *Biomedical Engineering, IEEE Transactions on* 58.3, pp. 681–688 (cit. on pp. 17, 24, 35, 51).

Nishikawa, D., Yu, W., Yokoi, H.i, and Kakazu, Y. (2001). "On-line learning method for EMG prosthetic hand control". In: *Electronics and Communications in Japan (Part III: Fundamental Electronic Science)* 84.10, pp. 35–46 (cit. on pp. 27, 43).

Oskoei, M. A. and Hu, H. (2006). "GA-based feature subset selection for myoelectric classification". In: IEEE, pp. 1465–1470 (cit. on p. 21).

— (2007). "Myoelectric control systems - A survey". In: *Biomedical Signal Processing and Control* 2.4, pp. 275–294 (cit. on pp. 17, 19, 21, 37, 51).

Østlie, K., Lesjø, I. M., Franklin, R. J., Garfelt, B., Skjeldal, O. H., and Magnus, P. (2012). "Prosthesis rejection in acquired major upper-limb amputees:

a population-based survey". In: *Disability and Rehabilitation: Assistive Technology* 7.4, pp. 294–303 (cit. on pp. 3, 11).

Ottobock Website (2020). `https://www.ottobock.de`. Accessed: 2020-11-24 (cit. on p. 27).

Paaßen, B., Schulz, A., Hahne, J. M., and Hammer, B. (2018). "Expectation maximization transfer learning and its application for bionic hand prostheses". In: *Neurocomputing* 298, pp. 122–133 (cit. on pp. 28, 42, 43).

Paninski, L., Fellows, M. R., Hatsopoulos, N. G., and Donoghue, J. P. (2004). "Spatiotemporal tuning of motor cortical neurons for hand position and velocity". In: *Journal of neurophysiology* 91.1, pp. 515–532 (cit. on p. 74).

Parker, P., Englehart, K., and Hudgins, B. (2006). "Myoelectric signal processing for control of powered limb prostheses". In: *Journal of Electromyography and Kinesiology* 16.6, pp. 541–548 (cit. on pp. 15, 17, 35, 51).

Pasquina, P. F., Evangelista, M., Carvalho, A. J., Lockhart, J., and Griffin, S. et al. (2015a). "First-in-man demonstration of a fully implanted myoelectric sensors system to control an advanced electromechanical prosthetic hand". In: *Journal of Neuroscience Methods* 244, pp. 85–93 (cit. on p. 97).

Pasquina, P. F., Perry, B. N., Miller, M. E., Ling, G. S. F., and Tsao, J. W. (2015b). "Recent advances in bioelectric prostheses". In: 5.2, pp. 164–170 (cit. on p. 97).

Peerdeman, B., Boere, D., Witteveen, H., Huis, R., Hermens, H., Stramigioli, S., Rietman, H., Veltink, P., and Misra, S. (2011). "Myoelectric forearm prostheses: State of the art from a user-centered perspective". In: *The Journal of Rehabilitation Research and Development* 48.6, p. 719 (cit. on pp. 17, 25, 51).

Peleg, D., Braiman, E., Yom-Tov, E., and Inbar, G. F. (2002). "Classification of finger activation for use in a robotic prosthesis arm". In: *IEEE Transactions on Neural Systems and Rehabilitation Engineering* 10.4, pp. 290–293 (cit. on p. 21).

Phinyomark, A., Khushaba, R. N., and Scheme, E. (2018). "Feature Extraction and Selection for Myoelectric Control Based on Wearable EMG Sensors". In: *Sensors* 18.5, p. 1615 (cit. on pp. 17, 19).

Phinyomark, A., Quaine, F., Charbonnier, S., Serviere, C., Tarpin-Bernard, F., and Laurillau, Y. (2013). "EMG feature evaluation for improving myoelectric pattern recognition robustness"". In: *Expert Systems with Applications* 40.12, pp. 4832–4840 (cit. on p. 18).

Pilarski, P. M., Dawson, M. R., Degris, T., Fahimi, F., Carey, J. P., and Sutton, R. S. (2011). "Online human training of a myoelectric prosthesis controller via actor-critic reinforcement learning". In: *2011 IEEE international conference on rehabilitation robotics*. IEEE, pp. 1–7 (cit. on p. 17).

Pistohl, T., Cipriani, C., Jackson, A., and Nazarpour, K. (2013). "Abstract and proportional myoelectric control for multi-fingered hand prostheses". In: *Annals of biomedical engineering* 41.12, pp. 2687–2698 (cit. on pp. 36, 39).

Pistohl, T., Joshi, D., Ganesh, G., Jackson, A., and Nazarpour, K. (2014). "Artificial proprioceptive feedback for myoelectric control". In: *IEEE Transactions on Neural Systems and Rehabilitation Engineering* 23.3, pp. 498–507 (cit. on p. 36).

Powell, M., Kaliki, R., and Thakor, N. (2014). "User training for pattern recognition-based myoelectric prostheses: Improving phantom limb movement consistency and distinguishability". In: *IEEE Transactions on Neural Systems and Rehabilitation Engineering* 22.3, pp. 522–532 (cit. on pp. 25, 28, 38).

Prahm, C., Schulz, A., Paaßen, B., Schoisswohl, J., Kaniusas, E., Dorffner, G., Hammer, B., and Aszmann, O. (2019). "Counteracting Electrode Shifts in Upper-Limb Prosthesis Control via Transfer Learning". In: *IEEE Transactions on Neural Systems and Rehabilitation Engineering* 27.5, pp. 956–962 (cit. on pp. 79, 97).

Radhakrishnan, S. M., Baker, S. N., and Jackson, A. (2008). "Learning a Novel Myoelectric-Controlled Interface Task". In: *Journal of Neurophysiology* 100.4, pp. 2397–2408 (cit. on pp. 26, 36, 38).

Radmand, A., Scheme, E., and Englehart, K. (2014). "A characterization of the effect of limb position on EMG features to guide the development of effective prosthetic control schemes". In: *2014 36th Annual International Conference of the IEEE Engineering in Medicine and Biology Society*. IEEE, pp. 662–667 (cit. on p. 21).

Rahimi, A., Benatti, S., Kanerva, P., Benini, L., and Rabaey, J. M. (2016). "Hyperdimensional biosignal processing: A case study for EMG-based hand gesture recognition". In: IEEE, pp. 1–8 (cit. on pp. 21, 37).

Resnik, L., Huang, H. H., Winslow, A., Crouch, D. L., Zhang, F., and Wolk, N. (2018). "Evaluation of EMG pattern recognition for upper limb prosthesis control: a case study in comparison with direct myoelectric control". In: *Journal of neuroengineering and rehabilitation* 15.1, p. 23 (cit. on p. 15).

Roy, S. H., De Luca, G., Cheng, M. S., Johansson, A., Gilmore, L. D., and De Luca, C. J. (2007). "Electro-mechanical stability of surface EMG sensors". In: *Medical & biological engineering & computing* 45.5, pp. 447–457 (cit. on p. 21).

Rupp, M. and Sayed, A. H. (1996). "Robustness of Gauss-Newton recursive methods: A deterministic feedback analysis". In: *Signal Processing* 50.3, pp. 165–187 (cit. on p. 73).

Samek, W., Vidaurre, C., Müller, K. R., and Kawanabe, M. (2012). "Stationary common spatial patterns for brain–computer interfacing". In: *Journal of neural engineering* 9.2, p. 026013 (cit. on p. 21).

Sartori, M., Durandau, G., Došen, S., and Farina, D. (2018). "Robust simultaneous myoelectric control of multiple degrees of freedom in wrist-hand prostheses by real-time neuromusculoskeletal modeling". In: *Journal of Neural Engineering* 15.6, p. 066026 (cit. on pp. 16, 38).

Scheme, E. and Englehart, K. (2011). "Electromyogram pattern recognition for control of powered upper-limb prostheses: state of the art and challenges for clinical use". In: *Journal of Rehabilitation Research and Development* 48.6, pp. 643–659 (cit. on pp. 3, 11, 15, 51, 97).

Scheme, E., Fougner, A., Stavdahl, Ø., Chan, A. D. C., and Englehart, K. (2010). "Examining the adverse effects of limb position on pattern

recognition based myoelectric control". In: *2010 Annual International Conference of the IEEE Engineering in Medicine and Biology*. IEEE, pp. 6337–6340 (cit. on pp. 3, 11, 15, 97).

Scheme, E. J., Englehart, K. B., and Hudgins, B. S. (2011). "Selective classification for improved robustness of myoelectric control under nonideal conditions". In: *IEEE Transactions on Biomedical Engineering* 58.6, pp. 1698–1705 (cit. on pp. 13, 15, 21, 97).

Sensinger, J. W., Lock, B. A., and Kuiken, T. A. (2009). "Adaptive Pattern Recognition of Myoelectric Signals: Exploration of Conceptual Framework and Practical Algorithms". In: *IEEE Transactions on Neural Systems and Rehabilitation Engineering* 17.3, pp. 270–278 (cit. on pp. 17, 28, 41).

Shehata, A. W., Engels, L. F., Controzzi, M., Cipriani, C., Scheme, E. J., and Sensinger, J. W. (2018a). "Improving internal model strength and performance of prosthetic hands using augmented feedback". In: *Journal of NeuroEngineering and Rehabilitation* 15.1, pp. 1743–0003 (cit. on p. 77).

Shehata, A. W., Scheme, E. J., and Sensinger, J. W. (2018b). "Audible Feedback Improves Internal Model Strength and Performance of Myoelectric Prosthesis Control". In: *Scientific Reports* 8.1, pp. 2045–2322 (cit. on p. 77).

Sherman, E. D. (1964). "A Russian bioelectric-controlled prosthesis: Report of a research team from the Rehabilitation Institute of Montreal". In: *Canadian Medical Association Journal* 91.24, p. 1268 (cit. on p. 15).

Shynk, J. J. (1989). "Adaptive IIR filtering". In: *ASSP Magazine, IEEE* 6.2, pp. 4–21 (cit. on pp. 53, 55, 59, 72).

Silva, K., Rand, S., Cancel, D.., Chen, Y., Kathirithamby, R., and Stern, M. (2015). *Three-dimensional (3-D) printing: a cost-effective solution for improving global accessibility to prostheses* (cit. on p. 30).

Smith, L. H., Kuiken, T. A., and Hargrove, L. J. (2016). "Evaluation of Linear Regression Simultaneous Myoelectric Control Using Intramuscular EMG". In: *IEEE Transactions on Biomedical Engineering* 63.4, pp. 737–746 (cit. on p. 23).

Souza, J. M., Cheesborough, J. E., Ko, J. H., Cho, M. S., Kuiken, T. A., and Dumanian, G. A. (2014). "Targeted Muscle Reinnervation: A Novel Approach to Postamputation Neuroma Pain". In: *Clinical Orthopaedics and Related Research* 472.10, pp. 2984–2990 (cit. on p. 16).

Spanias, J. A., Perreault, E. J., and Hargrove, L. J. (2015). "Detection of and compensation for EMG disturbances for powered lower limb prosthesis control". In: *IEEE Transactions on Neural Systems and Rehabilitation Engineering* 24.2, pp. 226–234 (cit. on pp. 20, 37).

Strazzulla, I., Nowak, M., Controzzi, M., Cipriani, C., and Castellini, C. (2017). "Online Bimanual Manipulation Using Surface Electromyography and Incremental Learning". In: *IEEE Transactions on Neural Systems and Rehabilitation Engineering* 25.3, pp. 227–234 (cit. on pp. 23, 26, 28, 36, 39).

Thomas, N., Ung, G., McGarvey, C., and Brown, J. D. (2019). "Comparison of vibrotactile and joint-torque feedback in a myoelectric upper-limb prosthesis". In: *Journal of neuroengineering and rehabilitation* 16.1, p. 70 (cit. on pp. 26, 37).

Al-Timemy, A. H., Bugmann, G., Escudero, J., and Outram, N. (2013). "Classification of finger movements for the dexterous hand prosthesis control with surface electromyography". In: *IEEE journal of biomedical and health informatics* 17.3, pp. 608–618 (cit. on p. 21).

User experience video (2018) (cit. on p. 71).

Velliste, M., Perel, S., Spalding, M. C., Whitford, A. S., and Schwartz, A. B. (2008). "Cortical control of a prosthetic arm for self-feeding". In: *Nature* 453.7198, p. 1098 (cit. on pp. 15, 29, 74).

Vidovic, M. M. C., Hwang H. J. Amsuess, S., Hahne, J. M., Farina, D., and Müller, K. R. (2015). "Improving the robustness of myoelectric pattern recognition for upper limb prostheses by covariate shift adaptation". In: *IEEE Transactions on Neural Systems and Rehabilitation Engineering* 24.9, pp. 961–970 (cit. on pp. 21, 26, 28, 39, 42).

Von Bünau, P., Meinecke, F. C., Király, F. C., and Müller, K. R. (2009). "Finding stationary subspaces in multivariate time series". In: *Physical review letters* 103.21, p. 214101 (cit. on p. 21).

Vujaklija, I., Farina, D., and Aszmann, O. C. (2016). "New developments in prosthetic arm systems". In: *Orthopedic research and reviews* 8, pp. 31–39 (cit. on pp. 3, 11, 97).

Vujaklija, I., Roche, A. D., Hasenoehrl, T., Sturma, A., Amsuess, S., Farina, D., and Aszmann, O. C. (2017). "Translating research on myoelectric control into clinics—Are the performance assessment methods adequate?" In: *Frontiers in neurorobotics* 11, p. 7 (cit. on p. 14).

Wheaton, L. A. (2017). "Neurorehabilitation in upper limb amputation: understanding how neurophysiological changes can affect functional rehabilitation". In: *Journal of neuroengineering and rehabilitation* 14.1, p. 41 (cit. on p. 29).

Widrow, B. and Stearns, S. D. (1985). *Adaptive signal processing*. Prentice-Hall (cit. on pp. 53, 56, 72).

Wubben, D., Rost, P., Bartelt, J. S., Lalam, M., Savin, V., Gorgoglione, M., Dekorsy, A., and Fettweis, G. (2014). "Benefits and impact of cloud computing on 5G signal processing: Flexible centralization through cloud-RAN". In: *IEEE signal processing magazine* 31.6, pp. 35–44 (cit. on p. 30).

Yang, D., Gu, Y., Jiang, L., Osborn, L., and Liu, H. (2017). "Dynamic training protocol improves the robustness of PR-based myoelectric control". In: *Biomedical Signal Processing and Control* 31, pp. 249–256 (cit. on p. 77).

Yeung, D., Farina, D., and Vujaklija, I. (2019). "Directional Forgetting for Stable Co-Adaptation in Myoelectric Control". In: *Sensors* 19.9, p. 2203 (cit. on pp. 27, 42).

Young, A., Smith, L., Rouse, E., and Hargrove, L. (2013). "Classification of Simultaneous Movements using Surface EMG Pattern Recognition". In: *Biomedical Engineering, IEEE Transactions on* 60.5, pp. 1250–1258 (cit. on pp. 17, 51, 77).

Young, A. J., Hargrove, L. J., and Kuiken, T. A. (2011). "The effects of electrode size and orientation on the sensitivity of myoelectric pattern recognition systems to electrode shift". In: *IEEE Transactions on Biomedical Engineering* 58.9, pp. 2537–2544 (cit. on pp. 13, 21, 79, 97).

Zardoshti-Kermani, M., Wheeler, B. C., Badie, K., and Hashemi, R. M. (1995). "EMG feature evaluation for movement control of upper extremity prostheses". In: *IEEE Transactions on Rehabilitation Engineering* 3.4, pp. 324–333 (cit. on p. 21).

Zhu, X., Liu, J., Zhang, D., Sheng, X., and Jiang, N. (2017). "Cascaded Adaptation Framework for Fast Calibration of Myoelectric Control". In: *IEEE Transactions on Neural Systems and Rehabilitation Engineering* 25.3, pp. 254–264 (cit. on pp. 26–28, 39, 40, 42).

Ziegler-Graham, K., MacKenzie, E. J., Ephraim, P. L., Travison, T. G., and Brookmeyer, R. (2008). "Estimating the prevalence of limb loss in the United States: 2005 to 2050". In: *Archives of physical medicine and rehabilitation* 89.3, pp. 422–429 (cit. on p. 11).